



Terms and Conditions of Use of Digitised Theses from Trinity College Library Dublin

Copyright statement

All material supplied by Trinity College Library is protected by copyright (under the Copyright and Related Rights Act, 2000 as amended) and other relevant Intellectual Property Rights. By accessing and using a Digitised Thesis from Trinity College Library you acknowledge that all Intellectual Property Rights in any Works supplied are the sole and exclusive property of the copyright and/or other IPR holder. Specific copyright holders may not be explicitly identified. Use of materials from other sources within a thesis should not be construed as a claim over them.

A non-exclusive, non-transferable licence is hereby granted to those using or reproducing, in whole or in part, the material for valid purposes, providing the copyright owners are acknowledged using the normal conventions. Where specific permission to use material is required, this is identified and such permission must be sought from the copyright holder or agency cited.

Liability statement

By using a Digitised Thesis, I accept that Trinity College Dublin bears no legal responsibility for the accuracy, legality or comprehensiveness of materials contained within the thesis, and that Trinity College Dublin accepts no liability for indirect, consequential, or incidental, damages or losses arising from use of the thesis for whatever reason. Information located in a thesis may be subject to specific use constraints, details of which may not be explicitly described. It is the responsibility of potential and actual users to be aware of such constraints and to abide by them. By making use of material from a digitised thesis, you accept these copyright and disclaimer provisions. Where it is brought to the attention of Trinity College Library that there may be a breach of copyright or other restraint, it is the policy to withdraw or take down access to a thesis while the issue is being resolved.

Access Agreement

By using a Digitised Thesis from Trinity College Library you are bound by the following Terms & Conditions. Please read them carefully.

I have read and I understand the following statement: All material supplied via a Digitised Thesis from Trinity College Library is protected by copyright and other intellectual property rights, and duplication or sale of all or part of any of a thesis is not permitted, except that material may be duplicated by you for your research use or for educational purposes in electronic or print form providing the copyright owners are acknowledged using the normal conventions. You must obtain permission for any other use. Electronic or print copies may not be offered, whether for sale or otherwise to anyone. This copy has been supplied on the understanding that it is copyright material and that no quotation from the thesis may be published without proper acknowledgement.

Spatial Modelling of Damage Accumulation in Bone Cement

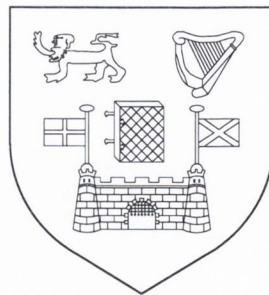
by

Elizabeth A. Heron

A thesis submitted to
the University of Dublin
for the degree of

Doctor of Philosophy

Department of Statistics,
University of Dublin, Trinity College



October, 2004



THESIS
7648

Declaration

This thesis has not been submitted as an exercise for a degree at any other University. Except where otherwise stated, the work described herein has been carried out by the author alone. This thesis may be borrowed or copied upon request with the permission of the Librarian, University of Dublin, Trinity College. The copyright belongs jointly to the University of Dublin and Elizabeth A. Heron.

Signature of Author..... *Elizabeth A. Heron*.....

Elizabeth A. Heron
29 October, 2004

Abstract

In this thesis we develop spatial models for damage accumulation in the bone cement of hip replacement specimens. A total hip replacement consists of an artificial cup, forming the socket portion of the joint, and a prosthesis inserted into the femur, replacing the ball part of the joint. Both components are fixated to the bone using an acrylic polymer known as bone cement. The dominant mode of failure of the hip replacement is the aseptic loosening of the components due to damage accumulation consisting of crack initiation and crack growth in the bone cement.

The data analysed come from a laboratory experiment in which 5 hip replacement specimens were subjected to a stress loading typical of normal use. Finite element stress measurements, together with start and end locations of each crack were provided.

As well as stress being a factor in damage accumulation, it is known that other spatially varying factors, for example pores, have an influence on crack initiation and growth. We develop two spatial models for crack initiation. Both models incorporate stress and allow for spatially varying latent factors to be modelled. A discrete model is proposed, in which crack counts in regions are modelled using an identity-link Poisson regression model. A continuous model for initiation is also presented that models the initiation of cracks as a spatial Poisson process, incorporating the influence of the latent factors through a Gamma random field.

Since damage accumulation consists of crack initiation and crack growth, we also propose a model for crack growth. It is known that cracks initiate with some length and that jumps occur in their growth; our model incorporates these features and the influence that stress has on crack growth. In the analysis of this model, evidence of spatial variability in the jump is presented.

All analysis is carried out through a Bayesian framework, employing MCMC techniques in order to sample from the posterior distribution of the parameters of each of the models.

Acknowledgements

I would first of all like to express my thanks to my supervisor Dr. Cathal Walsh. Cathal has given me many opportunities to broaden my knowledge; from attending conferences all over the world, giving talks, spending time abroad and not least of all introducing me to lots of statistics. Cathal has always been enthusiastic about my work, always patient and helpful, he has constantly encouraged me in all aspects of my academic career and it has always been fun to work with him.

Thank you to Prof. Patrick Prendergast and Dr. Alexander Lennon for providing the data on which this thesis is based and for the numerous questions they have answered. In particular I appreciate the time Dr. Alexander Lennon has taken in explaining the details of the experiment and for the diagrams that he has supplied. I appreciate the funding I have received from Trinity College in the form of an Ussher scholarship and the numerous travel grants of which I have availed. Thank you to the people of Fujitsu Siemens for their generous gift - the best piece of equipment I could have asked for - a very nice little blue laptop! This work has been carried out with the support of an Irish Research Council for Science, Engineering and Technology Basic Research Grant SC/02/187. Thank you to the members of the Statistics Department, both academic and non-academic, for always being helpful and for providing a good atmosphere in which to work. Thank you to the other postgraduate students: Sourabh, Claire, Breedette, Anne-Laure, Caroline, and Georgios, for an interesting and fun three years. I am also grateful to the members of the Statistics Department in Lancaster University where I spent some time, in particular Prof. Gareth Roberts, Prof. Robin Hendersen and Dr. Carmen Fernández and for the Marie Curie Fellowship which enabled me to travel there.

To my parents I express my thanks for everything that they have done and continue to do for me. Thank you to my brother for all of his support. Thank you to Alan Cahill for always being a really good friend. A very special thank you goes to my dear Raymond Russell with whom I have shared all the ups and downs of this time. Thank you for your patience and your support.

Contents

1	Introduction	1
1.1	Damage Accumulation in Bone Cement	1
1.2	Modelling Mechanical Failure	2
1.3	Overview of Chapters	3
1.3.1	Background	4
1.3.2	Statistical Methodology	4
1.3.3	Discrete Model for Crack Initiation	4
1.3.4	Continuous Model for Crack Initiation	5
1.3.5	Growth Model	5
1.4	Research Contributions	6
2	Background	7
2.1	Fatigue	7
2.2	Orthopaedic Hip Replacement	8
2.3	Bone Cement	9
2.4	Failure of the Hip Replacement	9
2.4.1	Stress	11
2.4.2	Pores	11
2.5	Other Factors Influencing Performance	12
2.6	The Experiment	13
2.6.1	The Experimental Model	14
2.6.2	Fatigue Testing	14

2.6.3	Crack Counting	14
2.7	Approaches to Modelling Fatigue Data	16
2.7.1	Survival Analysis	16
2.7.2	Modelling Crack Initiation	17
2.7.3	Modelling Crack Growth	18
2.7.4	Hierarchical Modelling of Crack Initiation and Growth	18
2.7.5	B-Models	19
2.8	What a Model Should Incorporate	19
3	Statistical Methodology	21
3.1	Bayesian Inference	21
3.1.1	Prior Distribution	22
3.1.2	Likelihood Function	22
3.1.3	Bayes' Theorem and The Posterior Distribution	23
3.1.4	Predictive Distribution	23
3.1.5	Estimating the Posterior Predictive Distribution	24
3.1.6	Prior Elicitation	24
3.2	Markov Chains	26
3.2.1	Basic Definitions	27
3.2.2	Transition Probabilities	28
3.2.3	Classification of States	28
3.2.4	Stationary Distribution	29
3.2.5	Stationary and Limiting Distribution Theorems	30
3.3	Markov Chain Monte Carlo	31
3.3.1	Monte Carlo Integration	31
3.3.2	Simulation Using Markov Chains	32
3.3.3	Metropolis-Hastings Algorithm	32
3.3.4	Metropolis and Random-Walk Metropolis Algorithms	34
3.3.5	Gibbs Sampling	34
3.3.6	Convergence	36

3.4	Data Augmentation	37
3.4.1	The Method	37
3.4.2	Example of Data Augmentation	38
3.5	Bayesian Kriging	40
4	Discrete Initiation Model	43
4.1	Modelling Approach	43
4.1.1	Approaches to Modelling Count Data	44
4.1.2	Identity-Link Poisson Regression Model	47
4.2	Model Specification	47
4.2.1	The Partition and the Intensity	48
4.2.2	Explanatory Variables	48
4.2.3	Poisson Regression Model with Identity Link	51
4.2.4	Prior Information	52
4.2.5	Posterior Distribution	53
4.3	Investigation of the Kernel Parameter ρ	54
4.3.1	Other Applications Using a Gaussian Kernel	54
4.3.2	Exploratory Analysis for ρ	55
4.3.3	Simulation Study	58
4.4	MCMC Algorithm	59
4.5	Results	59
4.5.1	Running the MCMC Algorithm	59
4.5.2	Estimates of the γ 's	60
4.5.3	Posterior Predictive Distribution for Counts	60
4.5.4	Zero-Inflated Poisson Distribution	61
4.5.5	Cross-Validation Predictive Density	62
4.6	Conclusions	63
5	Continuous Initiation Model	72
5.1	Poisson Random Field	72

5.1.1	Marked Poisson Process	72
5.1.2	Poisson Process on the Product Space	74
5.1.3	Intensity Measure	75
5.1.4	Regression Model with Identity-Link	75
5.1.5	Latent Spatial Covariate	76
5.1.6	Gamma Random Field	77
5.1.7	Simulation of a Gamma Random Field	78
5.1.8	Inverse Lévy Measure Algorithm	79
5.2	Likelihood	80
5.3	Prior Distributions	81
5.4	The Posterior Distribution	82
5.4.1	Inference for β_1 , β_2 , and ρ	82
5.4.2	Full Conditional Distributions for β_1 and β_2	83
5.4.3	Conditional Distribution for $\Gamma(ds)$	83
5.5	MCMC Algorithm	84
5.6	Results	85
5.6.1	Gamma Random Fields and Posterior Mean Intensity	85
5.6.2	Model Validation	86
5.7	Comparing Continuous and Discrete Models	87
5.7.1	Priors for Latent Factors	87
5.7.2	Loss of Information due to Aggregation	88
5.7.3	Computational Time	88
5.8	Conclusions	88
6	Growth Model	96
6.1	Preliminary Investigations	96
6.1.1	Crack Types	96
6.1.2	Crack Lengths	97
6.2	How Cracks Grow	99
6.3	Stochastic Process Model for Growth	99

6.3.1	Spatial Aspect to Growth	100
6.3.2	Stress	100
6.3.3	Jumps in Growth Rate	100
6.3.4	The Model	101
6.3.5	Prior Distributions	102
6.4	Posterior Distribution	103
6.4.1	Full Conditional Distributions	104
6.4.2	Simulation of I_{ijk^*} , B_{ijk} , Y_{ijk} , and h_{ijk^*}	105
6.5	MCMC Algorithm	106
6.6	Results	107
6.6.1	Convergence Assessment	107
6.6.2	Parameter Estimates	107
6.6.3	Heterogeneity of Specimens	107
6.6.4	Spatial Pattern of Jump Sizes	108
6.6.5	Growth Model Validation	109
6.7	Conclusions	110
7	Conclusions and Future Work	117
7.1	Conclusions	117
7.2	Comparison With Other Models	118
7.3	Further Work	119
7.3.1	Reliability Models	119
7.3.2	Pre-Crack Initiation	119
7.3.3	Growth Model Extension	120
7.4	Final Remarks	120
A	Calculations	121
A.1	Discrete Model	121
A.1.1	Data Augmentation for Crack Count	121
A.1.2	Full Conditional Distributions	123

A.2	Continuous Model	125
A.2.1	Full Conditional Distributions for β_1, β_2 and ρ	125
A.2.2	Full Conditional Distribution for $\Gamma(ds)$	127
A.3	Growth Model	129
A.3.1	Posterior Distribution	129
A.3.2	Full Conditional Distributions	130
B	Algorithms and Trace Plots	134
B.1	MCMC Algorithm for Discrete Initiation Model	134
B.2	MCMC Algorithm for Continuous Initiation Model	137
B.3	MCMC Algorithm for Growth Model	140
B.4	Trace Plots	141
	Bibliography	146

List of Figures

2.1	Schematic Diagram of a Hip Replacement	8
2.2	Failure Scenarios	10
2.3	Experimental Model	15
4.1	Load-Crack Locations, Specimens 1 - 3	45
4.2	Load-Crack Locations, Specimens 4 - 5	46
4.3	Boxplots and Histogram of Crack Counts	49
4.4	Stress Measurement Locations and Values	50
4.5	Kriged Stress Values	51
4.6	Gaussian Kernels	55
4.7	Estimated Log-Likelihoods for Fixed Values of ρ	56
4.8	Logarithm of Likelihood and Priors	57
4.9	Image Plots for Simulation Study of ρ	65
4.10	Posterior Median Estimates of Latent Contribution, Specimens 1 - 4	66
4.11	Posterior Median Estimates of Latent Contribution, Specimen 5	67
4.12	Posterior Predictive Counts and Actual Counts	67
4.13	Posterior Predictive Counts and Actual Counts (ZIP distribution)	68
4.14	Cross Validation Posterior Predictive Counts	69
4.15	Posterior Median Estimates of λ_{ij} 's, Specimens 1 - 4	70
4.16	Posterior Median Estimates of λ_{ij} 's Specimen 5	71
5.1	Single Realisation of a Simulated Gamma Random Field	80
5.2	Posterior Mean of Gamma Random Field, Specimens 1 - 4	90

5.3	Posterior Mean of Gamma Random Field for Specimen 5	91
5.4	Posterior Mean of the Poisson Intensity, Specimens 1 to 4	92
5.5	Posterior Mean of the Poisson Intensity, Specimen 5	93
5.6	Boxplots of Re-scaled γ 's for each Specimen	93
5.7	Scatter Plots of Residuals	94
5.8	Posterior Predictive Counts and Actual Counts for Each Specimen . .	95
6.1	Pre-Cracks and Load-Cracks	97
6.2	Boxplots of Logarithm of Crack Lengths	98
6.3	Trace Plots of Markov Chains	111
6.4	Credibility Intervals for $\frac{1}{\sqrt{\tau}}$, α , β and λ for Sensitivity Analysis	112
6.5	Credibility Intervals for M_I , $\frac{1}{\sqrt{\tau_I}}$, M_Y , and $\frac{1}{\sqrt{\tau_Y}}$ for Sensitivity Analysis	113
6.6	Spatial Representation of Average Jump Size, Specimens 1 - 4	114
6.7	Spatial Representation of Average Jump Size, Specimen 5	115
6.8	Prediction Analysis for Growth Model	116
B.1	Trace Plots of Parameters of the Discrete Model, β_1, β_2, ρ , and latent contribution	142
B.2	Trace Plots of Parameters of the Discrete Model, latent contributions and γ_{ij} 's	143
B.3	Trace Plots of Parameters of the Continuous Model, β_1, β_2, ρ	144
B.4	Trace Plots of Parameters of the Growth Model $\tau, \alpha, \beta, \tau_I, M_Y, \tau_Y$. .	145

List of Tables

4.1	Quantiles for β_1, β_2 and ρ from simulation study	58
4.2	Quantiles, Kernel Density Estimates and Priors for β_1, β_2 and ρ of the Discrete Model	60
5.1	Quantiles, Kernel Density Estimates and Priors for β_1, β_2 and ρ of the Continuous Model	89
6.1	Quantiles, Kernel Density Estimates and Priors for the Parameters of the Growth Model	108

Chapter 1

Introduction

The aim of this thesis is to develop spatial models for damage accumulation in the bone cement of hip replacement specimens. The spatial models we will develop incorporate both observed and unobserved factors that are influential in causing damage accumulation. In order to provide some motivation for this aim, we describe the hip replacement and the reasons as to why it fails. We also outline the structure of the thesis and summarise the research contributions made.

1.1 Damage Accumulation in Bone Cement

A common type of orthopaedic joint replacement is the total hip replacement. This replacement consists of two components, an artificial cup forming the socket and a prosthesis inserted into the femur, replacing the ball part of the joint. The components are fixated to the bone using an acrylic polymer known as bone cement.

The total hip replacement is considered to be a successful operation, with studies reporting over 90% of replacements still functioning well after 10 years (Huiskes and Verdonschot (1997)). For many patients though, the procedure is a failure and revision operations are not nearly as successful as primary ones (Malchau et al. (2000)). Also, the procedure is being carried out on younger patients, leading to the need for longer lasting replacements.

Failure of a hip replacement is a subjective term with much discussion as to when a replacement is said to have failed. Huiskes (1993) defines failure from a clinical point of view as the time at which a revision operation is required, due to excessive pain and impaired function. The dominant mode of failure is the aseptic loosening of the components of the replacement, due to damage accumulation (crack initiation and growth) in the bone cement.

It is known that, when in use, cyclic loads of several times a person's bodyweight are experienced at the hip (Bergmann et al. (1993)). Relative to the stresses that are applied at the hip, bone cement is a weak material (Huiskes (1993)). The cyclic loading results in compressive and tensile stresses along the femoral stem of the implant. These stresses are responsible for the initiation and growth of cracks in the bone cement.

As well as stress being a factor in crack initiation and growth in the bone cement, it is known that other influential factors exist. During the preparation of the bone cement, pores (air bubbles) may become trapped in the cement. It has been shown through retrieval studies (Jasty et al. (1991); Culleton et al. (1993)), that a link exists between crack initiation and the presence of pores in the cement. Pores have an impact on the stress in the cement. A raised stress state exists around a pore and this, coupled with stress concentrations in the micro-structure of the cement makes crack formation at pores highly likely.

There may also be inclusions in the cement, biological (e.g. blood) or non-biological (e.g., barium sulphate). These inclusions will also have an impact on the initiation and growth of cracks as they too change the structure of the cement.

1.2 Modelling Mechanical Failure

Given any sort of structure, the mechanical failure of that structure is dependent on its strength and on the stresses it experiences. Even if the structure experiences very high stresses, it will not fail, provided it is strong enough. But if the structure is weak and it experiences stresses that are beyond its limit, then it will fail.

Mechanical failure has been modelled in many different ways, depending on the understanding of the reasons for failure and on the tools and methods available for modelling. Obviously, the better the understanding of the reasons for failure, the better the model.

People have modelled failure in many ways. The simplest approach being the observation of the physical causes of stresses on structures and the drawing of conclusions based on these observations. A more sophisticated approach involves the construction of a mathematical model to quantify the influence that stress has on causing failure. The realisation that deterministic models were not sufficient to account for the random variability observed in the failure of structures led to the development of stochastic models for failure.

In the case of damage accumulation in the bone cement, random variability does exist. An obvious example of the variability being, that specimens subjected to the same stresses, under laboratory conditions, do not show the same damage accumulation patterns. This would obviously suggest the need for a stochastic model for damage accumulation. Incorporating stress into a stochastic model for damage accumulation is one way of approaching the task of modelling the variability.

It has also been observed that damage accumulation varies spatially. The incorporation of spatial coordinates of damage (crack locations), together with spatial stress information allows for an even closer examination of the relationship between damage and stress. This provides a more realistic model for damage accumulation.

The understanding of the physical process and the knowledge of other influential factors, but the inability to accurately measure or locate them, leads to a further extension. We can model, through latent variables, a spatial process, that accounts for the unobserved influential factors.

1.3 Overview of Chapters

In the following we present a brief outline of the research carried out.

1.3.1 Background

We describe in detail the structure of the orthopaedic hip replacement. We also introduce the concept of fatigue and examine the main reasons why these replacements fail, reviewing the literature on the impact of stress and of pores on causing damage accumulation in these implants. The data that we analyse come from experiments carried out on five specimens in a laboratory setting; each of the specimens was subjected to the same stress loading under similar conditions. The experimental model is described together with the methods by which the cracks were located and measured. We also present in this chapter a review of other statistical models that have been used for damage accumulation.

1.3.2 Statistical Methodology

We detail the statistical methods that we use throughout the analysis that we carry out in this thesis. All of our modelling is done in a Bayesian framework. We describe the Bayesian method in detail, highlighting the differences between this method and that of the Classical framework. We also address issues such as prior elicitation, which is an important aspect in carrying out any Bayesian statistical analysis.

The models that we present in this thesis are relatively complicated, often with many parameters, making direct simulation from these models difficult, if not impossible. To obtain estimates of the parameters of the models we use MCMC techniques in order to sample from the Posterior distributions. We describe in detail the Markov chain theory that underlies the MCMC techniques, as well as describing individual MCMC algorithms.

1.3.3 Discrete Model for Crack Initiation

We present a discrete spatial model for the initiation of cracks during the stress loading process. The model is discrete in the sense that we aggregate the data to form counts of cracks in a finite number of regions. We model the counts of cracks in

the regions as independent Poisson random variables, relating the Poisson intensity to both known (compression and tension) and unknown, or latent, factors through an identity-link regression model. We include the latent spatial parameters since we know from the literature that factors such as pores (air bubbles), which could not be measured during the experiment, have an impact on causing cracks to form. The latent factors are modelled by including a latent spatial parameter for each region. The influence of this parameter on crack formation in its own region, as well as in neighbouring regions, is governed by a Gaussian kernel. The distance over which the latent spatial parameters have an influence is determined by the variance parameter of the Gaussian kernel and we perform inference in order to estimate this parameter.

1.3.4 Continuous Model for Crack Initiation

A continuous spatial model for the initiation of cracks in the bone cement is presented in Chapter 5. Instead of aggregating the data, we use each of the data points (spatial coordinates) directly and model the initiation of the cracks as a spatial Poisson process. As in the case of the discrete model, we also incorporate both observed and unobserved factors that are influential in the formation of cracks in the bone cement. We model the intensity of the Poisson process, again using an identity link regression model, and this time we incorporate the latent factors using a Gamma random field. Thus the intensity due to the latent factors, that are influential in causing cracks to form but that were not measured, is modelled as a continuous surface.

1.3.5 Growth Model

Damage accumulation consists of both crack initiation and crack growth and so it is also necessary to model crack growth when examining damage accumulation. We present a model for the growth of the different types of fatigue cracks that are present during the stress loading. The model attempts to capture the actual physical process by which cracks grow, drawing on information from the literature about crack growth.

For example, cracks are known to have both active and dormant periods of growth. The model incorporates the effect of stress on the growth of the cracks. Cracks subjected to different stresses would be expected to show varying amounts of growth. It is also believed that cracks experience jumps in their growth rate and we model a jump in growth, showing visually that spatial variation does exist in the size of the jumps. We also carry out a sensitivity analysis which shows variability between the specimens with respect to the parameters of the growth model proposed.

1.4 Research Contributions

The following are the main contributions made by the research contained in this thesis:

1. The development of spatial models for crack initiation in the bone cement of hip replacement specimens. One model allows for the spatial modelling of crack counts without the need for actual spatial coordinates. The other model incorporates spatial coordinates of the crack locations allowing for a more detailed analysis to be carried out. Both of these models incorporate observed and unobserved factors (latent) and they constitute a new application of the methodology in an engineering setting.
2. The statistical modelling of the unobserved latent spatial factors is a new method of assessing the impact of the unmeasured covariates that are known to have an influence on crack formation.
3. The modelling of crack growth, incorporating the influence of stress, by adapting another available model and the detailing of how spatial modelling of crack growth may be carried out.

Chapter 2

Background

In this chapter we introduce the concept of fatigue with particular reference to fatigue in orthopaedic hip replacements. We examine the reasons why these replacements fail and detail a laboratory experiment which was carried out in order to investigate damage accumulation in the bone cement of the replacement. This experiment resulted in data which form the basis of our analysis in subsequent chapters. We also review other stochastic models that have been used to examine the initiation and growth of cracks in bone cement.

2.1 Fatigue

The deterioration of a structure that is subjected over time to an external loading, resulting in the inability of the structure to carry the intended loading, is known as fatigue. Crack initiation and crack growth are regarded as the basic causes of fatigue damage accumulation and ultimate fatigue failure (Sobczyk and Spencer (1992)). According to Sobczyk and Spencer (1992), between 50 and 90 percent of all mechanical failures in metallic structures are related to fatigue. Structures made from materials other than metal also experience crack initiation and growth, for example, orthopaedic joint replacements are load-bearing structures that experience fatigue.

2.2 Orthopaedic Hip Replacement

Orthopaedic joint replacements are used to replace human joints that no longer function as they should. In particular, an orthopaedic hip replacement is used to replace the ball and socket components of the hip joint. The replacement of a hip joint is a very common procedure with up to one million hip replacements being carried out annually (Huiskes and Verdonschot (1997)). Typically the hip replacement consists of a prosthesis, usually metallic, being inserted into the medullary cavity of the femur bone which has been hollowed out. The metal prosthesis is a replacement for the “ball” portion of the joint. The “socket” portion of the joint is replaced with an artificial cup (typically this is made from ultra high molecular weight polyethylene; UHMWPE). The prosthesis is held in place by an acrylic polymer (polymethylmethacrylate; PMMA) cement mantle that interlocks the prosthesis and the bone. See Figure 2.1.

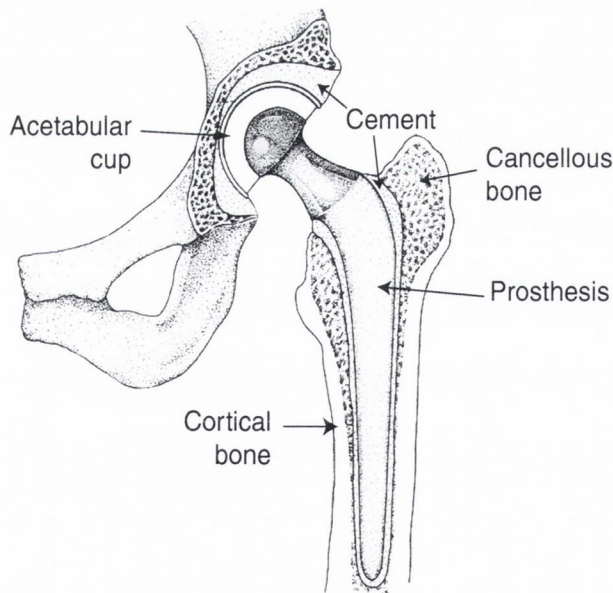


Figure 2.1: Schematic diagram of a hip replacement showing the prosthesis and acetabular cup inserted into the femur and pelvis respectively. Image courtesy of A.B. Lennon.

2.3 Bone Cement

The polymer cement used in the fixation of the joint replacement is often referred to as bone cement. The cement does not form any sort of chemical bond with either the metal prosthesis or the bone. The fixation occurs instead through a mechanical interlocking that arises between the surface of the implant and interdigitation with cancellous bone. An analogy given by Lennon (2002) for the function of the bone cement is that it performs a similar role to that of a “grout”.

Bone cement has a similar composition to Perspex/Plexiglas used in industrial settings. The bone cement is prepared in the operating theatre several minutes before the components of the joint replacement are inserted. It is prepared as a self-curing, dough-like resin thus ensuring that it is possible to insert the cement into the prepared cancellous bone and implant the prosthesis into the cement. The cement hardens within 10-15 minutes of initial preparation allowing enough time for the insertion. The bone cement may contain inclusions, for example, radiopaque fillers or antibiotics or biological inclusions such as blood or fat. For a more detailed description of bone cement and its composition see (Lennon 2002, pg. 13 -17).

2.4 Failure of the Hip Replacement

There are two main reasons for failure in cemented hip replacements: infection and mechanical (aseptic) loosening of the components. Due to improvements in surgical conditions, infection has been almost eliminated (cumulative revision rate for deep infection after ten years is 0.3% (Malchau et al. (2000))) and aseptic loosening of the components is now the dominant mode of failure, in particular aseptic loosening of the femoral stem (Malchau et al. (2000)).

According to Huiskes (1993) two interacting failure scenarios can account for the mechanical loosening of the hip replacement - particulate reaction scenario and the damage accumulation scenario. The particulate reaction scenario is a deterioration of the bone until it is no longer able to support the replacement. This deterioration

of the bone is caused by biological reactions to particulate wear debris. The damage accumulation scenario consists of the debonding of the prosthesis from the cement, together with the formation of cracks in the cement, until the prosthesis is no longer fixated to the bone, i.e., the prosthesis is free to move inside the femur. The two failure scenarios can interact, see Figure 2.2.

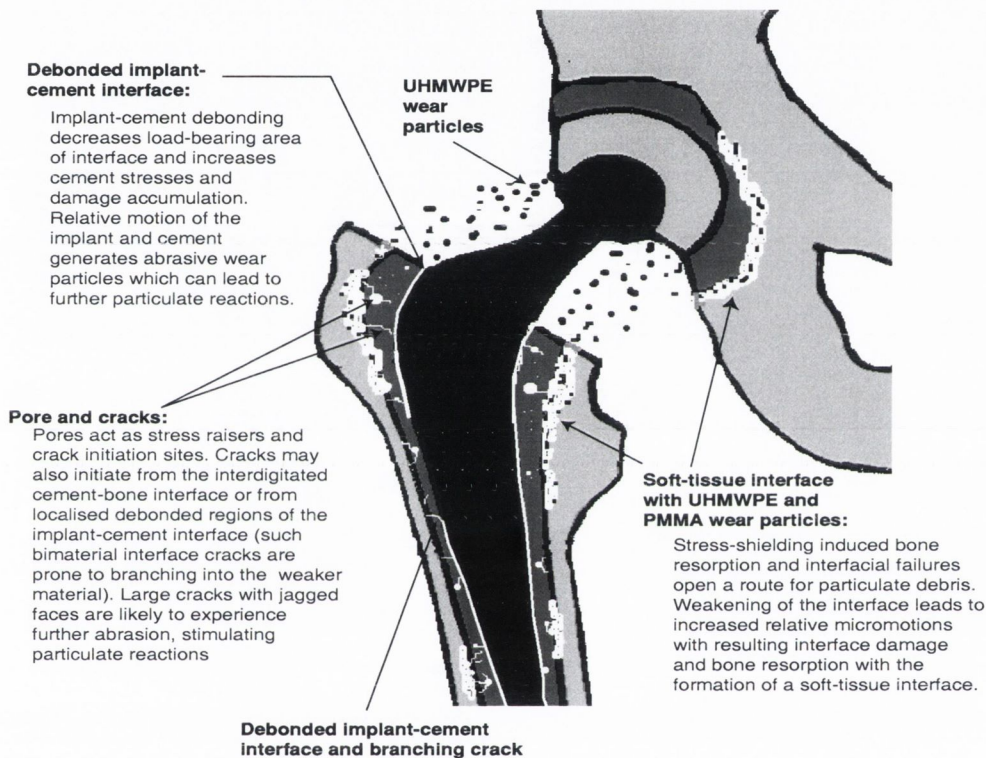


Figure 2.2: Particulate reaction senario and the damage accumulation senario and their interations. Image courtesy of A.B. Lennon.

Improvements have been made in resistance to the particulate reaction scenario but according to Lennon (2002) the reduction of damage accumulation within the cement has proved difficult. According to Lennon (2002) damage accumulation is likely to be the dominant mode of failure in the femoral part of the implant as the interface between the prosthesis and the cement experiences greater stress here.

2.4.1 Stress

According to Lennon and Prendergast (2001), the aseptic loosening in hip replacements is usually caused by fatigue failure of the cement mantle under cyclic loading. Maintaining the cement mantle is not simply a matter of reducing the peak stress in the mantle. Lennon and Prendergast (2001) highlight the situation where the influence of cement porosity may dominate the effect of stress to such an extent that failure may occur, not at the location of peak stress but instead where the pores are largest. In this case, recording the peak stress would not give sufficient information for investigating crack initiation and propagation.

2.4.2 Pores

Bone cement has a much lower fatigue resistance than Perspex/Plexiglas because of the way in which it is prepared (Lennon (2002)). During preparation, pores (air bubbles) become trapped in the cement. Retrieval studies carried out show that a link exists between the porosity in the bone cement in the hip replacement and damage accumulation (Jasty et al. (1991); Culleton et al. (1993)). According to Jasty et al. (1991) cracks initiate in the cement due to stress concentrations at the interface between the implant and the cement and also from pores in the cement. It has been observed that large numbers of pores form at the interface between the implant and the cement. Lennon (2002) provides more details on this.

The amount of porosity varies depending on the way in which the cement is mixed. Improvements in the mixing of the cement such as mixing under a vacuum and centrifuging, as opposed to manual mixing with a bowl and spoon, decrease the amount of air bubbles trapped but do not eliminate all pores (Wang et al. (1996)). According to Lennon (2002) the pores that do remain can often be very large (which can lead to early failure of the implant) in the case with vacuum mixing or the pores may be heterogeneously distributed in the case of centrifuging.

Damage accumulation, initiating mainly from pores was demonstrated in a physi-

cal model of the femoral stem of the hip replacement which was subjected to a bending load (McCormack and Prendergast (1999)). Another examination of the impact of pores can be seen in a time-lapse study of damage accumulation, in which it was noted that microcracks initiated from pores (Murphy and Prendergast (1999)). The existence of pores causes stress concentrations making crack initiation very likely. Also, pores often tend to cluster so that interactions occur which can result in cracks initiating and propagating in a different manner than would be expected.

Tsukrov and Kachanov (1997) examined the impact on stress of interactions between elliptical holes (pores or cracks) using a stress “feedbacks” method. In real materials pores often have strongly non-circular shapes and mixtures of holes of diverse shapes are typically to be found. Interactions between holes may produce both stress shielding and stress amplification, depending on factors such as the mutual positions of the holes, the hole eccentricities and the mode of the remote stress loading. Tsukrov and Kachanov (1997) also noted that different stress loading conditions produce different zones of shielding/amplification. The authors detail the effects of the interactions on stress of many different hole combinations, varying the relative distances between the holes, the number of holes and the hole shapes and sizes. For example, they examine the interaction between two circular holes, which are of equal size and that are experiencing remote tension in the direction normal to the line connecting the centres of the holes. They found that at distances of $1/100$ of the hole radius the interaction effect was very strong and the stress was amplified.

For more details on the impact of pores in crack formation and propagation see Lennon (2002).

2.5 Other Factors Influencing Performance

There are other factors that have an influence on how long a replacement lasts. The design of the prosthesis will certainly have an impact on the performance. Many different prosthesis models are available with varying femoral stem designs. The

longevity of the replacement is dependent on the design type, with different designs having different survival rates. A prosthesis design that suffices for the remaining life of all patients has yet to be found (Lennon and Prendergast (2001)).

The prosthesis needs to be carefully inserted so that it is well placed within the femur and that even pressurisation is achieved during the insertion, i.e., the surgeon's skill has an impact on the performance of the replacement. The condition of the surrounding bone will also have an effect on the longevity of the replacement as will the activity levels of the patient. The inclusions, both biological and non-biological previously mentioned will alter the structure of the cement. For example, both the presence of antibiotics and blood will weaken the cement, and so these too will have an influence on crack initiation and propagation.

However, under controlled laboratory conditions, variability exists in the damage accumulation in the bone cement and according to Lennon (2002) this variability is large enough that it might dominate, i.e., the other factors mentioned above would not have as great an impact on the performance of the replacement. There is also the possibility that these factors will interact.

Replacing the PMMA bone cement with a suitable alternative has yet to be successful (Lennon (2002)), but replacements do exist that use no bone cement. Instead the prosthesis is coated with a bioactive substance that allows a bond to form directly between the prosthesis and the bone. However these replacements have not performed as well as those using bone cement (Malchau et al. (2000)).

2.6 The Experiment

The data that are available for analysis come from an experiment which was carried out in a laboratory setting. Five specimens, each resembling as close as was possible a femoral hip replacement, were subjected under laboratory conditions to a stress loading. For full details of the design and experimental procedure see Lennon (2002).

2.6.1 The Experimental Model

The experimental model was designed in such a way as to retain the most important physical features of the femoral hip replacement, ensuring that it would behave in the laboratory in a similar fashion to a hip replacement in the human body. It was also necessary to design the model in such a way that measurements of damage accumulation could be made, i.e., that cracks could be observed and located.

The model consists of a femoral stem encased between layers of cement and strips of cancellous bone, see Figure 2.3(a). These are then held in two aluminium side plates which offer support similar to that which would be given by the cortical bone in the human body. The cancellous bone strips are made from bovine rib bone that has been cut and shaped to fit the length of the cavity in the aluminium side plates.

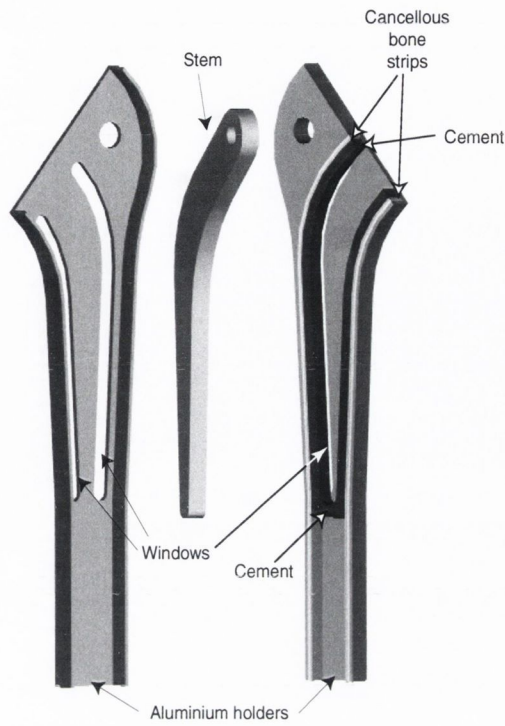
The side plates contain windows in which the cement is exposed and therefore available for observation. The cement that was used was mixed by hand and contained no inclusions (biological or otherwise). The particular type of cement that was used is translucent, enabling cracks to be stained and viewed by light transmission.

2.6.2 Fatigue Testing

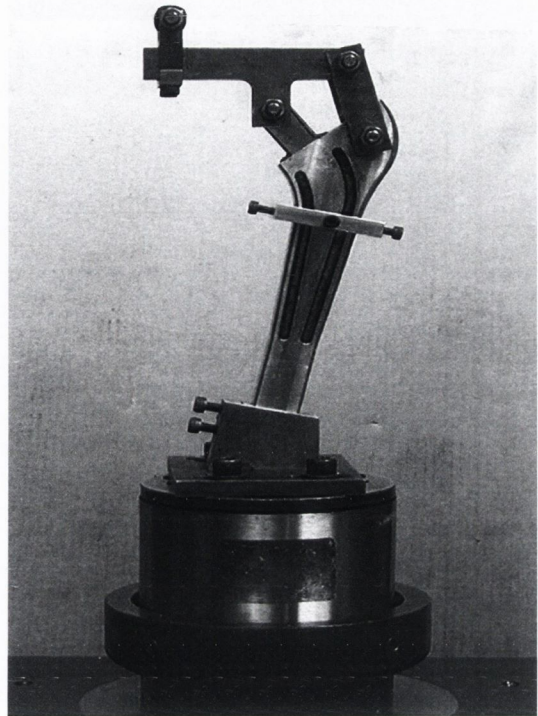
Stress loading was applied to the physical model in two ways. A load was applied to the prosthesis by means of a lever attached to the prosthesis head centre and a muscle loading was applied using a lever attached to the centre of the trochanter-like process of the aluminium holders. See Figure 2.3(b). Both loadings were applied simultaneously and were used to simulate what would occur in the human body, the prosthesis loading simulating the load that would be applied at the joint in a human body. For details on the actual load measurements see Lennon (2002).

2.6.3 Crack Counting

Before any testing was carried out dye penetrant was applied to the cement layers of each of the specimens. A magnified image of the cement surface was then projected



(a)



(b)

Figure 2.3: (a) shows an exploded view of the experimental model of the femoral stem encased in bone cement. (b) shows a photograph of a specimen mounted in the fatigue testing machine. The means by which muscle and joint loading are applied can be seen at the plates connecting the lever to the specimen and at the stem head, respectively. Images courtesy of A.B. Lennon.

onto a screen using an optical comparator. Any cracks which would have formed when the cement was curing (drying) were identified and traced onto acetate transparencies. The transparencies were digitally scanned and image analysis was carried out in order to obtain the position, length, and slope of each crack. In the literature these cracks, which form before the stress loading has been applied, are referred to as *pre-cracks*.

As would be expected not all cracks lay on the surface - some were seen to extend below the surface. For a crack of this type the focus of the optical comparator was changed in order to assess the full length of the crack. Cracks would also have formed

below the surface but would not have been stained with the dye and so could not have been identified. For this reason the data provide a conservative estimate of the number of cracks in each specimen.

After testing, this procedure of identifying and locating the cracks was repeated for each specimen. The cracks which have formed during the stress loading process are referred to as *load-cracks*.

2.7 Approaches to Modelling Fatigue Data

Since fatigue data is inherently random, with even data that have been produced under controlled laboratory conditions showing variability, the obvious approach in modelling this type of data is to use stochastic models. The choice of stochastic model should represent as fully as possible the essential aspects of the physical model.

2.7.1 Survival Analysis

Predicting lifetimes, for example, how long a hip replacement will last, is done by analysing lifetime data. When investigating lifetimes, components are tested until they fail, the lifetime of the component being the period from the start of observation until failure occurs. Survival analysis is concerned with the study of lifetimes and involves all aspects related to lifetimes data, from the recording of the data to the examination of factors that affect the lifetime of the components being considered.

A random variable Y is termed a survival random variable if an observed outcome of Y lies in the interval $[0, \infty)$. It is possible to define a survival function or reliability function S , as follows: $S(y) = \mathbb{P}(Y \geq y) = \int_y^\infty f(u)du$, where $f(u)$ is the probability density function.

As well as looking at the survival function it is often the case that we are interested in the instantaneous rate of failure of the component at a given time y , given that the component survives up to time y . This information is given by the hazard function $h(y) = f(y)/S(y)$. Essentially the hazard function says how the failure rate changes

with time. It is possible to construct many different kinds of hazard models. For example, if the risk of failure does not change over time, then a constant hazard model would be appropriate. What is often the case in engineering problems is that as time increases the imminent risk of failure also increases. What is termed a power hazard model is often proposed in this case. Here $h(y) = (\alpha y^{\alpha-1})/\beta^\alpha$, where $y > 0$ and in this case the lifetime variable Y can be modelled with a Weibull distribution.

Lifetime analysis for hip replacements has been carried out, see for example Malchau and Herberts (1998). For an examination of lifetime analysis and the techniques used, see Smith (2002).

2.7.2 Modelling Crack Initiation

McCormack et al. (1998) analysed fatigue data from an experiment in which hip replacement specimens were subjected in a laboratory setting to cyclic stress loading typical of normal use. In this experiment, cracks were observed in ten observational windows on the cement surface and the number of cracks in each window was recorded at 0, 0.5, 1, 2.5, and 5 million cycles. The length of each crack was also recorded. The number of cracks $X_{ij}(n)$ in window j of specimen i at n million cycles was modelled as a counting process, the process increasing by one each time a crack was initiated. The simplest counting process, that of a Poisson process, was chosen to model the number of cracks. The rate of the Poisson process λ_{ij} was modelled as $\lambda_{ij} = (\alpha_j + \beta_j Z_{ij})$, where Z_{ij} indicates the number of pre-load cracks, α_j may be interpreted as the expected rate of crack formation when no pre-load cracks were present, and β_j as the increase in the crack formation rate for each pre-load crack present.

Bayesian analysis was carried out and estimates of the posterior distributions for the parameters α_j and β_j were obtained. The authors acknowledge a lack of fit and suggest that it may be due to influential factors that have not been accounted for, such as stress levels or the location of pores. Also this model for initiation of cracks did not allow for any spatial data to be incorporated.

2.7.3 Modelling Crack Growth

A model for crack growth was also presented by McCormack et al. (1998). The average growth per million cycles over the observed life of each crack was examined. Cracks that did not grow or that appeared to shrink were ignored. A histogram of the logarithm of growth appeared to be bell-shaped and so a natural choice for the probability distribution to model the growth was the Lognormal distribution. Bayesian analysis was carried out and posterior estimates were obtained for the mean and variance parameters of the Lognormal distribution. According to the authors this model was satisfactory for all cracks except those that grew very quickly.

2.7.4 Hierarchical Modelling of Crack Initiation and Growth

The same data as were analysed by McCormack et al. (1998) were again analysed by Wilson (2005). Here, a hierarchical model for crack initiation and growth is proposed and a Bayesian analysis is carried out. The decision to use a hierarchical model is based on the fact that the variability between specimens and within specimens can be attributed to different influential physical factors. An example of within-specimen variability given by Wilson is that of random variations in the distribution of pores in the cement. Between-specimen variability could be due to the random differences in the mixing of the cement, for example.

A Poisson process, modelled as a function of local material properties of the cement, is proposed for the initiation of the cracks. The model proposed is similar to that of McCormack et al. (1998), again with the rate of the process being a function of the number of pre-load cracks.

The growth model proposed by Wilson models the physical process of crack growth. Through inspection of the data, the main features of the growth of the cracks may be observed. Cracks initiate with some length, some of the cracks then grow very slowly and some grow very quickly. Wilson models the way in which the cracks grow by allowing for large instantaneous jumps between periods of slower growth. We

follow this model in Chapter 6, adapting it to incorporate stress measurements and investigating how growth can be spatially modelled.

2.7.5 B-Models

Another approach to the stochastic modelling of the fatigue life of bone cement in the hip replacement is presented in Grasa et al. (2003). The authors propose a model, called a B-model, based on Markov chains. This type of model has been used to compute the probability of failure after a certain time or number of cycles, for different damage problems using results obtained through experimentation.

The basic idea of the model is the following. At a given time t (discrete) the component is at some damage level D_t , after starting at time 0 in state D_0 . There exist damage cycles of constant severity and associated with each damage cycle is a transition matrix P . The authors define the model so that given a damage state D_t , there are only two options for D_{t+1} , the next step in the chain. Either the chain will remain in the same state or it will advance to the next damage level, until finally it reaches a failure state b .

It is possible to examine the probability of being in any state at time t with the probability of being in state b tending to 1 as $t \rightarrow \infty$. The authors use this model to examine the probability of failure for different cement mixing techniques at different stress levels.

2.8 What a Model Should Incorporate

The engineering literature on fatigue in hip replacement specimens obviously regards stress as having an important role in causing cracks to form and grow in the bone cement. When a model for crack initiation was proposed that did not incorporate stress (McCormack et al. (1998)), the model did not perform very satisfactorily. As the data we are analysing contain stress measurements, we should construct a model that exploits these measurements fully.

As well as stress measurements being available in our data, we also have accurate spatial coordinates for each of the observed cracks. Again, our model should incorporate this information, as it is known that spatial variability exists in damage accumulation.

Together with the data available we also have the knowledge that pores have an effect on damage accumulation. Although their spatial distribution is unknown, a realistic model for damage accumulation should accommodate and account for their influence.

As there are two aspects to damage accumulation: crack initiation and crack growth both should be modelled. In the following chapters we construct and analyse models that fulfil the above criteria.

Chapter 3

Statistical Methodology

In order to analyse the data that we have available and in order to gain a better understanding of the processes that have given rise to the data, we will in subsequent chapters construct models and make inferences about the parameters of these models. To do this we draw on a wide range of statistical methods and in this chapter we detail many of these methods.

3.1 Bayesian Inference

When we carry out data analysis we are interested in summarizing the data and also in making inferences about the physical system or process that produced this data. We may also be interested in making predictions based on the data we have observed. Before we have collected any data, prior beliefs exist about the nature of the system or process. The modification of these beliefs in light of the observed data, through the use of Bayes' theorem, forms the basis of Bayesian inference.

One of the main differences between Bayesian and classical (frequentist) inference is that the parameters of the model are treated as random variables in Bayesian inference, whereas in classical inference they are assumed to have unique values (although these are unknown), (O'Hagan and Forster (2004)). Bayesian inference also differs from classical inference in that it is subjective and that previous knowledge or in-

formation about the system is important. It is subjective since one person's prior beliefs need not necessarily agree with another person's prior beliefs. Bayesian inference takes into account, through the use of what is called the prior distribution, any information available before any data are observed. For comprehensive introductions to Bayesian inference see, for example, Lee (1997) and O'Hagan and Forster (2004).

3.1.1 Prior Distribution

Let $\Theta = \{\theta_1, \theta_2, \dots, \theta_k\}$ represent the parameters of the distribution that models the data arising from the process, i.e., Θ represents characteristics which must be determined in order to obtain a complete description of the system or process. We are interested in knowing more about these unknown parameters, for example, obtaining point or interval estimates.

Before any data are observed we have some *a priori* beliefs about the values of Θ . These beliefs may be based on our own knowledge of the system or on an expert's knowledge or opinion. We use a probability density function $\pi(\Theta)$ to express these beliefs. This p.d.f, $\pi(\Theta)$, is referred to as the prior distribution. Choosing a prior that correctly reflects this *a priori* knowledge is not always an easy task, see Section 3.1.6.

3.1.2 Likelihood Function

Now suppose we observe some data: $X = \{X_1, X_2, \dots, X_n\}$, whose distribution depends on the unknown parameters Θ . How likely is it that we observe the data X given that the parameters take the value Θ ? The probability statement called the likelihood, $L(\Theta|X) = \mathbb{P}(X|\Theta)$, models the relationship between the parameters and the observed data, and provides an answer to this question. The likelihood function is obtained by calculating the joint probability of the observed data values as a function of the parameters. The likelihood function is used both in classical and Bayesian inference. In classical inference the likelihood is often maximized in order to find the

“most likely” values for Θ ; Chatfield (1983), pg. 123 provides a simple example.

If we were to consider $\mathbb{P}(X|\Theta)$ as a function of X for fixed Θ then $\mathbb{P}(X|\Theta)$ is a density function, i.e., $\int \mathbb{P}(X|\Theta)dX = 1$. Here, however, $\mathbb{P}(X|\Theta)$ is thought of as a function of Θ for fixed X and in this case $\int \mathbb{P}(X|\Theta)d\Theta$ does not necessarily integrate to one. Lee (1997) gives the example where X does not depend on Θ and in this case it is possible for the integral to equal ∞ .

3.1.3 Bayes' Theorem and The Posterior Distribution

We want to be able to express our beliefs about Θ given both our prior knowledge and the data that we have observed. The prior distribution takes into account prior beliefs about Θ while the likelihood function expresses the relationship between Θ and the observed data. Bayes' theorem provides a mechanism for combining both these sources of information. For random variables (continuous or discrete) Bayes' theorem states that

$$\mathbb{P}(\Theta|X) \propto \pi(\Theta)\mathbb{P}(X|\Theta),$$

where the constant of proportionality is given by:

$$\mathbb{P}(X) = \begin{cases} \int \pi(\Theta)\mathbb{P}(X|\Theta)d\Theta, & \text{(continuous)} \\ \sum_{\Theta} \pi(\Theta)\mathbb{P}(X|\Theta), & \text{(discrete)}. \end{cases}$$

This allows us to look at the conditional distribution of the parameters given the observed data, i.e., $\mathbb{P}(\Theta|X)$. $\mathbb{P}(\Theta|X)$ is termed the Posterior distribution and it is a summary of all that is known about Θ after we have observed data X . Thus we have

$$\text{Posterior} \propto \text{Prior} \times \text{Likelihood}.$$

3.1.4 Predictive Distribution

As well as carrying out inferences for the parameters of our model we may also be interested in making predictions based on the data we have observed and on our prior

knowledge. Suppose we are interested in some future (unobserved) observation Y , given that we have observed data X . We can look at the following distribution

$$\mathbb{P}(Y|X) = \int \mathbb{P}(Y|\Theta, X)\mathbb{P}(\Theta|X)d\Theta,$$

which is referred to as the predictive distribution. $\mathbb{P}(\Theta|X)$ is the posterior distribution and $\mathbb{P}(Y|\Theta, X)$ is the likelihood function for Y . If X and Y are independent given Θ , then the likelihood for Y reduces to $\mathbb{P}(Y|\Theta)$.

3.1.5 Estimating the Posterior Predictive Distribution

Suppose $\Theta_1, \dots, \Theta_n$ are samples from the posterior distribution $\mathbb{P}(\Theta|X)$ and suppose we are interested in obtaining the posterior predictive distribution $\mathbb{P}(Y|X)$. Often $\mathbb{P}(Y|X)$ is not known analytically, but we can approximate it with $\hat{\mathbb{P}}(Y|X)$, the Rao-Blackwellized estimator (Casella and Robert (1996); Gelfand and Smith (1990)):

$$\hat{\mathbb{P}}(Y|X) = \frac{1}{n} \sum_{i=1}^n \mathbb{P}(Y|X, \Theta_i),$$

that is, we use the numerical average of the conditional densities over the simulated values of Θ as an approximation.

3.1.6 Prior Elicitation

Prior distributions are the means by which *a priori* beliefs, regarding the value(s) of the parameter(s) Θ are expressed. This *a priori* information about Θ may be based on the researcher's knowledge or on the knowledge or opinions of an expert. The process of constructing a probability distribution, the prior distribution $\pi(\Theta)$, that expresses the knowledge and/or opinions that are available before any analysis is carried out, is termed prior elicitation. Strictly speaking prior elicitation should take place before any data are observed, but it is often the case that researchers turn to experts after the data have been collected.

The elicitation of a prior usually involves two steps. The first step is the choice of probability distribution and the second is the choice of values for the parameters of the chosen distribution.

The choice of distribution is often governed by the desire to have a mathematically tractable model. For example, conjugate priors are often used for this reason. A conjugate prior is a prior distribution that belongs to the same class of distributions as the posterior distribution. This has the advantage that the only change in going from the prior distribution to the posterior is to change the parameters of the distribution and this can often make analysis much simpler.

The choice of distribution is not so critical as long as a prior distribution is chosen that is quite flexible, i.e., changes in the parameters of the distribution give very different distributions. For example, in the case where a conjugate prior is chosen it is most likely that the “true” prior is not conjugate but the class of conjugate priors is large enough so that a prior distribution can be chosen that is very close to the “true” prior. See Lee (1997).

Choosing the parameters for the prior is important. Suppose we choose a Gamma prior, then the problem becomes how to assign values to the shape and scale parameters of the Gamma distribution. One method of obtaining values for the parameters is to consider what is known about Θ , for example, if we have an idea what the mean and standard deviation should be, then we can equate these with the mean and standard deviation of the prior distribution and hence obtain values for the parameters of the prior. According to Garthwaite et al. instead of eliciting prior information through moments, it is often better to elicit the information through quantiles. People’s ability to estimate statistical quantities, for example, means and variances, have been examined in psychological experiments. It is not easy for people to interpret what is meant by “variance”, for example, and so it is difficult to obtain a numerical value for this quantity, hence eliciting prior information through quantiles, which are easier to interpret, is often a better idea. For more ideas on specifying a prior distribution see also O’Hagan (1998).

The situation where very little prior information exists must also be considered. For example, suppose no expert is available or the expert cannot give very much information. It is possible to specify what is termed a non-informative prior. (Up until now we have been considering informative priors). Suppose the range of values that the random quantity of interest can take is finite. It would be possible to use a Uniform prior over this range, i.e., all possible values in the range would be given equal probability. It is also possible to choose parameters for other prior distributions so that the distribution appears to be flat over the range of possible values for Θ .

When Θ takes values over an infinite range, a prior that is sometimes used is the following: $\pi(\Theta) = 1/c$, for all values of Θ , where c is some constant. This prior is not a probability density function, as $\int \pi(\Theta)d\Theta = \infty$ and is termed an improper prior density for this reason. Sometimes when improper priors are combined with likelihoods they result in proper posterior densities and so in some cases it is possible to use improper priors.

Objections to improper priors are for obvious reasons, i.e., they are not probability density functions and so one must be very careful, as the posterior is not guaranteed to be a proper density. See Lee (1997) for more details on improper priors and Uniform priors.

3.2 Markov Chains

In this section we introduce a special type of stochastic process called the Markov chain. Some definitions and main results are presented as they form the theory behind the iterative simulation techniques that will be introduced in the next section. For a more detailed study of Markov chains see Ross (2003) or Grimmett and Stirzaker (2001).

3.2.1 Basic Definitions

Definition 3.1 A stochastic process can be defined as a collection of random variables $\{\theta_t : t \in T\}$, where T is called the index set. The $\{\theta_t\}$ take values in a set S , called the state space, i.e., $\theta_t = s; s \in S, t \in T$.

If the index set is assumed to be countable, then we have a *discrete time stochastic process*. Without loss of generality it will be assumed to be the set of natural numbers \mathbb{N} . In general the state space will be a subset of \mathbb{R}^d .

Note that in what follows we are assuming a discrete state space, as it is possible to present the main theories of Markov chains in this way. Extending the theory to more general state spaces is of course possible.

Definition 3.2 A stochastic process $\{\theta_t : t \in T\}$ is called a discrete time Markov chain with countable state space S if:

1. $\forall n \geq 0, \mathbb{P}(\theta_n \in S) = 1;$
2. Markov property: $\forall n \geq 0$ and $\forall j, i, i_{n-1}, \dots, i_0 \in S :$

$$\mathbb{P}(\theta_{n+1} = j | \theta_n = i, \theta_{n-1} = i_{n-1}, \dots, \theta_0 = i_0) = \mathbb{P}(\theta_{n+1} = j | \theta_n = i).$$

Less formally stated, a Markov chain is a stochastic process where given the present state, past and future states are independent of each other.

Definition 3.3 A discrete time Markov chain $\{\theta_n\}$ with countable state space S is said to be time homogeneous (or homogeneous) if the conditional probabilities

$$\mathbb{P}(\theta_{n+1} = j | \theta_n = i),$$

are independent of $n, \forall i, j \in S$. This is also known as stationarity.

From here on we will assume that our state space S is discrete and that our Markov chain is homogeneous. We will now examine the probabilities for moving around this state space.

3.2.2 Transition Probabilities

Definition 3.4 A transition probability $P_{ij} = \mathbb{P}(\theta_{n+1} = j | \theta_n = i)$ is a function that satisfies:

1. $P_{ij} \geq 0, \forall i, j \in S$;
2. $\sum_{j \in S} P_{ij} = 1, \forall i \in S$, i.e., $P_{i \cdot}$ is a probability distribution. Thus the transition matrix

$$P := \begin{pmatrix} P_{11} & P_{12} & \dots & P_{1s} \\ P_{21} & P_{22} & \dots & P_{2s} \\ \vdots & \vdots & & \vdots \\ P_{s1} & P_{s2} & \dots & P_{ss} \end{pmatrix}$$

is a stochastic matrix. It is also called the Markov matrix.

We will denote by P_{ij}^m the probability of a chain moving from state i to state j in exactly m steps. If we let π^0 denote the initial distribution of the chain and we denote by π^n the marginal distribution of the chain at stage n , then

$$\pi^n = \pi^0 P^n.$$

3.2.3 Classification of States

We will now consider some properties of the states themselves.

Definition 3.5 A state $i \in S$ is said to be recurrent (persistent) if the Markov chain starting in i returns to i with probability 1, and it is said to be transient if it has positive probability of not returning to i . A recurrent state is said to be positive recurrent if the expected time to return to the state is finite, otherwise the state is null recurrent.

Recurrent states are infinitely often visited with probability 1. A Markov chain is said to be recurrent if all its states are recurrent. Similarly a Markov chain is said to be a positive recurrent chain if all its states are positive recurrent.

Definition 3.6 State j is accessible from state i if there exists an n such that $P_{ij}^n > 0$. States i and j communicate if i is accessible from j and j is accessible from i . States that communicate with each other are said to be in the same class.

Definition 3.7 A Markov chain is irreducible if it has only one class, i.e., all states can communicate with each other.

Definition 3.8 The period of a state i , denoted by d_i , is the greatest common divisor of the set

$$\{n \geq 1 : P_{ii}^n > 0\}.$$

A state i is said to be aperiodic if $d_i = 1$.

For an irreducible chain all states have the same period. A chain is periodic with period d if all its states have period $d > 1$ and aperiodic if all its states are aperiodic.

Definition 3.9 A chain that is positive recurrent and aperiodic is said to be ergodic.

3.2.4 Stationary Distribution

In using Markov chains for simulation it is necessary to study the behaviour of the chain as the number of iterations $n \rightarrow \infty$. In looking at this asymptotic behaviour of the chain a key concept is that of the stationary distribution of the chain.

Definition 3.10 A distribution π , is said to be a stationary distribution of a Markov chain with transition matrix P if

$$\pi P = \pi.$$

If the marginal distribution at any given n is π then the distribution at $n + 1$ is $\pi P = \pi$, i.e., once the chain reaches a stage where π is its distribution, then the chain keeps this distribution. The stationary distribution is also known as the invariant or equilibrium distribution. It can be shown that if π exists and $\lim_{n \rightarrow \infty} P_{ij}^n = \pi_j$ then, independently of the initial distribution of the chain, π^n will approach π as $n \rightarrow \infty$. In this case the distribution is also referred to as the limiting distribution.

3.2.5 Stationary and Limiting Distribution Theorems

We present two definitions that are necessary for the consideration of the stationary and limiting distribution theorems.

Definition 3.11 *The first passage time is defined to be the probability that the first visit to state j , given that the chain started in state i , takes place at the n^{th} step, i.e.,*

$$f_{ij}^n = \mathbb{P}(\theta_n = j, \theta_{n-1} \neq j, \dots, \theta_1 \neq j | \theta_0 = i).$$

Definition 3.12 *The mean recurrence time μ_i of a state i is defined as*

$$\mu_i = \mathbb{E}(T_i | \theta_0 = i) = \begin{cases} \sum_n n f_{ii}^n & \text{if state } i \text{ is recurrent;} \\ \infty & \text{if state } i \text{ is transient,} \end{cases}$$

where $T_i = \min\{n \geq 1 : \theta_n = i\}$.

The following two theorems are stated but not proved; see for example Grimmett and Stirzaker (2001) for detailed proofs. These theorems will be important when we consider simulating Markov chains in order to draw samples from some distribution of interest.

Theorem 3.1 *An irreducible Markov chain has a stationary distribution π if and only if all its states are positive recurrent. In this case π is unique and is given by $\pi_i = \frac{1}{\mu_i}$ where μ_i is the mean recurrence time of state i .*

Theorem 3.2 *For an irreducible aperiodic chain:*

$$\lim_{n \rightarrow \infty} P_{ij}^n = \frac{1}{\mu_j}; \quad \forall i, j \in S.$$

Combining these two theorems we have that if a Markov chain is irreducible and ergodic then

$$\lim_{n \rightarrow \infty} P_{ij}^n = \frac{1}{\mu_j} = \pi_j.$$

3.3 Markov Chain Monte Carlo

Suppose we are interested in simulating from some probability distribution $\pi(x)$, which we will refer to as the target distribution. A Markov chain Monte Carlo (MCMC) method is a method used to simulate from an ergodic Markov chain whose stationary distribution is the target distribution $\pi(x)$. The Monte Carlo part of MCMC refers to the use of Monte Carlo integration to form sample averages in order to approximate expectations.

MCMC techniques are used in the analysis of complex statistical models where, for example, they provide a means of simulating from high dimensional distributions when otherwise it would either be very difficult or impossible to perform direct simulation. High dimensional distributions often appear, for example, in the context of hierarchical modelling or in models for spatial data. Gamerman (1997) and Gilks et al. (1996) provide a more detailed and comprehensive treatment of MCMC with many applications. In order to examine how MCMC techniques work we examine first what is meant by Monte Carlo integration and then show how it is possible to construct a Markov chain that has as its stationary distribution the target distribution $\pi(x)$.

3.3.1 Monte Carlo Integration

We look at Monte Carlo integration in the Bayesian setting. Let $\mathbb{P}(\Theta|X)$ be the posterior distribution of Θ , where Θ could be a vector of random variables; $\Theta = \{\theta_1, \dots, \theta_k\}$. In the Bayesian setting Θ is the set of parameters of interest. Suppose we want to evaluate

$$\mathbb{E}[f(\Theta)] = \int f(\Theta)\mathbb{P}(\Theta|X)d\Theta,$$

where f is some function of interest. Suppose we can obtain n samples, $\Theta^{(1)}, \dots, \Theta^{(n)}$ of Θ from the posterior $\mathbb{P}(\Theta|X)$. These samples can be used to form an approximation as follows:

$$\mathbb{E}[f(\Theta)] \approx \frac{1}{n} \sum_{i=1}^n f(\Theta^{(i)}).$$

Drawing samples and using the above approximation is a Monte Carlo method of evaluating the expectation. When the $\Theta^{(1)}, \dots, \Theta^{(n)}$ are independent, the approximation is made more accurate by increasing n .

3.3.2 Simulation Using Markov Chains

In order to use Monte Carlo integration we need to be able to generate random samples from the target distribution. For standard distributions, for example, the Normal, Gamma, etc., it is straightforward to simulate from these distributions as there are many algorithms for simulation available (Press et al. (1992)). For distributions that are not of known form, and where there are high dimensional parameter spaces, it is possible to use techniques based on Markov chains.

Suppose we simulate a homogeneous Markov chain, i.e., we generate a sequence of random variables $\{X_0, X_1, \dots\}$, where the X_{t+1} is sampled from $\mathbb{P}(X_{t+1}|X_t)$, i.e., the next state only depends on the present state and not on any other states and the distribution $\mathbb{P}(\cdot|\cdot)$ does not depend on time, see Section 3.2. Given certain conditions the chain will eventually converge to its unique stationary distribution ϕ . The number of iterations taken before the chain has reached its stationary distribution is known as the burn-in period. All subsequent random variables that are generated will be dependent samples approximately from the stationary distribution ϕ .

As mentioned above, for Monte Carlo integration we require independent samples from the distribution. However, it is possible to carry out Monte Carlo integration where the samples are not independent, so long as they are drawn from the full support of the distribution. We now need to construct a Markov chain whose stationary distribution is not just an arbitrary distribution but the target distribution.

3.3.3 Metropolis-Hastings Algorithm

The Metropolis-Hastings algorithm is a method of ensuring that the stationary distribution of a generated Markov chain is the desired distribution. The Metropolis-

Hastings algorithm was first proposed by Metropolis et al. (1953) and then generalised by Hastings (1970).

The basic idea of the algorithm is as follows. Given a state X_t at time t the next state is chosen by first sampling a candidate Y from some proposal distribution $q(\cdot|X_t)$. The candidate is then accepted, i.e., $X_{t+1} = Y$ with probability $\alpha(X_t, Y)$ where

$$\alpha(X, Y) = \min \left\{ 1, \frac{\pi(Y)q(X|Y)}{\pi(X)q(Y|X)} \right\}. \quad (3.1)$$

If the candidate state Y is not accepted then the chain remains in the same state, i.e., $X_{t+1} = X_t$. This algorithm has the advantage that there is no need to determine the normalizing constant of the target distribution $\pi(\cdot)$ since it divides out in the acceptance probability $\alpha(\cdot, \cdot)$.

The fact that $q(\cdot|X_t)$ can take any form and still yield π as the stationary distribution of the chain can be seen from the following. The transition kernel for the Metropolis-Hastings algorithm is:

$$\begin{aligned} \mathbb{P}(X_{t+1}|X_t) &= q(Y|X_t)\alpha(X_t, Y), \quad \text{if } X_t \neq Y, \\ \mathbb{P}(X_{t+1}|X_t) &= 1 - \int q(Y|X_t)\alpha(X_t, Y)dY, \quad \text{if } X_t = X_{t+1}, \end{aligned}$$

$\mathbb{P}(X_{t+1}|X_t)$ being the acceptance of the candidate state Y if $X_t \neq Y$ and if $X_t = X_{t+1}$, the rejection of all candidate states Y . From the definition of the acceptance probability, Equation 3.1, it follows that

$$\pi(X_t)q(X_{t+1}|X_t)\alpha(X_t, X_{t+1}) = \pi(X_{t+1})q(X_t|X_{t+1})\alpha(X_{t+1}, X_t). \quad (3.2)$$

Combining Equation 3.2 with the transition kernel we have that

$$\pi(X_t)\mathbb{P}(X_{t+1}|X_t) = \pi(X_{t+1})\mathbb{P}(X_t|X_{t+1}). \quad (3.3)$$

Equation 3.3 is known as the *detailed balance equation*. If we integrate Equation 3.3 with respect to X_t we have that

$$\begin{aligned} \int \pi(X_t)\mathbb{P}(X_{t+1}|X_t)dX_t &= \int \pi(X_{t+1})\mathbb{P}(X_t|X_{t+1})dX_t, \\ &= \pi(X_{t+1}), \end{aligned}$$

i.e., we have obtained the marginal distribution for X_{t+1} given that X_t comes from the stationary distribution π . Thus, once X_t is from the stationary distribution, any subsequent samples will also be from the stationary distribution.

3.3.4 Metropolis and Random-Walk Metropolis Algorithms

The Metropolis algorithm consists of a symmetric proposal distribution, i.e., $q(Y|X_t) = q(X_t|Y)$ and so the acceptance probability reduces to

$$\alpha(X_t, Y) = \min \left\{ 1, \frac{\pi(Y)}{\pi(X_t)} \right\}.$$

A special case of the Metropolis algorithm is the Random-Walk Metropolis algorithm. For this algorithm the proposal distribution is of the form:

$$q(Y|X_t) = q(|X_t - Y|).$$

An example of such a proposal distribution is $Y \sim \text{Normal}(X_t, \sigma^2)$.

It is important to choose the proposal distribution for a random-walk carefully. If the moves proposed are small, i.e., $|X - Y|$ are small, then the acceptance rate (the number of times a move is accepted divided by the total number of steps in the chain) will be relatively high and it will take the chain a long time to explore the target distribution (poor mixing). On the other hand if the moves proposed are large, they will generally be rejected and the acceptance rate will be low and the chain will fail to move. Both of these extremes need to be avoided. Where the target and proposal distributions are Normal, optimal acceptance rates of approximately 0.45 for one dimensional problems are suggested, with this rate being reduced as the number of dimensions increases (Chib and Greenberg (1995)).

3.3.5 Gibbs Sampling

Gibbs sampling is a stochastic simulation method that uses Markov chains to sample from a distribution of interest; it is an MCMC technique. The term Gibbs sampling comes from an application in image processing where samples were drawn from a

Gibbs distribution. In Geman and Geman (1984) the authors discussed Bayesian restoration of images and the Gibbs distribution, specifically looking at sampling schemes. But it wasn't until Gelfand and Smith (1990) and Gelfand et al. (1990) that the idea of Gibbs sampling began to be used in general. They pointed out that this method could be used to sample from, not only the Gibbs distribution, but from many other posterior distributions.

Gibbs sampling provides a method of sampling from the posterior distribution of interest by means of successively sampling from the full conditional distributions. Suppose $\mathbb{P}(\theta_1, \dots, \theta_k)$ is the distribution of interest. Let $\mathbb{P}_i(\theta_i|\theta_{-i})$ be the full conditional distribution for θ_i , $i = 1, \dots, k$, where $\theta_{-i} = \theta_1, \dots, \theta_{i-1}, \theta_{i+1}, \dots, \theta_k$. Suppose also that the full conditional distributions are easy to sample from, i.e., suppose that $\mathbb{P}_i(\theta_i|\theta_{-i})$ is of some known distribution. The Gibbs sampling algorithm is then as follows:

1. Initialise $\theta_1^{(0)}, \dots, \theta_k^{(0)}$;
2. Generate

$$\begin{aligned} \theta_1^{(j)} &\sim \mathbb{P}_1(\theta_1|\theta_2^{(j-1)}, \dots, \theta_k^{(j-1)}); \\ \theta_2^{(j)} &\sim \mathbb{P}_2(\theta_2|\theta_1^{(j)}, \dots, \theta_k^{(j-1)}); \\ &\vdots \\ \theta_k^{(j)} &\sim \mathbb{P}_k(\theta_k|\theta_1^{(j)}, \dots, \theta_{k-1}^{(j)}), \end{aligned}$$

for $j = 1, \dots$ until convergence is reached.

The $\theta_1^{(j)}, \dots, \theta_k^{(j)}$ drawn after convergence has been reached are a sample from $\mathbb{P}(\theta_1, \dots, \theta_k)$. Note that proposed new values for the θ_i are always accepted, no accept/reject step is required. Gibbs sampling defines a Markov chain, since the probability of moving to $\theta^{(j)}$ only depends on $\theta^{(j-1)}$ and not on the previous moves.

3.3.6 Convergence

For each of the MCMC schemes detailed, we know that the stationary distribution is the target distribution and that after a number of iterations (burn-in) the chain will have reached its stationary distribution. After burn-in the chain is said to have converged. The question is how long should burn-in be before we can say we are sampling from the target distribution, i.e., before we can say we have reached convergence?

A number of diagnostic tools for assessing convergence exist. For example, Brooks and Roberts (1998) and Cowles and Carlin (1996) provide details of tools based on a statistical approach to the assessment of convergence.

For practical applications, trace plots of sampled values are often examined. A chain that has the same qualitative behaviour (Gamerman (1997)) after a number of iterations indicates convergence of that chain.

Iterative simulations can be slow-moving and it is important to note this when making inferences based on finite-length sequences. For example, the random walk can remain for many iterations in a region that has been influenced by the starting point of the chain. Gelman and Rubin (1992) provide a tool for assessing convergence that is based on running multiple independent chains whose starting values are chosen from a distribution that is more variable than the target distribution (overdispersed). Their method examines between-chain variance and within-chain variance: as chains become longer (and hence closer to convergence) the between-chain variance will become smaller. The multiple sequences are analysed to form a distributional estimate (t-distribution) of the target random variable given the simulations so far. The t-distribution will lie somewhere between the starting (overdispersed) distribution and the target distribution and it provides a basis for an estimate of how close the simulation process is to convergence.

3.4 Data Augmentation

The method of augmenting observed data with unobserved data in order to construct an iterative optimization algorithm or a sampling algorithm is termed *data augmentation*. This method is often used during the calculation of maximum likelihood estimates or posterior modes, where it allows easier analysis of a problem. It is also often used to facilitate Gibbs sampling.

The paper by Dempster et al. (1977) on the EM algorithm had an influence in popularising the idea of data augmentation for deterministic algorithms. The Data Augmentation algorithm of Tanner and Wong (1987) for posterior sampling popularised the method for stochastic algorithms. It was here that the term data augmentation originated. This same method may also be seen in the physics literature where it is termed the method of auxiliary variables. The paper by Swendsen and Wang (1987) on sampling from the Ising and Potts models and their generalisations was influential in this area. A detailed discussion of data augmentation may be found in van Dyk and Meng (2001). It should be noted that implementing data augmentation schemes requires skill and experience as the choice of scheme depends very much on the model being considered.

3.4.1 The Method

Two cases where data augmentation may be used are first if we have incomplete data and second where the likelihood function is intractable. Even in well-defined experiments, it is often the case that we have missing values that make the estimation of parameters difficult. The likelihood function can often be difficult to analyse for some reason. The introduction of latent data (unobserved supplementary data in the case of incomplete data, or unobserved random variables in the likelihood case) make analysis easier.

According to Tanner and Wong (1987) the method of data augmentation applies whenever the data can be augmented in such a way that:

1. it becomes easier to analyse the augmented data;
2. it is easy to generate the augmented data, given the parameter(s).

In the case of analysing posterior densities, suppose we have observed data X whose distribution depends on some parameter θ , where θ is the parameter of interest, i.e. we are interested in the distribution:

$$\mathbb{P}(\theta|X).$$

Let $\pi(\theta)$ be the prior on θ . Suppose now that the likelihood function $\mathbb{P}(X|\theta)$ is not readily available, but suppose we can augment the data X easily with latent (unobserved) data Z from the predictive density $\mathbb{P}(Z|X)$ such that the augmented data (X, Z) is easy to analyse, i.e., the posterior distribution:

$$\mathbb{P}(\theta, Z|X) \propto \mathbb{P}(X, Z|\theta)\pi(\theta),$$

becomes easy to analyse because the likelihood $\mathbb{P}(X, Z|\theta)$ is available. Data augmentation consists of successively sampling θ and Z , then calculating the marginal distribution of θ , i.e.,

$$\mathbb{P}(\theta|X).$$

3.4.2 Example of Data Augmentation

Example 3.1 *Poisson Model*

We now present an example of data augmentation which is a simplified version of how we will later on in this thesis (Sections 4.2.5 and 5.4) implement the method of data augmentation. The introduction of the augmented data set (N_1, N_2) in this example allows for the use of the Gibbs sampler and also for the estimation of the parameters λ_1 and λ_2 which are not identified by the data N . When we implement this method during the analysis of initiation models for the crack data in the following chapters, together with facilitating the use of the Gibbs sampler, the data augmentation will allow us to identify the proportion of the intensity of the Poisson model that is due to various crack causing factors.

Suppose we have the following Poisson model:

$$N \sim \text{Poisson}(\lambda_1 + \lambda_2).$$

We wish to make inferences about the parameters λ_1 and λ_2 , i.e. we are interested in $\mathbb{P}(\lambda_1|N)$ and $\mathbb{P}(\lambda_2|N)$. Suppose we choose Gamma priors for both λ_1 and λ_2 . Consider first the joint distribution:

$$\begin{aligned} \mathbb{P}(\lambda_1, \lambda_2|N = n) &\propto \mathbb{P}(N = n|\lambda_1, \lambda_2)\pi(\lambda_1)\pi(\lambda_2), \\ &= \frac{\exp(-(\lambda_1 + \lambda_2))(\lambda_1 + \lambda_2)^n}{n!}\pi(\lambda_1)\pi(\lambda_2). \end{aligned}$$

It is not so easy to analyse the conditional posterior distributions for λ_1 and λ_2 , i.e. $\mathbb{P}(\lambda_1|\lambda_2, N = n)$ and $\mathbb{P}(\lambda_2|\lambda_1, N = n)$ respectively, as they are not of known form. What we can do though, is augment the data as follows. Introduce two new random variables N_1 and N_2 , where we define N_1 as:

$$\mathbb{P}(N_1 = n_1|N = n) \sim \text{Binomial}\left(n, \frac{\lambda_1}{\lambda_1 + \lambda_2}\right),$$

and $N_2 = N - N_1$. We must show that the random variables we have defined, namely N_1 and N_2 , both have Poisson distributions with parameters λ_1 and λ_2 respectively.

Lemma 3.1 $N_1 \sim \text{Poisson}(\lambda_1)$.

Proof:

$$\begin{aligned} \mathbb{P}(N_1 = n_1) &= \sum_{n=n_1}^{\infty} \mathbb{P}(N_1 = n_1|N = n)\mathbb{P}(N = n), \\ &= \sum_{n=n_1}^{\infty} \binom{n}{n_1} \left(\frac{\lambda_1}{\lambda_1 + \lambda_2}\right)^{n_1} \left(\frac{\lambda_2}{\lambda_1 + \lambda_2}\right)^{n-n_1} \frac{e^{-(\lambda_1 + \lambda_2)}(\lambda_1 + \lambda_2)^n}{n!}, \\ &= \sum_{n=n_1}^{\infty} \frac{1}{n_1!n_2!} (\lambda_1)^{n_1} (\lambda_2)^{n_2} e^{-\lambda_1} e^{-\lambda_2}, \\ &= \frac{e^{-\lambda_1} (\lambda_1)^{n_1}}{n_1!} \sum_{n_2=0}^{\infty} \frac{e^{-\lambda_2} (\lambda_2)^{n_2}}{n_2!}, \\ &= \frac{e^{-\lambda_1} (\lambda_1)^{n_1}}{n_1!}, \end{aligned}$$

where $\lambda = \lambda_1 + \lambda_2$. Therefore $N_1 \sim \text{Poisson}(\lambda_1)$. With a similar argument to that used in Lemma 3.1 it is possible to show that $N_2 \sim \text{Poisson}(\lambda_2)$. We must now show that the random variables N_1 and N_2 are independent.

Lemma 3.2 $\mathbb{P}(N_1 = n_1, N_2 = n_2) = \mathbb{P}(N_1 = n_1)\mathbb{P}(N_2 = n_2)$.

Proof:

$$\begin{aligned} \mathbb{P}(N_1 = n_1, N_2 = n_2) &= \mathbb{P}(N_1 = n_1, N - N_1 = n_2), \\ &= \mathbb{P}(N_1 = n_1, N = n_1 + n_2), \\ &= \mathbb{P}(N = n_1 + n_2)\mathbb{P}(N_1 = n_1 | N = n_1 + n_2), \\ &= \frac{e^{-\lambda}(\lambda)^{n_1+n_2}}{(n_1 + n_2)!} \binom{n_1 + n_2}{n_1} \left(\frac{\lambda_1}{\lambda_1 + \lambda_2}\right)^{n_1} \left(\frac{\lambda_2}{\lambda_1 + \lambda_2}\right)^{n_2}, \\ &= \frac{e^{-\lambda_1}(\lambda_1)^{n_1}}{n_1!} \frac{e^{-\lambda_2}(\lambda_2)^{n_2}}{n_2!}. \end{aligned}$$

Given the random variable $N \sim \text{Poisson}(\lambda_1 + \lambda_2)$ we have constructed the independent random variables $N_1 \sim \text{Poisson}(\lambda_1)$ and $N_2 \sim \text{Poisson}(\lambda_2)$. Thus

$$\begin{aligned} \mathbb{P}(\lambda_1, \lambda_2 | N_1 = n_1, N_2 = n_2) &\propto \mathbb{P}(N_1 = n_1, N_2 = n_2 | \lambda_1, \lambda_2)\pi(\lambda_1)\pi(\lambda_2), \\ &= \mathbb{P}(N_1 = n_1)\mathbb{P}(N_2 = n_2)\pi(\lambda_1)\pi(\lambda_2). \end{aligned}$$

It is possible to show that $\mathbb{P}(\lambda_1 | \lambda_2, N_1, N_2)$ and $\mathbb{P}(\lambda_2 | \lambda_1, N_1, N_2)$ both have Gamma distributions since we have chosen a Gamma prior for both λ_1 and λ_2 . Hence for the algorithm we simulate $n_1 \sim \text{Binomial}\left(n, \frac{\lambda_1}{\lambda_1 + \lambda_2}\right)$, and $n_2 = n - n_1$, we can then simulate λ_1 and λ_2 given n_1 and n_2 .

3.5 Bayesian Kriging

It is sometimes necessary that we interpolate the data that we have available in order to estimate responses at locations other than those given. Kriging is a method

used for the interpolation or prediction of spatial data. See Cressie (1993), Diggle and Ribeiro Jr. (2000) and WinBUGS (June 2003) for more details. Consider a continuous study region $A \in \mathbb{R}^2$. We have a set of locations (x_i, y_i) , $i = 1, \dots, N$, and at each of these locations we have a scalar measurement (response) $Y_i = Y(x_i, y_i)$, where in principle the Y_i 's can be located anywhere in A . We consider the real-valued stochastic process:

$$\{Y(x, y) : (x, y) \in A\}.$$

The Y_i can be thought of as a “noisy” version of an underlying random variable $S(x_i, y_i)$, which is the value at location (x_i, y_i) of another process $\{S(x, y) : (x, y) \in \mathbb{R}^2\}$. $S(\cdot)$ is sometimes referred to as the signal. The stochastic process $S(x, y)$ is a stationary Gaussian process, i.e., the joint distribution of $S(x_1, y_1), \dots, S(x_n, y_n)$ is a multivariate Normal for any integer n and set of locations $\{(x_i, y_i)\}$, the expectation $\mathbb{E}[S(x, y)] = \mu(x, y)$ for all locations (x, y) , the variance of $S(x, y)$ is σ^2 for all locations and the correlation between $S(x_1, y_1)$ and $S(x_2, y_2)$ depends only on Euclidean distance (isotropic). The mean of the Gaussian process $S(\cdot)$ can be expressed as $\mu(x, y) = \sum_k \beta_k X_k(x, y)$, where $X_k(x, y)$ are a set of k spatially-referenced explanatory variables.

The model for the data can then be expressed as:

$$Y \sim \text{MVN} \left(\mu, \sigma^2 \sum + \tau^2 I \right),$$

where \sum is an $N \times N$ correlation matrix, i.e., $\sum_{ij} = f(d_{ij}; \Theta)$, $f(\cdot)$ is a correlation function, τ^2 is the variance of the nugget effect (small scale variation and measurement error) and d_{ij} is Euclidean distance. Equivalently, conditional on $S(\cdot)$, $Y_i \sim \text{Normal}(S(x_i, y_i), \tau^2)$.

Suppose we are interested in predicting responses T_j , $j = 1, \dots, M$ at locations (x_j, y_j) . The parameters $\{\beta_k\}$, σ^2 and Θ must be estimated and in Bayesian kriging we choose an appropriate prior distribution for each of them. From the properties of the multivariate Normal distribution and Bayes' theorem, it can be shown that the

conditional distribution for T given Y is as follows:

$$\begin{aligned}\mathbb{P}(T|Y) &\sim \text{MVN}(\mu_{T|Y}, \Sigma_{T|Y}), \\ \mu_{T|Y} &= \mu_1 + \text{Cov}(T, Y)\text{Var}(Y)^{-1}(Y - \mu_1), \\ \Sigma_{T|Y} &= \text{Var}(T) - \text{Cov}(T, Y)\text{Var}(Y)^{-1}\text{Cov}(Y, T),\end{aligned}$$

and thus we can obtain estimates for the responses T_j , $j = 1, \dots, M$.

Chapter 4

Discrete Initiation Model

As was mentioned previously, damage accumulation is defined to be the initiation and growth of fatigue cracks. In order to model damage accumulation it is necessary to model the initiation of the cracks in the bone cement. As discussed, various models have been proposed for the initiation of these cracks. We now present a model that utilises the spatial information that is available in the data, namely the crack locations (given as x and y coordinates). Local properties of the bone cement such as irregularities in the cement due to pores or air bubbles (unmeasured), or local stresses (measured) have an impact on the initiation of cracks. We propose a spatially discrete model for crack initiation that incorporates both the observed and unobserved factors that influence crack initiation.

4.1 Modelling Approach

As detailed in Chapter 2, the data collected consist of crack locations for each crack in each of the five specimens, together with stress measurements (compression and tension) obtained through a finite element analysis. The crack locations consist of spatial coordinates of both the start and end points of each crack. The stress measurements are identical for the five specimens, as only one set of stress measurements was taken. In this chapter we wish to model the initiation of cracks during the stress

loading. We will only be concerned with those cracks that have formed during the stress-loading (i.e, load-cracks) and not with the cracks which have formed prior to the loading. Also we will only be considering the start locations of the load-cracks. See Figures 4.1 and 4.2 (left hand side) for images of the load-crack start locations in each of the five specimens.

Various models for crack initiation have been proposed, see Section 2.7. We wish to model the initiation of the cracks as a spatial process. Having observed the crack locations (and hence counts of cracks in regions are available) together with estimates of the stress intensities, we would like to make inferences about the underlying process that has given rise to the cracks. In doing so we would like to make use of the spatial information available to model the relationship between stress (both compression and tension), unobserved covariates and crack initiation.

4.1.1 Approaches to Modelling Count Data

An approach when considering data consisting of actual spatial coordinates, such as we have, is to aggregate the data over some grid/partition and then model the resulting count data (Ickstadt and Wolpert (1997)). The grid, often referred to as a “lattice” (Cressie (1993)), denotes a countable collection of (spatial) sites and it is often possible to specify neighbourhood information for the lattice. In disease mapping, where the number of disease cases in each geographical region is of interest, the data are often supplied as count data (Elliott et al. (2000)).

The choice then becomes how to model the count data. One method in modelling the count data is to perform a variance stabilizing transformation and then treat the count data as having a Normal distribution (Cressie (1993)), but as noted in Ickstadt and Wolpert (1997) this Gaussian model does not respect the discrete nature of the count data.

A natural choice when dealing with count data is to use the Poisson distribution. A type of model sometimes used is the log-linear Poisson model. In this case the count data are modelled as Poisson and the logarithms of the intensity can then be

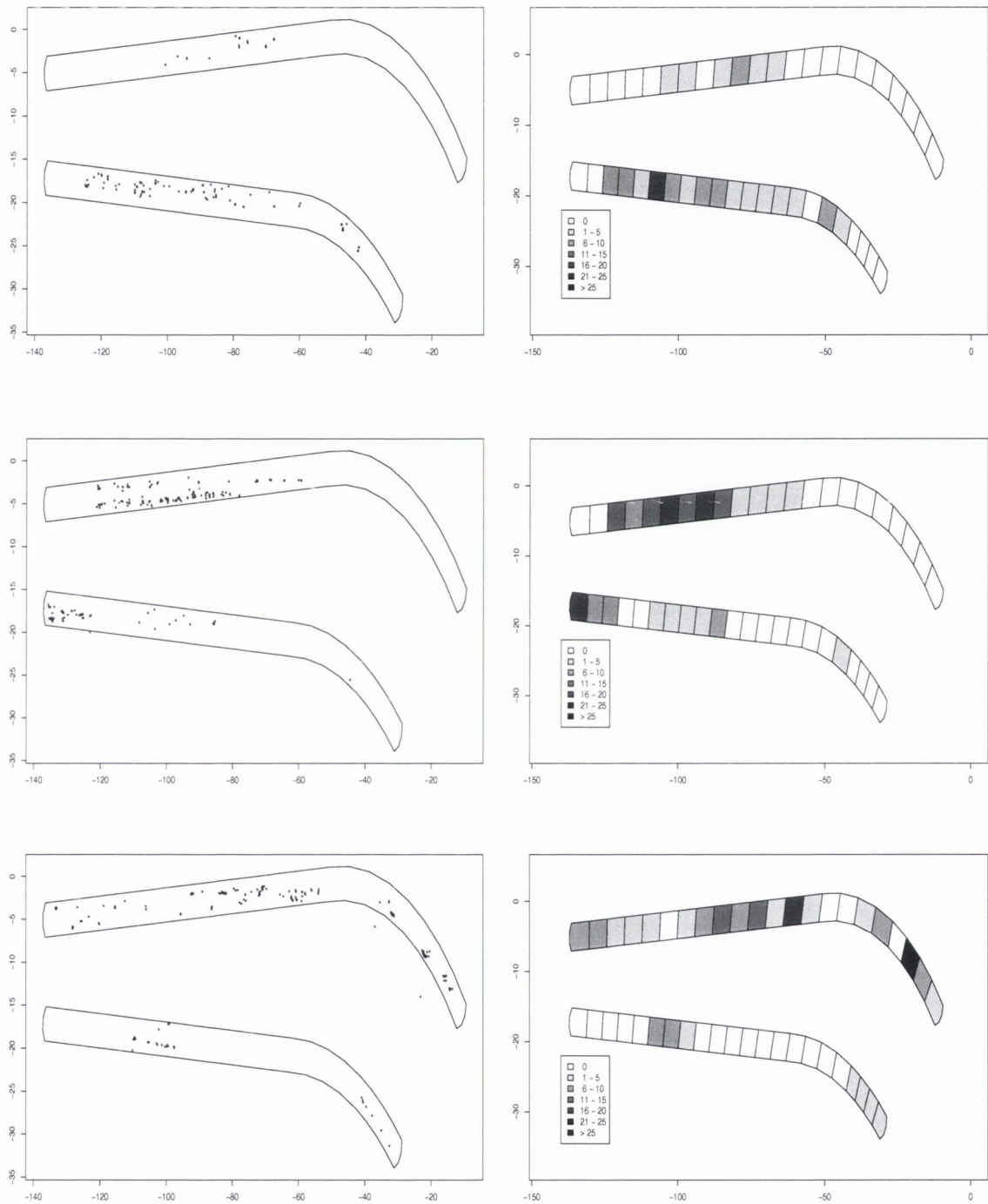


Figure 4.1: Diagrams on the left indicate individual crack locations for specimens 1 to 3 (top to bottom) with corresponding image diagrams on the right of the windows divided into an arbitrary grid of polygons shaded according to the observed number of cracks.

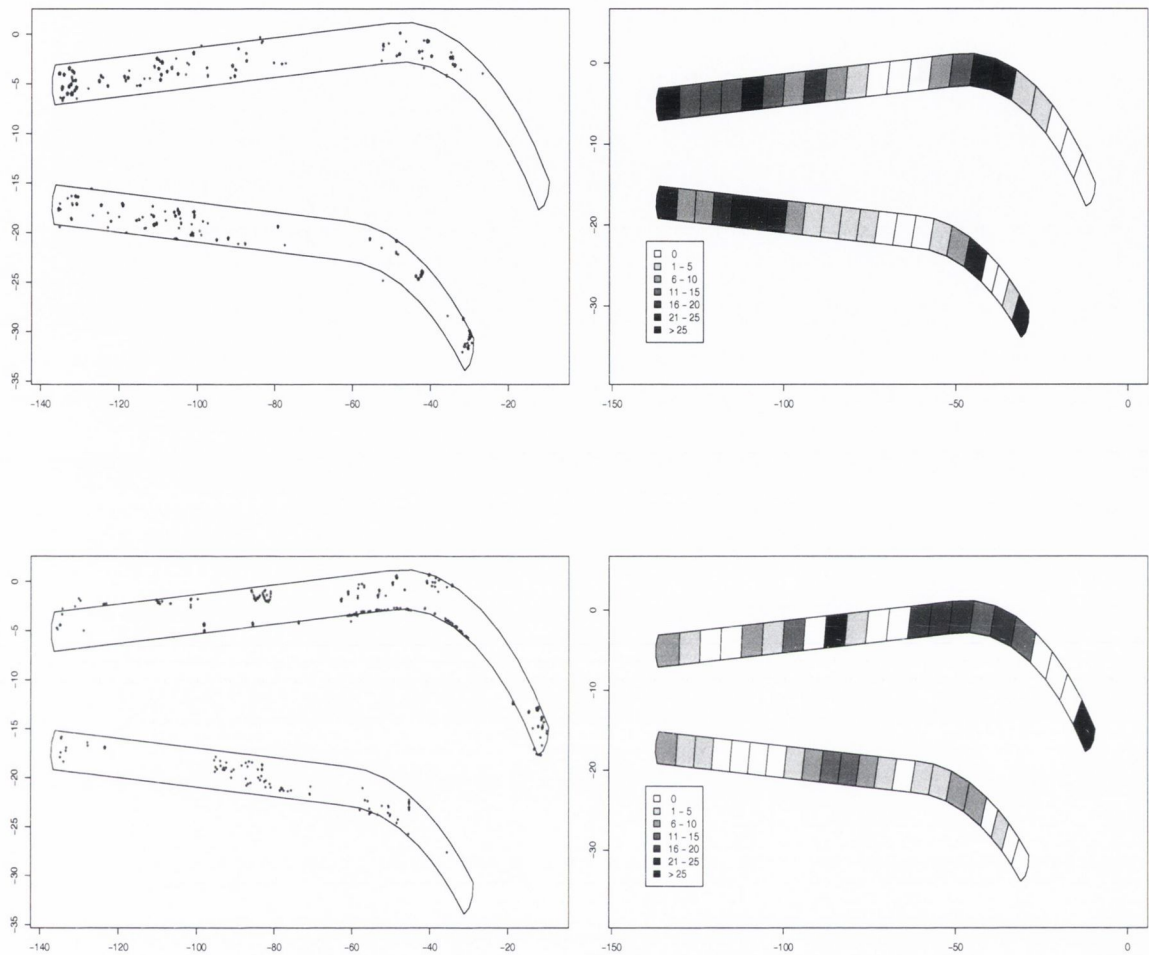


Figure 4.2: Diagrams on the left indicate individual crack locations for specimens 4 and 5 (top and bottom respectively) with corresponding image diagrams on the right of the windows divided into an arbitrary grid of polygons shaded according to the observed number of cracks. (Due to the non-uniformity of the bone strips used in the experimental model described in Section 2.6.1, some cracks appear to be outside of the windows, but are in fact inside.)

modelled with a Gaussian random field. Unfortunately if the level of aggregation is not the desired level and we wish to aggregate the regions or refine the partition the model does not scale so easily. We would expect sums for the intensity if we aggregate regions but instead we get products. Thus the choice of lattice is very important as the analysis would have to be repeated if a new level of aggregation is desired.

4.1.2 Identity-Link Poisson Regression Model

An alternative model for the Poisson random variable is to model it using an identity-link Poisson regression model. As already mentioned, when a logarithmic-link is proposed, attempting to aggregate the partition leads to products for the Poisson means of the new aggregated regions instead of sums, as would be desired. The identity-link does not have this problem as it is consistent under aggregation and refinement of the partition. Poisson regression models with identity link functions have been used in various applications, for example, in spatial epidemiology (Best et al. (2000b)) and in the examination of forest inhomogeneity (Ickstadt and Wolpert (1997)).

Thus we choose a partition of our windows and count the number of cracks in each of the regions of the partition and model the count as a Poisson random variable which in turn is modelled with an identity-link regression model.

The next step is then to consider how to relate the Poisson random variables, one associated with each region, to both the observed and unobserved factors that are believed to have an influence on the Poisson random variables. In our case how to relate the Poisson random variables to stress and any influential unobserved factors.

4.2 Model Specification

To begin we choose an arbitrary partition of both the lateral and medial windows and we introduce some notation and specify the factors which we believe have an influence on the Poisson intensity.

4.2.1 The Partition and the Intensity

We choose to divide the lateral and medial windows into an arbitrary grid/partition consisting of 22 polygons in each window. Figures 4.1 and 4.2 (right hand side) indicate the crack count for this arbitrary grid for each of the specimens. Each polygon is shaded according to the number of cracks observed in the polygon. Figure 4.3 also gives details of the counts for this arbitrary grid.

Let P_{ij} denote polygon j of specimen i , $i = 1, \dots, 5$; $j = 1, \dots, 44$. We denote by $N(P_{ij}) = N_{ij}$ the count of cracks in polygon P_{ij} . We model the crack count in each polygon as having an independent Poisson distribution with some unknown intensity, μ_{ij} . As we are modelling the crack count in a Bayesian setting, the intensity can be considered as a random variable.

Dobson (2002) describes the events of a Poisson process as being related to varying amounts of “exposure” which need to be taken into account when modelling the intensity. Consider the simple example given by Dobson where counts of occupational injuries are being modelled as Poisson distributed; each worker is exposed for the period that they are at work, so the Poisson rate (one-dimensional intensity) may be defined in terms of this time spent at work. In our spatial context this “exposure” may be thought of as the area of the polygons, giving

$$\mathbb{E}(N_{ij}) = \mu_{ij} = A_j \lambda_{ij},$$

where A_j is the area of polygon P_{ij} (note, not all A_j are equal) and λ_{ij} is the unit-area intensity.

The influence that any explanatory variables have on the crack counts N_{ij} is modelled by μ_{ij} through λ_{ij} . This immediately raises the question of what explanatory variables are available in this case?

4.2.2 Explanatory Variables

As well as individual crack locations, the data provided also include a finite element analysis of the stress measurements. Figure 4.4 gives locations and measurements for

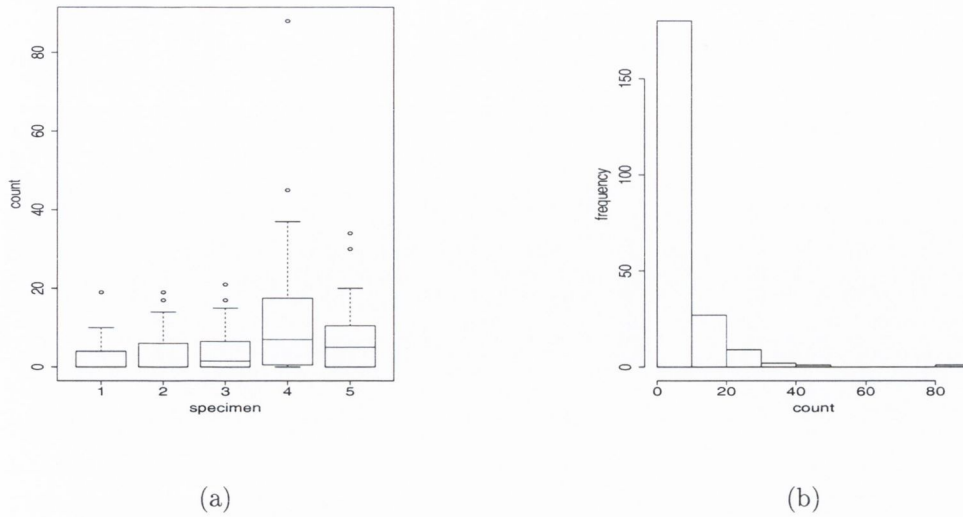


Figure 4.3: (a) shows a boxplot of the count of cracks in the polygons for each of the specimens. (b) shows a histogram of the count of cracks for all specimens.

the finite element stress analysis, (note that positive stress measurements denote tension, negative values indicate compression). Instead of using the stress measurements as presented, we have kriged the stress measurements in order to obtain estimates of the stress at the centroids of each of the polygons. This allows us to relate the count of cracks in a polygon to a single stress measurement at the centroid of the polygon.

In carrying out Bayesian kriging (see Section 3.5) we assume the nugget variance is negligible and so set $\tau^2 = 0$. For each of the given stress measurements S_n at location n , we set $\mu_n = \beta$ and we choose the correlation function $\sum_{nm} = \exp(-\phi d_{nm})$, where d_{nm} is the Euclidean distance between locations n and m . For the unknown parameters β, σ^2 and ϕ we choose Gaussian, Gamma and Uniform priors, respectively. We carry out inference to estimate these parameters and then predict the stress measurements at the centroids of each of the polygons.

See Figure 4.5 for an image detailing the kriged values of the stress. We denote by C_j and T_j the compression and tension respectively at the centroid of polygon P_{ij} for all $i = 1, \dots, 5$. Note that only one of C_j and T_j will be non-zero for a given polygon centroid, as compression and tension cannot both be present at a given location.

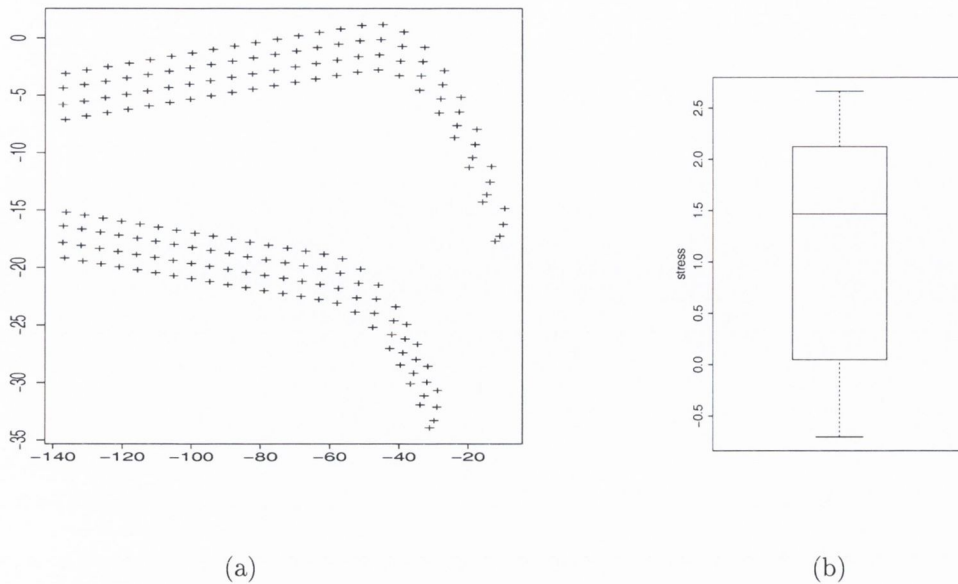


Figure 4.4: (a) indicates the locations at which finite element measurements of stress were calculated. (b) shows the spread of stress intensities that were calculated (measured) in the finite element analysis.

Both compression and tension have an effect on crack initiation and we would like to estimate the effect that each has, see Section 2.4.1.

Another factor that has an impact on the initiation of cracks is the distribution of pores (air bubbles) in the bone cement. As detailed in Section 2.4.2 the mixing of the cement is a very important step during the operation as it is possible for air bubbles to become trapped in the cement while it is being prepared. As also detailed in Section 2.4.2 the pores have an impact on the initiation of the cracks in the cement. In the experiment from which our data come, it was not possible to locate pores within the cement. Thus we do not have any idea as to the distribution of the pores in each of the specimens. We would like to incorporate this important factor in our model for the initiation of cracks and to do this we model the unobserved distribution of pores using hidden or latent spatial variables, which will also model excess variability due to other unobserved factors.

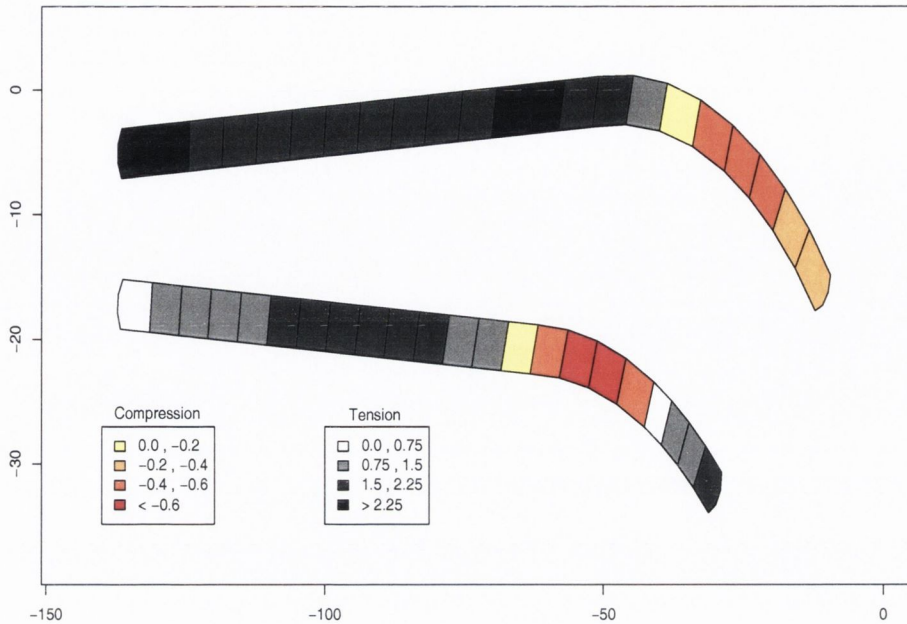


Figure 4.5: Kriged values of compression and tension for each of the polygons.

4.2.3 Poisson Regression Model with Identity Link

We model the dependence of the random unit area intensity λ_{ij} on the explanatory variables (stress, latent) using a Poisson regression model with identity link (Dobson (2002)):

$$\lambda_{ij} = \beta_1 C_j + \beta_2 T_j + \sum_{k=1}^{44} \omega_{jk} \gamma_{ik}, \quad i = 1, \dots, 5; \quad j = 1, \dots, 44, \quad (4.1)$$

where β_1 is the coefficient of compression and β_2 is the coefficient of tension. We choose to model the effect of compression and tension without a specimen effect. The reason for this is that we have only one set of stress measurements for all of the specimens and so we do not expect to be able to model a specimen effect. $\{\gamma_{ij}\}$ is defined to be the set of latent factors with one factor for each polygon. These latent factors represent the effect in polygon P_{ij} of the unobserved spatially distributed factors that have an influence on crack initiation. The amount of influence that these factors have on causing cracks to form in a given polygon is governed by ω_{jk} , a Gaussian kernel

which depends on Euclidean distance, i.e.,

$$\omega_{jk} = \frac{1}{2\pi\rho^2} \exp\left(-\frac{|d_{jk}|^2}{2\rho^2}\right),$$

where d_{jk} is the Euclidean distance from the centroid of polygon P_{ij} to the centroid of polygon P_{ik} . If a polygon is far away from the polygon whose crack count we are modelling then the kernel will be relatively small and so the influence from the latent factor in this polygon will be small. This influence is controlled by the parameter ρ . We make the following assumption: when considering the crack count in a particular polygon, the latent factors associated with the polygons in the other window do not have any influence in causing cracks to form in this polygon. We make this assumption as there is no physical link between the windows in the experimental model, see Figure 2.3(a). Thus, in Equation 4.1 the kernel $\omega_{jk} = 0$ if polygon P_{ik} is not in the same window as polygon P_{ij} .

4.2.4 Prior Information

The parameters $\beta_1, \beta_2, \{\gamma_{ij}\}$, and ρ are all uncertain. β_1 quantifies the influence of compression on cracks forming, β_2 quantifies the influence of tension on the initiation of cracks, and the $\{\gamma_{ij}\}$ quantify the influence of unobserved, spatially varying factors on crack formation. The parameter ρ indicates over what distance the effect of the latent spatial variables is felt, answering the question: Do these unobserved spatially varying factors only have an influence locally or is their influence more far-reaching? All of these parameters are of interest and we would like to estimate each of them. We will make inferences about each of these parameters using Bayesian analysis.

In order to model these parameters using a Bayesian analysis, we must choose prior distributions for each of them. We choose independent prior distributions. For the coefficients of compression and tension we choose independent prior distributions as physically compression and tension will not both be present in a given polygon. For each of $\beta_1, \beta_2, \{\gamma_{ik}\}$ we choose Gamma priors. One reason for choosing Gamma priors is that the mean of the Poisson must be non-negative; another is our belief that

each of these corresponding factors positively influences the formation of cracks. We also have reason to believe from communications with engineers that tension stresses have a greater impact in crack initiation than do compression stresses and our priors should reflect this knowledge. We choose the following priors:

$$\begin{aligned}\pi(\beta_1) &\sim \text{Gamma}(\alpha_1 = 1, b_1 = 0.1), \\ \pi(\beta_2) &\sim \text{Gamma}(\alpha_2 = 3, b_2 = 0.1), \\ \pi(\gamma_{ij}) &\sim \text{Gamma}(\alpha_g = 1, b_g = 0.1), \forall i, j.\end{aligned}$$

We return to the question of inference for ρ in Section 4.3.

4.2.5 Posterior Distribution

The joint posterior distribution is proportional to the product of the joint likelihood and independent priors:

$$\begin{aligned}\mathbb{P}(\beta_1, \beta_2, \{\gamma_{ij}\}, \rho | \{N_{ij}\}) &\propto \mathbb{P}(\{N_{ij}\} | \beta_1, \beta_2, \{\gamma_{ij}\}, \rho) \pi(\beta_1) \pi(\beta_2) \pi(\rho) \prod_{ij} \pi(\gamma_{ij}), \\ &= \prod_{ij} \left\{ \frac{\exp(-\mu_{ij}) (\mu_{ij})^{N_{ij}}}{N_{ij}!} \pi(\gamma_{ij}) \right\} \pi(\beta_1) \pi(\beta_2) \pi(\rho).\end{aligned}$$

In order to make inferences about the unknown parameters of interest we make use of the MCMC techniques that are available, see Section 3.3. By using the technique of data augmentation, see Section 3.4, the full conditional distributions for β_1, β_2 , and $\{\gamma_{ij}\}$ are of known form, (they have Gamma distributions). The choice of prior distributions (Gamma) for each of these parameters has also made this possible as we are exploiting the conjugacy of the prior distributions. In augmenting the data we introduce a set of new random variables, $\{N_{ijk}\}$, by breaking up the count N_{ij} of cracks in each polygon into a sum of counts, where each of these new counts represents the number of cracks that are attributable either to compression, tension or one of the latent factors. See Appendix A.1.1 for full details.

With the inclusion of this data augmentation step the full conditional distributions for β_1, β_2 , and $\{\gamma_{ik}\}$ are available in known form. This makes the use of the Gibbs

sampler, see Section 3.3.5, a natural choice of MCMC technique to use in order to draw samples from the full posterior distribution. It can easily be shown (see Appendix A.1.2) that the full conditional distributions are as follows:

$$\begin{aligned}\mathbb{P}(\beta_1|\beta_2, \{\gamma_{ik}\}, \rho) &\sim \text{Gamma}\left(\sum_{ij} N_{ij1} + \alpha_1, 5 \sum_j C_j A_j + b_1\right); \\ \mathbb{P}(\beta_2|\beta_1, \{\gamma_{ik}\}, \rho) &\sim \text{Gamma}\left(\sum_{ij} N_{ij2} + \alpha_2, 5 \sum_j T_j A_j + b_2\right); \\ \mathbb{P}(\gamma_{ik}|\beta_1, \beta_2, \rho) &\sim \text{Gamma}\left(\sum_j N_{ijk+2} + \alpha_g, \sum_j \omega_{jk} A_j + b_g\right).\end{aligned}$$

See Appendix A.1.1 for definitions of N_{ij} .

4.3 Investigation of the Kernel Parameter ρ

The Gaussian kernel, $\omega_{jk} = \exp\{-|d_{jk}|^2/(2\rho^2)\}/(2\pi\rho^2)$, governs the influence on the crack count in polygon P_{ij} arising from the latent variable γ_{ik} in polygon P_{ik} . The parameter $\rho > 0$ determines how rapidly this influence declines with increasing distance from the centre of polygon P_{ij} . As ρ gets larger, the kernel ω_{jk} becomes flatter, as ρ becomes smaller the kernel becomes more peaked and the latent variables associated with far away (relative to ρ) polygons have less of an influence on the crack count in polygon P_{ij} . See Figure 4.6.

4.3.1 Other Applications Using a Gaussian Kernel

Best et al. (2000b) used this type of kernel in their identity link spatial regression model which related the prevalence of respiratory illness in children in Huddersfield, UK, to NO_2 concentrations and unmeasured factors. The authors treated ρ as fixed or certain. Several different fixed values for ρ were considered and the value for ρ that was chosen was the one that gave results that were most consistent with the data. Best et al. (2000a), again examining the prevalence of respiratory illness in children using an identity link regression model, chose a Lognormal prior for ρ . The

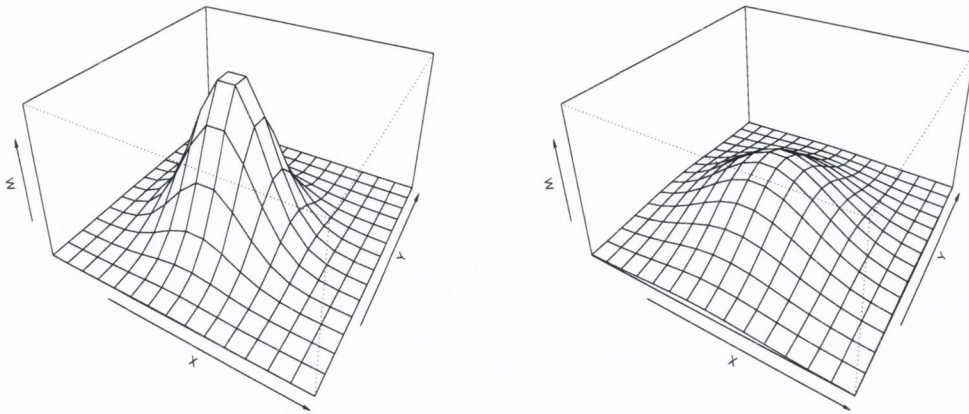


Figure 4.6: Gaussian kernels for two values of ρ . On the left $\rho = 2$ and on the right $\rho = 3$. The x and y ranges are $(1, 15)$ for both plots.

mean and variance of this Lognormal prior reflected the fact that spatial effects on a small scale would not be detectable and those on a much larger scale would appear as large-scale trends. Wolpert and Ickstadt (1998a) analyse the density and spatial correlation of hickory trees and they also use a Gaussian kernel in their analysis, again with Lognormal prior with appropriate mean and variance parameters.

4.3.2 Exploratory Analysis for ρ

As an initial examination of the parameter ρ we look at the log-likelihood function for each specimen, for $i = 1, \dots, 5$

$$\mathbb{P}(\{N_{ij}\} | \beta_1, \beta_2, \{\gamma_{ij}\}, \rho_m) = \sum_j \{-\mu_{ij} + N_{ij} \log(\mu_{ij}) - \log(N_{ij}!)\},$$

where

$$\begin{aligned} \mu_{ij} &= (\beta_1 C_j + \beta_2 T_j + \sum_k \omega_{jk} \gamma_{ik}) A_j, \\ \omega_{jk} &= \frac{1}{2\pi\rho_m^2} \exp\left\{-\frac{|d_{jk}|^2}{2\rho_m^2}\right\}, \end{aligned}$$

for the range of ρ values $0.01 = \rho_1 < \rho_2 < \dots < \rho_m < \dots < \rho_M = 20$. This was done as follows. For each ρ_m we calculated

$$\hat{\mathbb{P}}(\{N_{ij}\}|\beta_1, \beta_2, \{\gamma_{ij}\}, \rho_m) = \frac{1}{T} \sum_{t=1}^T \mathbb{P}(\{N_{ij}\}|\beta_1^{(t)}, \beta_2^{(t)}, \{\gamma_{ij}^{(t)}\}),$$

where $\beta_1^{(t)}$, $\beta_2^{(t)}$, and $\{\gamma_{ij}^{(t)}\}$ are the parameter estimates obtained at each iteration of the MCMC algorithm when ρ is fixed at the value ρ_m . Thus $\hat{\mathbb{P}}(\{N_{ij}\}|\beta_1, \beta_2, \{\gamma_{ij}\}, \rho_m)$ is an estimate of $\mathbb{E}[\mathbb{P}(\{N_{ij}\}|\beta_1, \beta_2, \{\gamma_{ij}\})]$ with respect to the posterior distribution $\mathbb{P}(\beta_1, \beta_2, \{\gamma_{ij}\}|\rho, \{N_{ij}\})$. For each ρ_m we then plot $(\rho_m, \hat{\mathbb{P}}(\{N_{ij}\}|\beta_1, \beta_2, \{\gamma_{ij}\}, \rho_m))$ as can be seen in Figure 4.7.

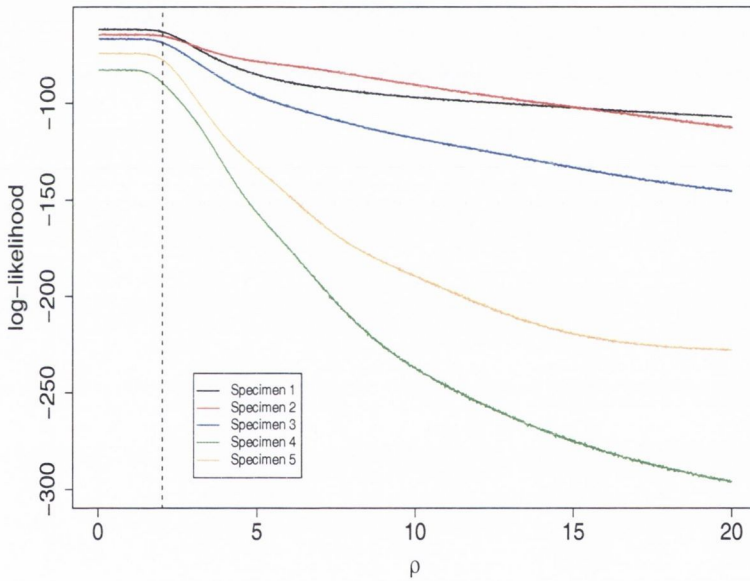


Figure 4.7: Estimated log-likelihood, $\hat{\mathbb{P}}(\{N_{ij}\}|\beta_1, \beta_2, \{\gamma_{ij}\}, \rho_m)$ calculated for $\rho_m \in [0.01, 20]$ for each of the five specimens. The log-likelihood was estimated using sample values for β_1, β_2 , and $\{\gamma_{ij}\}$ from the posterior distribution obtained from the MCMC program. The dashed black line is at $\rho = 2$.

The log-likelihood was calculated by running the MCMC algorithm, Section B.1, for each of the specimens individually, with ρ having a fixed value, for an appropriate burn-in period. One thousand samples were then taken for each of β_1, β_2 and $\{\gamma_{ij}\}$

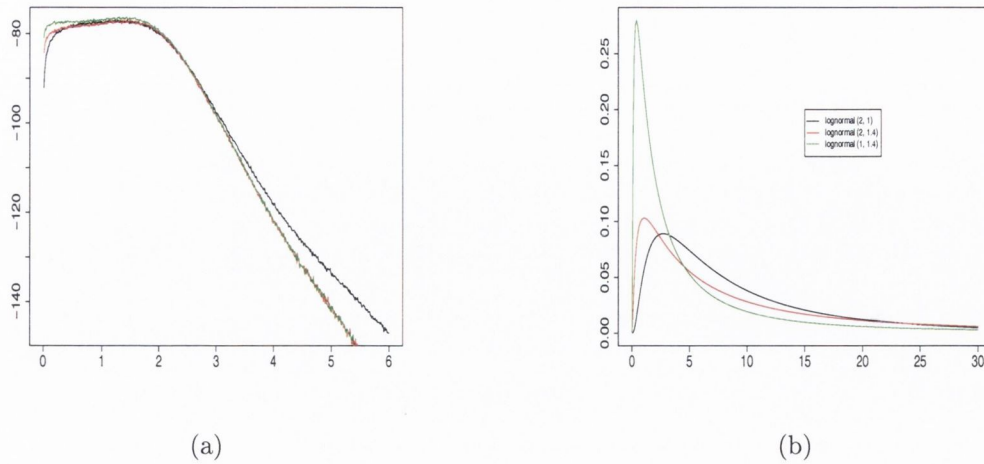


Figure 4.8: (a) shows the logarithm of the likelihood times different priors for Specimen 5. (b) shows Lognormal priors for different parameters, these are the corresponding priors used in Figure (a).

and averaged. The plots for each of the five specimens clearly show that values less than approximately 2 are to be favoured for ρ . As ρ becomes larger, i.e., the kernel becomes more diffuse, the log-likelihood decreases. This is as we would expect in light of engineering intuition that the influence of the latent factors is of a localised nature. Based on the information from the likelihood and from the range over which it is believed the latent variables have an influence, it would be possible to treat ρ as fixed and carry out inference for the other parameters.

We also examined the effect of including a Lognormal prior for ρ . Figure 4.8(a) shows the logarithm of the likelihood times a Lognormal prior for ρ with different mean and variance parameters for the prior, Figure 4.8(b) shows the Lognormal priors used. The Lognormal prior has the effect of making small values for ρ , ($\rho < 2$), i.e., kernels that are peaked, less likely, meaning the latent influence is not so localised. The prior parameters should reflect the beliefs as to the range over which interactions from latent factors are to be expected. For a given value of ρ , most of the Gaussian kernel will lie within a radius of 2ρ of the centroid of the polygon. A polygon is

approximately 6 units across. We would like a prior for ρ to allow influence outside a given polygon and so the prior mean for ρ should reflect this.

4.3.3 Simulation Study

In order to investigate the identifiability of the parameters, in particular ρ , we carried out a simulation study. Fixing the parameters at known values we simulated count data from a Poisson distribution, using the statistical package R, for 44 polygons of the same area as each of the polygons in the experimental model. Inputting the resulting simulated count data, we used the MCMC algorithm in order to obtain estimates of our known parameters. We choose a Lognormal prior distribution for ρ with parameters: $\mu = 1$ and $\sigma = 1.4$, giving a prior mean of ≈ 7.2 . As was noted by Best et al. (2000b), the likelihood function for ρ is complicated and doesn't facilitate Gibbs sampling. Instead we use a Gaussian random walk. The full MCMC algorithm with details of the random walk step can be found in Section B.1. The data were simulated with the following values: $\beta_1 = 0.01$, $\beta_2 = 0.03$ and $\rho = 3$. See Figure 4.9 for image plots of the stresses, γ 's, simulated counts, and the resulting γ estimates. Table 4.1 presents quantiles of the parameters: β_1, β_2 and ρ . From these results it appears that the parameters are reasonably well estimated.

Parameter	Quantiles		
	5%	50%	95 %
β_1	0.001	0.007	0.025
β_2	0.009	0.02	0.033
ρ	2.68	3.14	3.48

Table 4.1: Quantiles for β_1, β_2 and ρ for the simulated data.

4.4 MCMC Algorithm

We now present a brief outline of the MCMC algorithm for obtaining samples from the posterior distribution for each of the parameters: $\beta_1, \beta_2, \{\gamma_{ij}\}$, and ρ . A more detailed algorithm is contained in Appendix B.1.

Algorithm

1. Initialise $\beta_1, \beta_2, \{\gamma_{ij}\}, \rho$, and set the iteration counter $r = 0$.
2. Calculate the Gaussian kernel $\omega_{jk}^{(r)}$ for each pair of polygons P_{ij} and P_{ik} .
3. Simulate $N_{ijk}^{(r)}$ for all i, j, k .
4. Using Gibbs sampling simulate $\beta_1^{(r)}, \beta_2^{(r)}$ and $\{\gamma_{ij}^{(r)}\}$.
5. Propose ρ_{test} from $\text{Normal}(\rho^{(r-1)}, \sigma)$ and accept ρ_{test} with probability α , otherwise $\rho^{(r)} = \rho^{(r-1)}$.
6. Set $r = r + 1$ and repeat Step 2 through 5.

4.5 Results

4.5.1 Running the MCMC Algorithm

We now present the estimates of the β parameters and the parameter ρ based on data for the five specimens. See Table 4.2 for quantiles and kernel density estimates for each of the parameters. The estimates for the parameters are based on sample values obtained from the posterior distribution by running the MCMC algorithm detailed in Section B.1. We computed 15,000 iterations of the program attributing the first 3,000 to burn-in. We examined each of the chains visually in order to inspect for lack of convergence. The chains appeared to have converged. We also ran multiple independent chains from various starting points. No evidence for lack of convergence

was found. Trace plots of some parameters may be found in Appendix B.4, Figures B.1 and B.2.

4.5.2 Estimates of the γ 's

We present the estimates for the latent parameters in the form of image plots. For each polygon we present the posterior median value of $A_j \sum_k \omega_{jk} \gamma_{ik}$, obtained from the MCMC algorithm. These plots show an estimate of the latent contribution to the intensity. See Figures 4.10 and 4.11. These may be compared with the median intensity for each of the polygons presented in Figures 4.15 and 4.16.

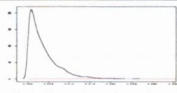
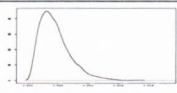
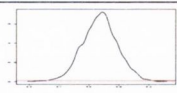
Parameter	Quantiles			KDE's and Priors
	5%	50%	95 %	
β_1	$1.9e^{-4}$	$2.5e^{-3}$	$1.1e^{-2}$	
β_2	$5.1e^{-4}$	$1.6e^{-3}$	$3.8e^{-3}$	
ρ	2.14	2.24	2.33	

Table 4.2: Quantiles and plots of kernel density estimates and priors (red) for the parameters β_1 , β_2 and ρ based on data from all five specimens.

4.5.3 Posterior Predictive Distribution for Counts

We calculate the posterior predictive distribution for the count of cracks in each polygon using the Rao-Blackwellized estimator (Section 3.1.5):

$$\hat{\mathbb{P}}(N_{ij}|\{N_{ij}\}) = \frac{1}{R} \sum_{r=1}^R \mathbb{P}(N_{ij}|\{N_{ij}\}, \beta_1^{(r)}, \beta_2^{(r)}, \rho^{(r)}, \{\gamma_{ij}^{(r)}\}), \quad (4.2)$$

where R is the total number of iterations after burn-in. This was carried out as follows

$$\mathbb{P}(N_{ij} = n | \dots) = \frac{\exp(-\mu_{ij}^{(r)}) (\mu_{ij}^{(r)})^n}{n!} = f_{rn}, \quad (4.3)$$

and the estimator is given by the following:

$$\hat{\mathbb{P}}(N_{ij} | \{N_{ij}\}) = \frac{1}{R} \sum_{r=1}^R f_{rn} = \bar{f}_n, \quad n = 0, 1, \dots$$

We then calculate the cumulative sum of (\bar{f}_n) and obtain 95% quantiles for the predicted counts. This was done for the count in each polygon of each specimen. In Figure 4.12 we show for each of the polygons of Specimen 3 the actual count and the median posterior predicted count (and 95% quantiles), based on this estimate.

4.5.4 Zero-Inflated Poisson Distribution

One point to note when examining Figure 4.12 is that the zero counts appear not to be so well modelled. The overabundance of observed zero counts could be modelled by treating the zero counts differently from the non-zero counts. One way of doing this is to consider a zero-inflated Poisson Distribution (Ridout et al. (1998)). N has a zero-inflated Poisson (ZIP) distribution if

$$\mathbb{P}(N = n) = \begin{cases} \pi_0 + (1 - \pi_0) \exp(-\mu), & n = 0; \\ (1 - \pi_0) \frac{\exp(-\mu) \mu^n}{n!}, & n > 0, \end{cases}$$

where π_0 is the proportion of zero counts, $0 \leq \pi_0 < 1$. For the ZIP distribution

$$\mathbb{E}(N) = (1 - \pi_0)\mu;$$

$$\text{Var}(N) = (1 - \pi_0)\mu(1 + \pi_0\mu).$$

Thus the ZIP distribution has a variance that is greater than its mean, allowing for overdispersion.

We re-calculate the posterior predictive for the count of cracks in each polygon again using the Rao-Blackwellized estimator, Equation 4.2 and replace Equation 4.3 with the ZIP distribution, where π_0 is the proportion of polygons having zero count.

For each of the polygons of Specimen 3 we present the actual count and the median posterior predicted count (and 95% quantiles), based on this estimate obtained using the ZIP distribution, see Figure 4.13. It would appear from this figure that the zero counts are better modelled using this distribution.

4.5.5 Cross-Validation Predictive Density

We will carry out a cross-validation analysis by omitting the count, for each polygon in turn, and examining the resulting predictive densities. It is not possible to omit a full specimen from the analysis as the latent factors, the γ_{ij} 's are specimen specific. For our purposes the set of cross-validation densities is given by $\{\mathbb{P}(N_{ij}|\{N_{-ij}\})\}$ where $\{N_{-ij}\}$ denotes all counts excepts the count N_{ij} for polygon P_{ij} . The density $\mathbb{P}(N_{ij}|\{N_{-ij}\})$ gives an indication of what values of N_{ij} are likely when we fit the model but leave out the count N_{ij} . We then compare the true N_{ij} with this density and see how likely it is under the model we have chosen. More details of the method can be found in Gilks et al. (1996).

We carry out this cross-validation in the following way. For specimen i we omit the count for polygon j and input all other data into the MCMC algorithm. All parameters β_1, β_2, ρ and $\{\gamma_{ij}\}$ are estimated as usual. At each iteration m of the MCMC algorithm a count $N_{ij}^{(m)}$ is simulated from a Poisson distribution where the parameter of the distribution is given by $\mu_{ij}^{(m)} = (\beta_1^{(m-1)}C_j + \beta_2^{(m-1)}T_j + \sum_k \omega_{jk}\gamma_{ik}^{(m-1)})A_j$.

For N_{ij} we then calculate the posterior predictive distribution as follows:

$$\mathbb{P}(N_{ij}|\{N_{-ij}\}) = \int \mathbb{P}(N_{ij}|\theta, \{N_{-ij}\})\mathbb{P}(\theta|\{N_{-ij}\})d\theta,$$

where $\theta = \beta_1, \beta_2, \rho, \{\gamma_{ij}\}$. We again use a Rao-Blackwellized estimate:

$$\hat{\mathbb{P}}(N_{ij}|\{N_{-ij}\}) = \frac{1}{M} \sum_{m=1}^M \mathbb{P}(N_{ij}|\beta_1^{(m)}, \beta_2^{(m)}, \rho^{(m)}, \{\gamma_{ij}^{(m)}\}),$$

where M is the total number of iterations after burn-in.

The results of this analysis are presented for Specimen 3 in Figure 4.14. Here we have omitted the count for each polygon in turn and predicted the count for

this polygon. As can be seen from the figure, all true counts, except one, lie within the 95% predicted intervals. This would suggest that the model is an adequate one. Another indication of the adequacy of the model is given by calculating the percentage of counts that fall into the 50% equal-tailed predictive intervals. This percentage is 47.7%, which suggests that the interval lengths are of the right size. We would expect with a reasonably well-fitting model, that approximately 50% of the observed data would lie in the predictive intervals.

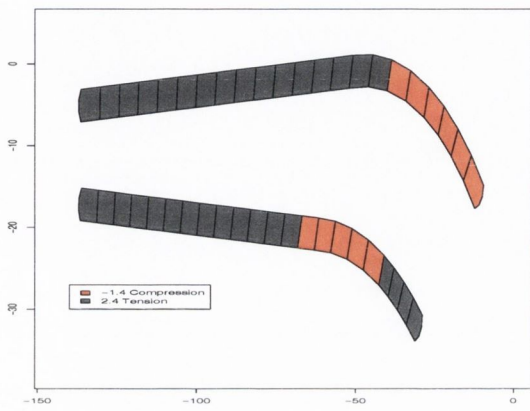
4.6 Conclusions

In this chapter we have presented a spatial regression based approach to modelling the influence that both measured (stress) and unmeasured (latent) factors have in causing cracks to initiate in the bone cement during stress loading. One of the most important aspects of the model is the detection of latent spatial factors and the estimation of the distance over which these factors appear to have an influence. We present an in-depth examination of the variance parameter ρ^2 of the Gaussian kernel, showing through a simulation study that it is possible with reasonable accuracy to estimate this parameter.

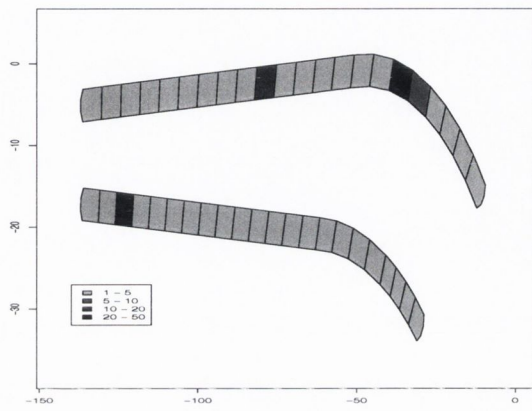
The estimates that we obtain for ρ suggest that the latent random effects have a short-range influence and this finding agrees with the literature. The partition size that we have chosen may be too large for us to determine if the influence is of a shorter range. A refinement of the partition may be considered, i.e., refining the areas of the polygons upon which the latent spatial factors are defined. The choice of refinement may be difficult, each time we refine the partition we may believe that a further refinement is desirable. The ultimate refinement is to treat the latent spatial effects as a continuous random field, as we do in Chapter 5.

Using a finite partition of the area has advantages, namely that in future experiments it would be possible to apply this model to data where counts of cracks have been taken as opposed to the more time consuming task of locating each crack and

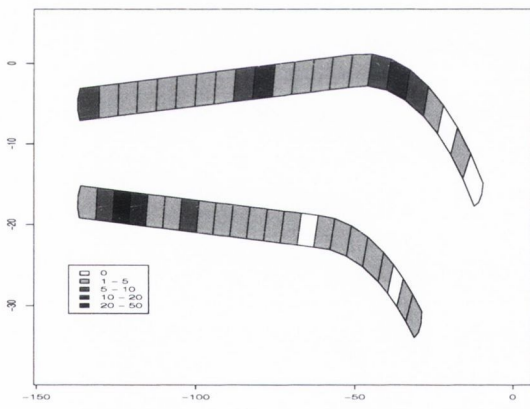
obtaining its coordinates.



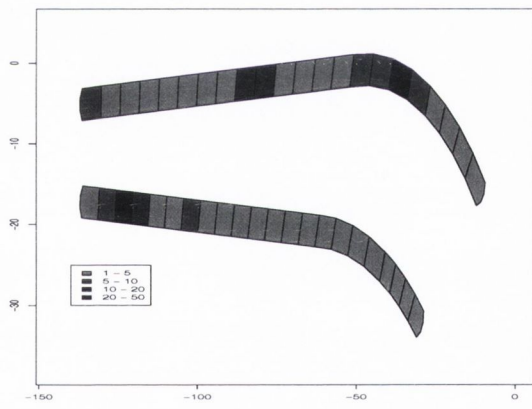
(a) Stress



(b) γ 's

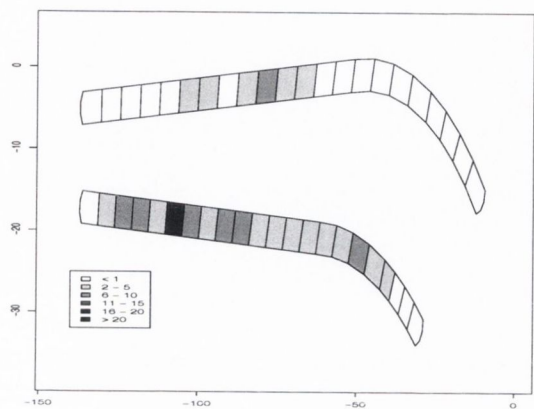


(c) Simulated Counts

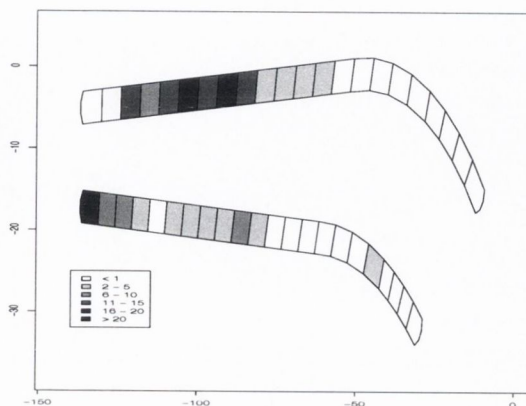


(d) Median Estimates of γ 's

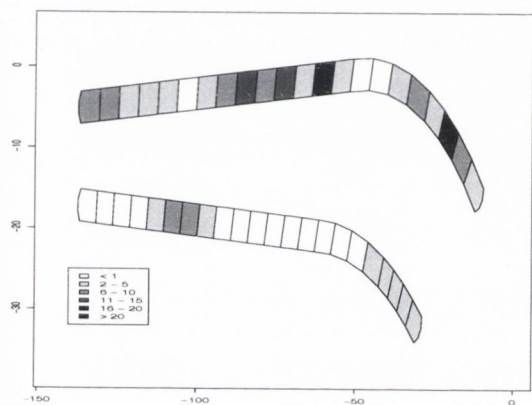
Figure 4.9: Image plots for the simulation study, showing (a) stress, (b) γ 's, (c) simulated Poisson counts and (d) estimated γ 's.



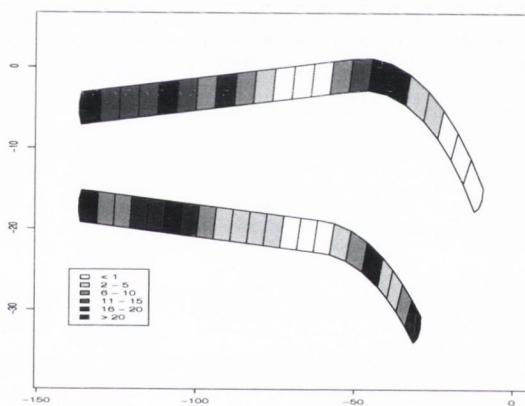
(a) Specimen 1



(b) Specimen 2

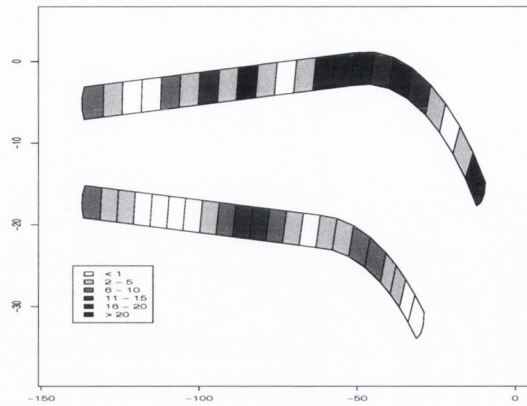


(c) Specimen 3



(d) Specimen 4

Figure 4.10: The posterior median estimates of the latent contribution, $A_j \sum_k \omega_{jk} \gamma_{ik}$ for each polygon, (Specimens 1 to 4).



(a) Specimen 5

Figure 4.11: The posterior median estimates of the latent contribution, $A_j \sum_k \omega_{jk} \gamma_{ik}$ for each polygon of Specimen 5.

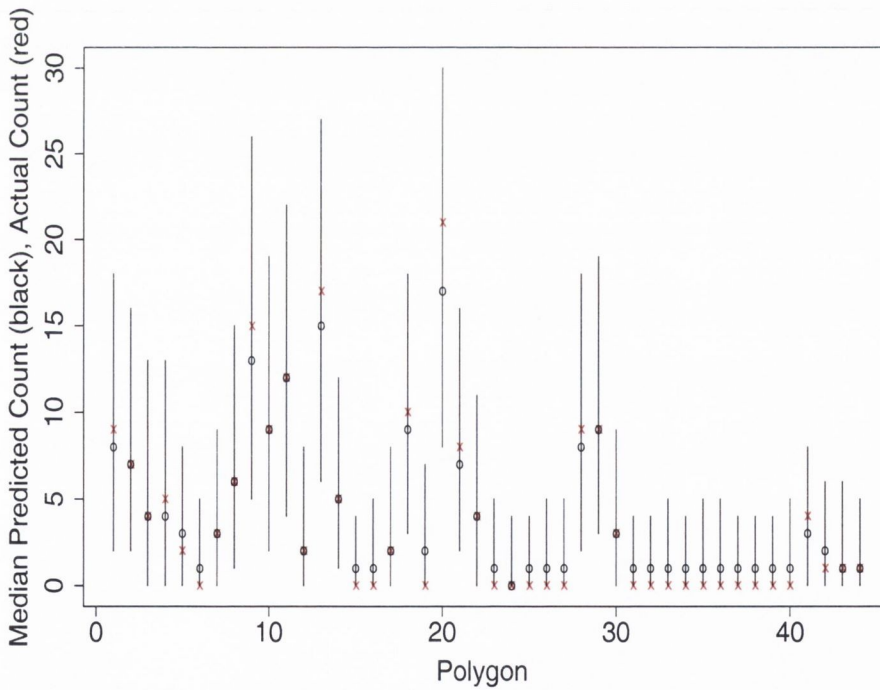


Figure 4.12: For each polygon (x-axis) of Specimen 3 we show the actual count (red star), and the median posterior predicted count (black circle), together with 95% quantiles for the predicted counts.

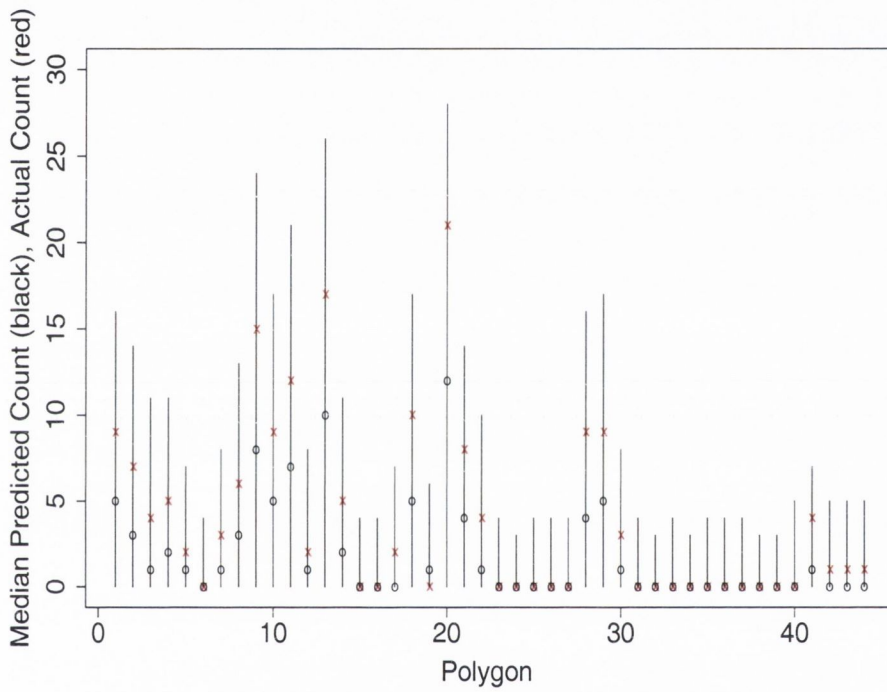


Figure 4.13: For each polygon (x-axis) of Specimen 3 we show the actual count (red star), and the median posterior predicted count (black circle), together with 95% quantiles for the predicted counts, based on the ZIP distribution.

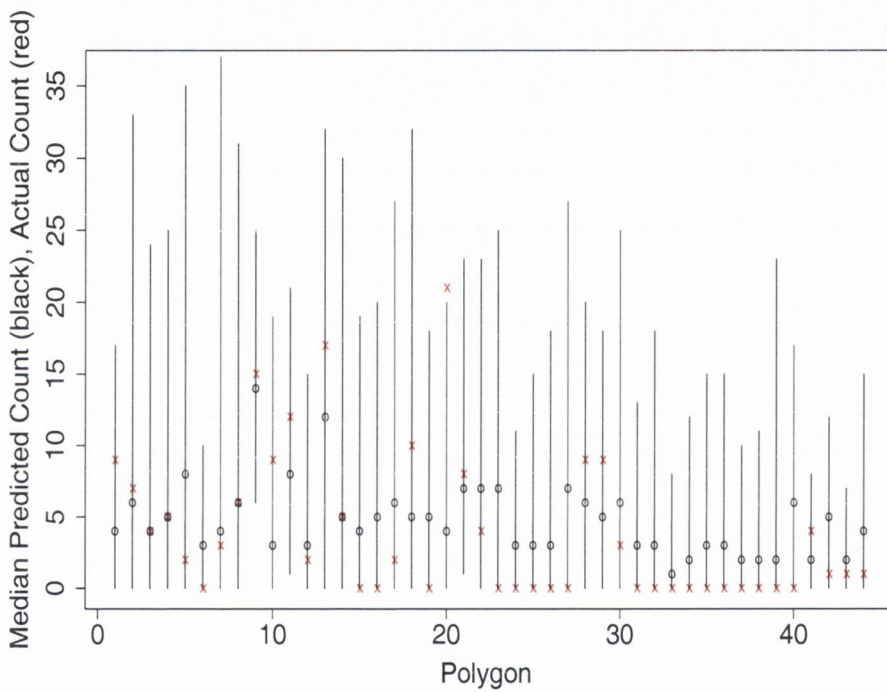
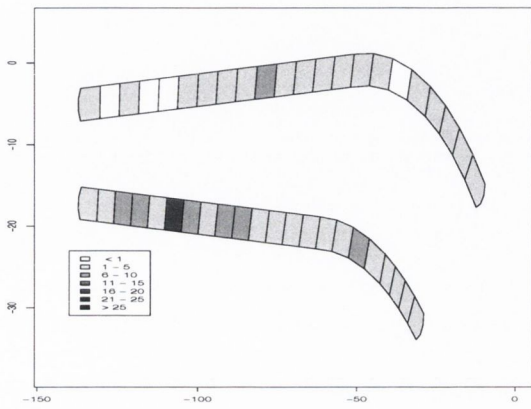
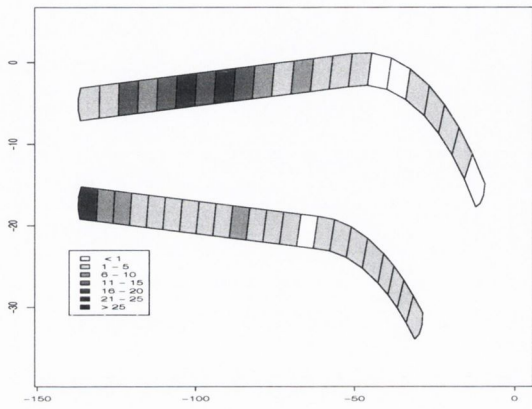


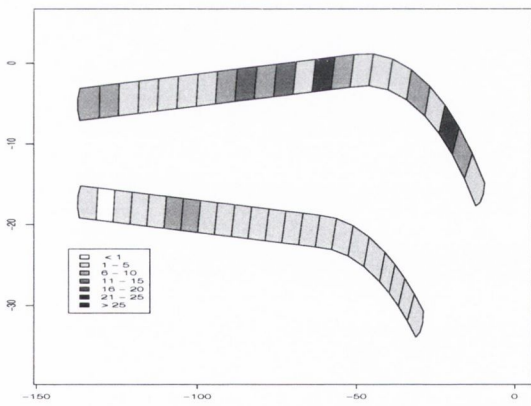
Figure 4.14: For each polygon (x-axis) of Specimen 3 we show the actual count (red star), and the median posterior predicted count (black circle), together with 95% quantiles for the predicted counts, based on carrying out the analysis with the count for the relevant polygon omitted.



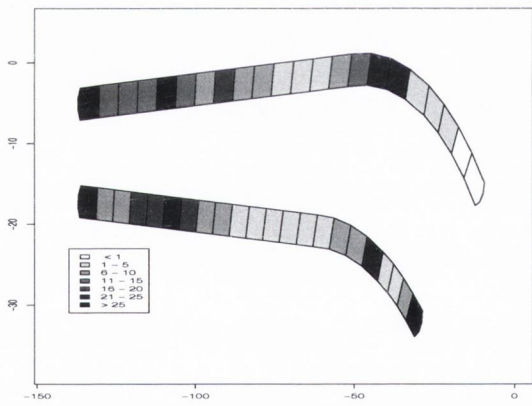
(a) Specimen 1



(b) Specimen 2

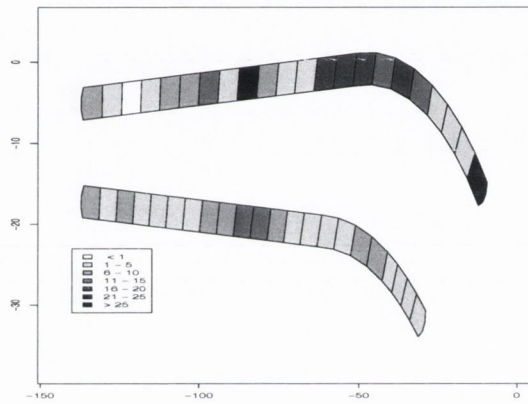


(c) Specimen 3



(d) Specimen 4

Figure 4.15: Posterior medians of λ_{ij} 's for Specimens 1 to 4.



(a) Specimen 5

Figure 4.16: Posterior medians of λ_{ij} 's for Specimen 5

Chapter 5

Continuous Initiation Model

We propose a spatial model for the initiation of cracks in the bone cement, this time using a continuous spatial field. The discrete model presented in Chapter 4 necessitated the choice of an arbitrary grid and the aggregation of the data in order to form counts of cracks in regions. This model allows the crack locations to be modelled without having to aggregate the data. This model also incorporates the observed (stress) and unobserved (latent) spatial factors which influence the formation of cracks in the bone cement again using an identity-link Poisson regression model. The latent spatial factors are modelled using a Gamma random field. Similar models have been used in an epidemiological study (Best et al. (2000a)) and in the modelling of origin/destination trip data (Ickstadt and Wolpert (1999)) which are based on Bayesian hierarchical point process models which were developed by Wolpert and Ickstadt (1998a).

5.1 Poisson Random Field

5.1.1 Marked Poisson Process

Consider again the load-crack locations. This time, instead of creating a discrete lattice or grid of polygons and counting the number of cracks in each polygon, we look

at the coordinates of the start locations of the cracks, i.e., the actual measurements that were presented in the data. We denote by l_{ij} the spatial coordinates (location) of crack j of specimen i . Let us consider what we mean by a spatial point process. See Cox and Isham (1980), Cressie (1993) and Diggle (2003) for a detailed introduction to spatial point processes.

Definition 5.1 *A spatial point process is a stochastic mechanism which generates a countable set of events in Euclidean space.*

A particular type of point process is the Poisson process, see Kingman (1993).

Definition 5.2 *A Poisson process on \mathbb{R}^2 is a random countable subset S of \mathbb{R}^2 , such that*

1. *for any disjoint measurable subsets A_1, A_2, \dots, A_n of \mathbb{R}^2 , the random variables $N(A_1), N(A_2), \dots, N(A_n)$ are independent;*
2. *$N(A)$ is Poisson distributed with mean $\mu(A)$, $0 \leq \mu(A) \leq \infty$, i.e.,*

$$\mathbb{P}(N(A) = n) = \frac{e^{-\mu(A)} \mu(A)^n}{n!}, \quad n = 0, 1, \dots$$

where $N(A) = \#\{S \cap A\}$, the measurable sets are the Borel sets, and

$$\mu(A) = \int_A \lambda(x) dx, \quad x \in \mathbb{R}^2,$$

where $\lambda(x)$ is a non-negative valued function called the intensity function.

If $\lambda(x)$ is constant, then the process is referred to as a homogeneous or uniform Poisson process, otherwise the process is termed an inhomogeneous Poisson process. Note that the intensity function is the two-dimensional analogue of the rate function of the one-dimensional Poisson process.

The set of crack locations $\{l_{ij}\}$ can be thought of as a random countable subset of some space $\mathcal{L} \subset \mathbb{R}^2$. In particular we can model this set of crack locations as a Poisson process L on \mathcal{L} , i.e., for any disjoint measurable subsets A_1, A_2, \dots, A_n of \mathcal{L} , the random variables $N(A_1), N(A_2), \dots, N(A_n)$ are independent and Poisson distributed.

For each crack location, we now obtain, through kriging, the stress value at that location and denote this stress value by either $C(l_{ij}) = C_{ij}$, if it is a compression stress, or $T(l_{ij}) = T_{ij}$ if it is a tension stress. Note, as in the case where we obtained through kriging the stress values at the centroids of the polygons, only one of either compression or tension can be present at a single location, not both. For each crack location l_{ij} we can consider the attribute vector a_{ij} , where a_{ij} is defined to be either of the form $(C_{ij}, 0)$ or $(0, T_{ij})$, depending on whether there is a compression or tension value at the crack location l_{ij} . In a similar way as we did with the set of crack locations we can consider the set of attribute vectors $\{a_{ij}\}$ as lying in some space $\mathcal{A} \subset \mathbb{R}^2$. We would like to combine both the crack locations and the attribute vectors in a model. To do so we define a particular type of point process, namely a marked point process.

Definition 5.3 *A marked point process is a point process in which a real-valued random variable, or vector of random variables, called a mark, is attached to each point (Cox and Isham (1980)).*

Trivially a marked Poisson process is a marked point process where the underlying process is Poisson. See also Kingman (1993) for more details, in particular on marked Poisson processes.

Thus we have associated a vector of random variables (attribute vector), taking values in some space $\mathcal{A} \subset \mathbb{R}^2$, with each point of the random set $\{l_{ij}\}$, i.e. with each point of the Poisson process L , hence we have defined a marked Poisson process.

5.1.2 Poisson Process on the Product Space

Consider the product space $\mathcal{X} = \mathcal{L} \times \mathcal{A}$, the pair $x = (l, a)$, $x \in \mathcal{X}$, $l \in \mathcal{L}$, $a \in \mathcal{A}$ can be regarded as a random point in this product space \mathcal{X} and the set of points $\{x = (l, a) : l \in L\}$ forms a random countable subset of $\mathcal{L} \times \mathcal{A}$. A fundamental result is that this set of coordinates $\{x\}$ of marked points in the product space is a Poisson process. See Kingman (1993), pg. 55 for a detailed proof. Thus we have a spatial

Poisson process

$$N(dx) \sim \text{Poisson}(\Lambda(dx)), \quad (5.1)$$

defined on the product space \mathcal{X} . $\Lambda(dx)$ is an uncertain and inhomogeneous intensity measure, making $N(dx)$ a doubly-stochastic Poisson process or Cox process,

Definition 5.4 *A doubly-stochastic spatial Poisson process or spatial Cox process is a stochastic process in which the intensity is replaced by a random process $\Lambda(x)$ defined in \mathbb{R}^n , where, conditional on $\Lambda(x)$ the stochastic process is an inhomogeneous spatial Poisson process, (Cox and Isham (1980), Kingman (1993)).*

$\Lambda(dx)$ can also be referred to as a random field (Cox and Isham 1980, pg. 147).

5.1.3 Intensity Measure

The intensity measure $\Lambda(dx)$ can be modelled as a product of the intensity at a point x and a reference measure $\omega(dx)$ on \mathcal{X} . In this case $\omega(dx)$ is an area-weighted reference measure. This is similar to the discrete case where the intensity was a product of a unit-area intensity and the area of the polygon. Thus we have

$$\Lambda(dx) = \Lambda(x)\omega(dx),$$

and the total number of cracks in \mathcal{X} is given by

$$N(\mathcal{X}) \sim \text{Poisson} \left(\int_{\mathcal{X}} \Lambda(x)\omega(dx) = \Lambda(\mathcal{X}) \right).$$

5.1.4 Regression Model with Identity-Link

In a similar way as in the discrete case we model the intensity at a point using a regression model with identity link that incorporates both the observed (compression and tension) and unobserved factors (latent factors representing the unknown spatial distribution of pores or other influential factors) that are believed to have an influence on crack initiation. The intensity at a point x is given by

$$\Lambda(x) = C(l)\beta_1 + T(l)\beta_2 + X_3\beta_3, \quad \forall x \in \mathcal{X},$$

where the coefficients β_1 and β_2 are indicators of the influence of compression and tension, respectively, on causing cracks to initiate. The third term $X_3\beta_3$ in the identity link regression model represents the influence of the unobserved (latent) factors, which we will define subsequently.

5.1.5 Latent Spatial Covariate

As in the discrete case where we considered a set of latent spatial variables, one for each region (polygon), we also include a latent spatial covariate here. If unobserved covariates vary continuously over the space, it is important to include them in the analysis and, as we have reason to believe that the distribution of pores varies continuously, we incorporate a latent spatial covariate to account for this. We are no longer considering discrete regions but want to model the intensity over continuous space. Suppose to start with we introduce a set of M random locations $\{s_m\}_{m \in M}$ in $\mathcal{S} \subset \mathbb{R}^2$ where \mathcal{S} is some region such that $\mathcal{L} \subset \mathcal{S}$ and with each of these we associate a set of random latent magnitudes $\{\gamma_m\}_{m \in M}$, not necessarily all equal. Each of the s_m 's can be considered as analogous to the polygon centroids and each of the γ_m 's as analogous to the random variables γ_{ij} , associated with each polygon in the discrete model.

In a similar way as in the discrete case we choose to model the influence, that the latent magnitudes $\{\gamma_m\}_{m \in M}$ have on causing cracks to form, with a Gaussian kernel $k(l, s_m)$ depending on Euclidean distance, for any location $l \in \mathcal{L}$. Thus we are modelling the unobserved factors that influence the formation of cracks as point sources of not necessarily equal magnitudes, and whose influence decreases with increasing distance from the point source, and the rate at which the influence decreases is determined by the Gaussian kernel.

We consider the following

$$\sum_{m=1}^M k(l, s_m)\gamma_m. \quad (5.2)$$

The magnitudes $\{\gamma_m\}$ together with the locations $\{s_m\}$ are an approximation to

any unobserved spatially varying latent covariate. Suppose now we increase the set, $\{s_m, \gamma_m\}$, in the limit this leads to a random field, which we denote by $\Gamma(ds)$,

$$\Gamma(ds) = \sum_m \gamma_m \delta_{s_m}(ds).$$

5.1.6 Gamma Random Field

We now introduce a particular type of random field, namely the Gamma random field.

Definition 5.5 *A random field $\Gamma(ds) \sim \text{Gamma}(\alpha(ds), b(s))$ is said to be a Gamma random field with shape measure $\alpha(ds)$ and scale function $b(s)$ over some set \mathcal{S} if*

- $A \subset \mathcal{S}$, $\Gamma(A) \sim \text{Gamma}(\int_A \alpha(s)ds, b(s))$;
- *If two sets $A, B \subset \mathcal{S}$ are disjoint, then $\Gamma(A)$ and $\Gamma(B)$ are independent, (independent increments).*

Note that the distribution is exact if $b(s)$ is constant on A , otherwise it is an approximation. Gamma random fields offer a means by which we can model uncertainty about both the location and the size of factors (for example, the pores in the cement) that we believe have an influence on the formation of cracks. Wolpert and Ickstadt (1998a) introduced the idea of using Gamma random fields in their class of Bayesian hierarchical models used to analyse spatially dependent count data. As an illustrative example, they modelled the density and spatial correlation of hickory trees. The incorporation of a Gamma random field and Gaussian kernel in order to model latent spatial covariates was also used in the analysis of the effect of traffic pollution on respiratory disorders in children (Best et al. (2000a)). It has also been used in the analysis of origin/destination trip data (Ickstadt and Wolpert (1999)).

The influence of all latent spatial point sources on a point $l \in \mathcal{L}$, Equation 5.2, now has the following integral form

$$\int_{\mathcal{S}} k(l, s) \Gamma(ds).$$

The intensity for the marked Poisson process then becomes

$$\Lambda(x) = C(l)\beta_1 + T(l)\beta_2 + \int_S k(l, s)\Gamma(ds). \quad (5.3)$$

For notational simplicity let $X_1(x)\beta_1 = C(l)\beta_1$, $X_2(x)\beta_2 = T(l)\beta_2$, and $X_3(x)\beta_3 = \int_S k(l, s)\Gamma(ds)$. The intensity can now be written as

$$\Lambda(x) = \sum_{k=1}^3 X_k(x)\beta_k.$$

5.1.7 Simulation of a Gamma Random Field

Since the Gamma random field is not observed it is necessary to have some way of simulating the field. The Gamma random field can be simulated using the Inverse Lévy Measure (ILM) algorithm, see Wolpert and Ickstadt (1998a) and Wolpert and Ickstadt (1998b) for full details. The ILM algorithm is based on an idea regarding characteristic functions of infinitely-divisible distributions and particular positive measures which are termed ‘‘Lévy measures’’. The algorithm is used to draw random samples from Gamma and other non-negative independent-increment random fields. According to Wolpert and Ickstadt (1998a) the work of Lévy (1937) and others suggests that a Gamma process can be constructed from a Poisson process. The following theorem summarizes how this can be done, see Wolpert and Ickstadt (1998a) for a detailed proof.

Theorem 5.1 *Let $\alpha(s) \geq 0$ and $b(s) > 0$ be measurable functions on a space S . Let $\{\sigma_m\}$ be independent identically distributed draws from any probability distribution $\Pi(ds)$ on S , and let $\tau_m \geq 0$ be the successive jump times of a standard Poisson process. Set $\tau(u, s) = E_1(u/b(s))\alpha(s)$ and $\gamma_m = \inf[u \geq 0 : \tau(u, \sigma_m) \leq \tau_m]$, that is,*

$$\gamma_m = E_1^{-1}(\tau_m/\alpha(\sigma_m))b(\sigma_m),$$

or $\gamma_m = 0$ if $\alpha(\sigma_m) = 0$. Then the random field $\Gamma(\phi) = \sum_{m < \infty} \gamma_m \phi(\sigma_m)$ for bounded measurable $\phi(s)$ has the Gamma process distribution $\Gamma(ds) \sim \text{Gamma}(\alpha(ds), b(s))$ for the measure $\alpha(ds) = \alpha(s)\Pi(ds)$.

Note: $E_1(t) = \int_t^\infty e^{-u} u^{-1} du$ denotes the exponential integral function, see Abramowitz and Stegun (1964), pg. 228. See Wolpert and Ickstadt (1998b) for details on how to approximate this function and its inverse.

Suppose we want to sample from the Gamma random field $\Gamma(ds) \sim (\alpha(ds), b(s))$, over the set S . A single realization of this Gamma random field will be discrete, and will consist of countably many point masses of random magnitudes γ_m at locations $s_m \in S$. The theory allows for the sample locations to be drawn from any distribution Π , provided that whenever a set A exists such that $\alpha(A) > 0$ then $\Pi(A) > 0$. For example it is possible to exploit information about where points associated with the latent variables would be expected to lie and to sample heavily from those areas. If such information is not available then the Uniform distribution on S is a good choice from which to sample.

5.1.8 Inverse Lévy Measure Algorithm

The following is the ILM algorithm to sample from a Gamma random field $\Gamma(ds) \sim \text{Gamma}(\alpha(ds), b(s))$:

1. Set M to be large.
2. Choose a distribution $\Pi(ds)$ on S from which it is easy to sample.
3. Generate M independent identically distributed draws $\{\sigma_m\}$ from $\Pi(ds)$.
4. Generate the first M jump times $\{\tau_m\}$ of a standard Poisson process; to do this simulate M independent exponential random variables $\{e_m\}$ and set $\tau_m = \sum_{i=1}^m e_i$.
5. Set $\gamma_m = E_1^{-1}\{\tau_m/\alpha(\sigma_m)\}b(\sigma_m)$, for $m = 1, \dots, M$.
6. $\Gamma(ds) \approx \Gamma_M(ds) = \sum_m \gamma_m \delta_{\sigma_m}(ds)$.

Figure 5.1 shows a single realisation of a Gamma random field. The code for this plot was written in R and it is an adaptation of S-Plus code that is available in Wolpert and Ickstadt (1998b).

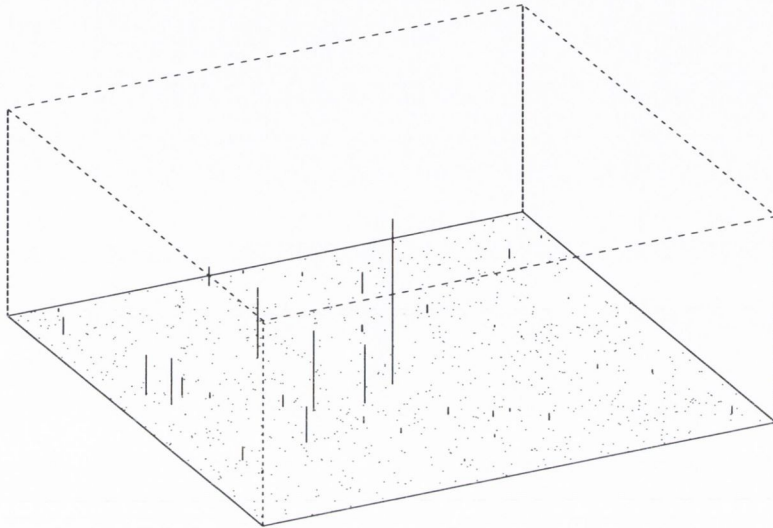


Figure 5.1: A single realisation of a simulated Gamma random field with $\alpha(ds) = 10$ and $b(s) = 2$. The Gamma random field was simulated with $\Pi(ds)$ Uniform on $(0, 1) \times (0, 1)$ and $M = 1000$.

5.2 Likelihood

The Poisson regression model with identity-link (see Equations 5.1 and 5.3) is the model we have chosen: $N(\mathcal{X}) \sim \text{Poisson}(\Lambda(\mathcal{X}) = \Lambda)$. The joint likelihood for all crack locations for all five of the specimens may be written as follows

$$\mathbb{P}(\{N_{ij}\} | \beta_1, \beta_2, \{\Gamma_{ij}(ds)\}, \rho) = \prod_{ij} \frac{\exp(-\Lambda_{ij}) \Lambda_{ij}^{N_{ij}}}{N_{ij}!},$$

where the indexing sets are specimen: $i = 1, 2, \dots, 5$ and window: $j = 1, 2$ and $N_{ij} = N_i(\mathcal{X}_j)$. Note that the index j previously referred to cracks. We model the lateral and medial windows separately since there is no physical link in the laboratory model between the two windows, see Section 4.2.3 and Figure 2.3(a). Thus N_{ij} is the total number of cracks in window j of specimen i . The intensity is given by

$$\Lambda_i(\mathcal{X}_j) = \Lambda_{ij} = \beta_1 \int_{\mathcal{X}_j} X_1(x)\omega(dx) + \beta_2 \int_{\mathcal{X}_j} X_2(x)\omega(dx) + \int_{\mathcal{X}_j} \int_{S_j} k(x, s)\Gamma_{ij}(ds)\omega(dx),$$

where \mathcal{X}_j is the lateral ($j = 1$) or the medial ($j = 2$) window and S_j is a rectangular region containing the lateral window ($j = 1$) or the medial window ($j = 2$).

5.3 Prior Distributions

As in the discrete model we performed inference on the unknown parameters $\beta_1, \beta_2, \{\gamma_{ij}\}$ and ρ . Similarly we wish to carry out inference on β_1, β_2 and ρ and also on the Gamma random field $\Gamma_{ij}(ds)$. For β_1, β_2 and ρ we use similar priors as in the discrete case,

$$\pi(\beta_1) \sim \text{Gamma}(\alpha_1, b_1),$$

$$\pi(\beta_2) \sim \text{Gamma}(\alpha_2, b_2),$$

$$\pi(\rho) \sim \text{Lognormal}(\mu, \sigma),$$

as we are still making use of the same prior information that is available for analysing this data.

For the prior for the Gamma random field $\Gamma_{ij}(ds)$ we choose a Uniform shape measure $\alpha(ds)$ on a rectangular region surrounding each of the lateral and medial windows separately and we choose a constant scale parameter b .

5.4 The Posterior Distribution

The joint posterior distribution for all the data can be written as follows:

$$\mathbb{P}(\beta_1, \beta_2, \{\Gamma_{ij}(ds)\}, \rho | \{N_{ij}\}) \propto \prod_{ij} \left\{ \frac{\exp(-\Lambda_{ij})(\Lambda_{ij})^{N_{ij}}}{N_{ij}!} \pi(\Gamma_{ij}(ds)) \right\} \pi(\beta_1) \pi(\beta_2) \pi(\rho).$$

5.4.1 Inference for β_1 , β_2 , and ρ

We want to perform inference on the parameters β_1 , β_2 , ρ , and $\{\Gamma_{ij}(ds)\}$. In order to do this we employ MCMC techniques. The first of which is data augmentation, see Section 3.4. In the discrete model, given a count of crack start locations in a particular polygon during each iteration of the algorithm, we divided the count into cracks which we attributed to compression, cracks which we attributed to tension, and cracks we attributed to the unobserved latent factors. We do something similar here. For each crack (k) in window (j) of specimen (i) we have a point $x_{ijk} = (l_{ijk}, a_{ijk})$ in the product space \mathcal{X}_j . During each iteration of the algorithm, we assign to each of these points an indicator $I_{ijk} \in \{1, 2, 3\}$, where $\mathbb{P}(I_{ijk} = n) \propto X_n(x_{ijk})\beta_n$, $n = 1, 2, 3$. And we introduce the random variables $N_{in}(\mathcal{X}_j) = N_{ijn}$ defined as

$$N_{ijn} = \#\{k : I_{ijk} = n\},$$

and hence

$$N_{ij} = \sum_{n=1}^3 N_{ijn}$$

See Appendix A.2.1 for full details on how this is carried out. The inclusion of this data augmentation step facilitates the use of the Gibbs sampler in order to draw samples from the full conditional distributions for β_1 and β_2 . For the parameter ρ we use a random-walk Metropolis step, calculating the full conditional distribution for ρ for use in the acceptance probability, see Appendix A.2.1 for details.

5.4.2 Full Conditional Distributions for β_1 and β_2

For full details on how these full conditional distributions may be obtained see Appendix A.2.1. The conditional distributions for β_1 and β_2 are as follows:

$$\mathbb{P}(\beta_1 | \beta_2, \rho, \{\Gamma_{ij}\}) \sim \text{Gamma} \left(\sum_{ij} N_{ij1} + \alpha_1, 5 \sum_j \int_{\mathcal{X}_j} X_1(x) \omega(dx) + b_1 \right), \quad (5.4)$$

and

$$\mathbb{P}(\beta_2 | \beta_1, \rho, \{\Gamma_{ij}\}) \sim \text{Gamma} \left(\sum_{ij} N_{ij2} + \alpha_2, 5 \sum_j \int_{\mathcal{X}_j} X_2(x) \omega(dx) + b_2 \right). \quad (5.5)$$

5.4.3 Conditional Distribution for $\Gamma(ds)$

We consider $\Gamma(ds)$ the Gamma random field over the space S . The following method and results apply also to $\Gamma_{ij}(ds)$, the Gamma random field over the space S_j for all i and j . Full details on how the full conditional distribution for $\Gamma(ds)$ is obtained using data augmentation may be found in Wolpert and Ickstadt (1998a).

Consider $N_3(dx)$, it is a finite integer-valued measure on \mathcal{X} and as such can be represented as the sum of a random number of unit point masses at points x_n , which need not necessarily be distinct. Again we use the technique of data augmentation in order to obtain the full conditional distribution of $\Gamma(ds)$ in known form. For each of these x_n 's select an additional random variable $s_n \in \mathcal{S}$, i.e., a point in the auxiliary space S , where

$$\mathbb{P}(s_n) = \frac{k(x_n, s_n) \Gamma(ds_n)}{\sum_n k(x_n, s_n) \Gamma(ds_n)}.$$

Now we have pairs of points (x_n, s_n) , $x_n \in \mathcal{X}$, $s_n \in S$. We introduce a new random measure Z on $\mathcal{X} \times S$ such that

$$Z(dx, ds) = \sum_n \delta_{(x_n, s_n)}(dx, ds).$$

Note that $Z(\mathcal{X} \times \mathcal{S}) = N_3$. Let $Z_1(dx) = Z(dx \times \mathcal{S}) = N_3(dx)$, i.e. $Z_1(dx)$ recovers the unaugmented data and let $Z_2(ds) = Z(\mathcal{X} \times ds)$, i.e. $Z_2(ds)$ recovers the augmented data. The following result now holds:

Lemma 5.1

$$\mathbb{P}(\Gamma(ds)|N_1, N_2, Z_2(S), \beta_1, \beta_2) \sim \text{Gamma}\left(\alpha(ds) + Z_2(ds), b(s) + \int_{\mathcal{X}} k(x, s)\omega(dx)\right).$$

See Appendix A.2.2 for a proof of Lemma 5.1.

5.5 MCMC Algorithm

We present in the following a brief outline of the MCMC algorithm used to sample from the posterior distribution of the continuous initiation model in order to obtain samples for the parameters: β_1, β_2, ρ and $\Gamma_{ij}(ds)$. A more detailed algorithm is contained in Appendix B.2.

Algorithm

1. Initialise $\beta_1, \beta_2, \rho, X_3\beta_3$, and set the iteration counter $r = 0$.
2. For each crack set $\Lambda_{ijk}^{(r)} = C_{ijk}\beta_1^{(r-1)} + T_{ijk}\beta_2^{(r-1)} + X_3^{(r-1)}\beta_3^{(r-1)}$.
3. Simulate Bernoulli variables to indicate whether each crack is attributable to compression, tension or latent factors. Set N_{ij1} = number of cracks due to compression, N_{ij2} = number of cracks due to tension and N_{ij3} = number of cracks due to latent factors.
4. For each crack attributable to latent factors simulate a corresponding location σ_{ij*} in S .
5. For each σ_{ij*} carry out a random-walk Metropolis step proposing a new location $\sigma_{ij\text{test}}$. Set $s_{ijk} = \sigma_{ij\text{test}}$ if the new step is accepted, otherwise $s_{ijk} = \sigma_{ij*}$, $k = 1, \dots, N_{ij3}$.
6. Simulate the Gamma random field.
7. Simulate the parameters $\beta_1^{(r)}, \beta_2^{(r)}$.

8. Carry out a random-walk Metropolis step for ρ , proposing ρ_{test} , if accepted $\rho^{(r)} = \rho_{\text{test}}$, otherwise $\rho^{(r)} = \rho^{(r-1)}$.
9. $r = r + 1$. Repeat steps 2 through 9.

5.6 Results

We now present the results obtained from carrying out inference on the unknown parameters of the model using the MCMC algorithm detailed above. Table 5.1 shows quantiles, kernel density estimates and priors for β_1 , β_2 , and ρ . The estimates for these parameters are based on sample values obtained from the posterior distribution by running the MCMC algorithm. We computed 6,000 iterations of the program; the first 1000 of these iterations were attributed to burn-in. For each parameter we examined a trace plot of its chain and from this inspection there was no evidence for lack of convergence. We also ran multiple independent chains from various starting points and again, after an initial burn-in, there was no reason to believe the chains had not converged. Trace plots of some parameters may be found in Appendix B.4, Figure B.3.

5.6.1 Gamma Random Fields and Posterior Mean Intensity

For each specimen we present, in image form, the posterior mean of its Gamma random field. This field models spatially the latent factors that have been influential in causing cracks to form in that specimen. See Figures 5.2 and 5.3.

For each of the specimens we also examine the range of the Gamma random field, boxplots of these results may be found in Figure 5.6. From this figure it would appear that the range of the contribution (on the logarithm scale) to the intensity, is of the same magnitude for each of the specimens, i.e., there is no specimen variability as regards the range of the Gamma random field. This suggests that the influence that the latent factors have on causing cracks to form is the same across specimens.

Figures 5.4 and 5.5 show the posterior mean intensity $\mathbb{E}(\Lambda_i)$ as an image plot with stars indicating the crack locations.

5.6.2 Model Validation

As in the discrete initiation model, it is not possible to carry out cross-validation by omitting a specimen and carrying out the analysis as the Gamma random field is specific to the specimen as it is modelling spatially varying factors that are specimen specific. Instead, to examine the fit of the model we examine residuals as follows. For each of the regions in Figure 5.7(a), which correspond to the polygons in the discrete initiation model, P_{ij} , we calculate the standardised residuals r_{ij} for region j of specimen i using the following approximation

$$r_{ij} = \frac{1}{T} \sum_{t=1}^T \frac{(N_{ij} - \Lambda(P_{ij})^{(t)})}{\sqrt{\Lambda(P_{ij})^{(t)}}},$$

where

$$\Lambda(P_{ij}) = \int_{P_{ij}} \Lambda(x) \omega(dx),$$

and T is the total number of iterations. We plot these standardised residuals against the predicted counts

$$\hat{N}_{ij} = \frac{1}{T} \sum_{t=1}^T \Lambda(P_{ij})^{(t)}$$

in Figure 5.7(b). This plot suggests that, in general, there is no unmodelled trend in the residuals, which we would hope for if the model is a reasonable fit. Although, there are a small number of large residuals. When we further examine the residuals by plotting them against both specimen and window, in Figures 5.7(c) and 5.7(d) respectively, it appears that the large residuals are associated with Specimens 1, 2, and 4, mostly. There appears to be no distinction between windows as to how well the model fits.

We also examine the predictive count for each of the specimens. A plot of this analysis may be seen in Figure 5.8. In general the model appears to predict the count

of cracks in each of the specimens well, as all of the true counts lie within the 90% quantiles, and are all close to the median predicted values.

5.7 Comparing Continuous and Discrete Models

We now compare the discrete and continuous models for initiation that we have presented. We examine how comparable the priors are for the latent factors in both of the models. We highlight the important issue of information being lost through aggregation of the data in the discrete model. We also address the issue of the computational time taken by each of the two algorithms, the discrete and continuous, used to carry out inference for the models.

5.7.1 Priors for Latent Factors

For the discrete crack initiation model we have chosen a $\text{Gamma}(1, 0.1)$ prior for the latent factors $\{\gamma_{ij}\}$. In the continuous model we have chosen a prior with a uniform shape parameter and a constant scale parameter b . We can compare these two prior distributions in the following manner. For the discrete model the intensity per unit area due to the latent factors is approximately equal to $\gamma_{ij}/(2\pi\rho^2)$, as the latent contribution from outside a polygon is small. The prior mean intensity for each of the γ_{ij} 's is equal to 10, giving a prior unit area mean intensity due to the latent factors of approximately 0.33.

For the continuous initiation model the prior unit area intensity is given by

$$\int_{S_j} k(x, s)\Gamma_{ij}(ds) \approx \frac{1}{(2\pi\rho^2)} \frac{\Gamma(GK)}{b} = \frac{\alpha(s)}{b},$$

where GK is a Gaussian kernel, whose area is obviously $2\pi\rho^2$. This prior unit area intensity is equal to 0.6 as we have chosen $\alpha(s) = 0.6$ and $b = 1$. Thus, as regards prior mean intensity, the priors are comparable.

5.7.2 Loss of Information due to Aggregation

The discrete model cannot be expected to perform as well as the continuous model in modelling crack initiation, as information, specifically spatial information, will have been lost due to the aggregation of the data for this model. Although the identity-link in the discrete model facilitates the aggregation and refinement of the initial partition, in order to examine results for this model a partition must be chosen. The choice of partition will determine how much information will have been lost in the analysis. In contrast, no information is lost in the continuous model as no aggregation is carried out.

In determining the parameter ρ , the range over which the latent factors have an influence, the continuous model will perform better than the discrete model with a more accurate estimate, as the choice of partition in the discrete model will have an influence on the estimation of this parameter.

5.7.3 Computational Time

The continuous model does require more time for preparation and initial setup and running of the algorithm in comparison to the discrete model. But if the chosen partition for the discrete model has to be reviewed and either refined or aggregated, then the speed of the discrete model is lessened. In comparison, the continuous model does not require this.

5.8 Conclusions

In this chapter we have presented a continuous spatial model for crack initiation that models the data (crack locations) at the finest level of aggregation, i.e., as a continuous spatial process. This model incorporates the spatially varying stress together with latent influential factors, which we have modelled as a continuous surface using a Gamma random field.

Again, as in the case of the discrete model one of the important aspects of the model is the detection of the range over which the latent factors exert an influence, i.e., the estimation of the parameter ρ . This model suggests that the latent factors have an influence on crack formation up to a distance of just under 4mm.

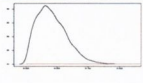
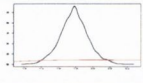
Parameter	Quantiles			Histogram of Samples
	5%	50%	95 %	
β_1	0.003	0.015	0.034	
β_2	0.024	0.031	0.04	
ρ	1.5	1.78	2.06	

Table 5.1: Quantiles, and histograms of sample values for β_1, β_2 , and ρ .

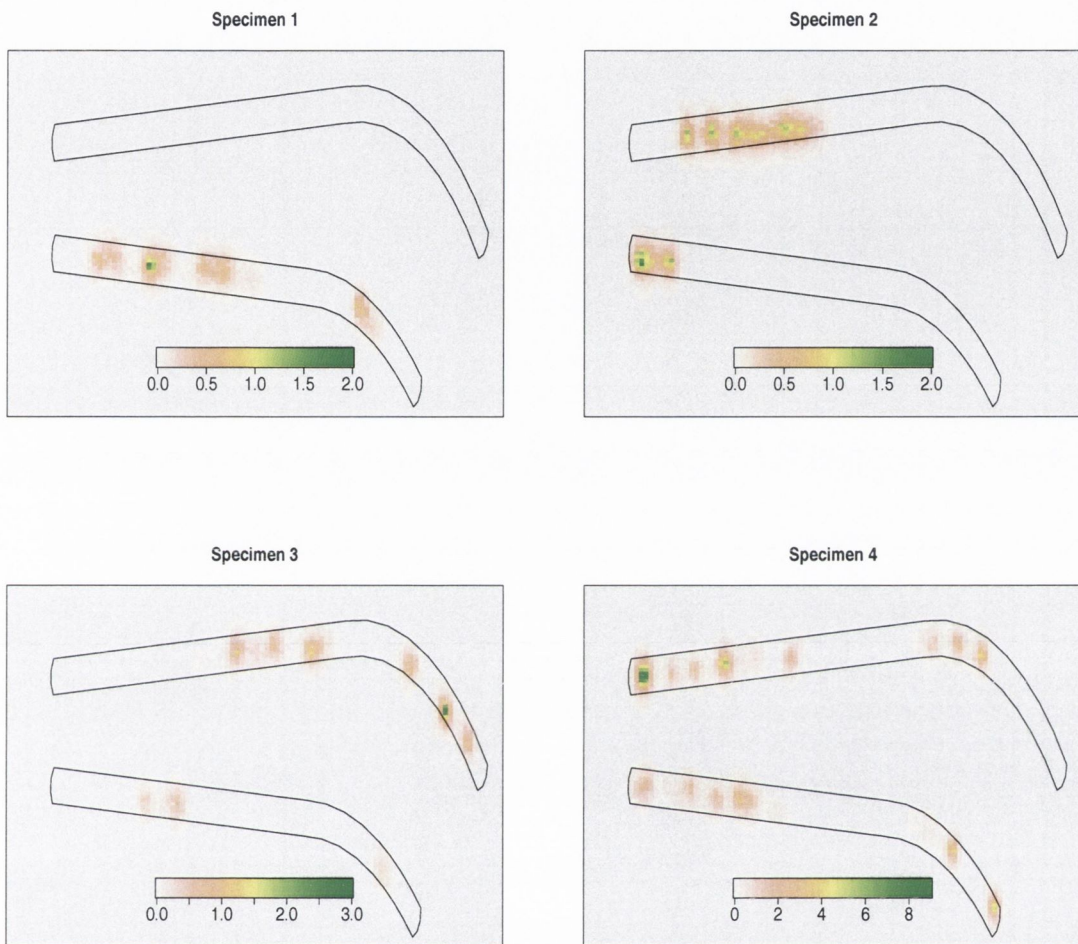


Figure 5.2: Image plots for Specimens 1 - 4 indicating the posterior mean of the Gamma random field over the two windows. The posterior mean is calculated on a 100×100 grid and the Gamma random field in each grid segment G is obtained by calculating $\int_G \Gamma(ds) \approx \sum_m \{\gamma_m : \sigma_m \in G\}$ at each iteration of the program and averaging over the iterations.

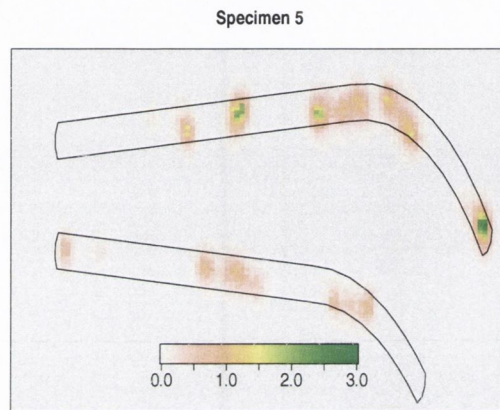
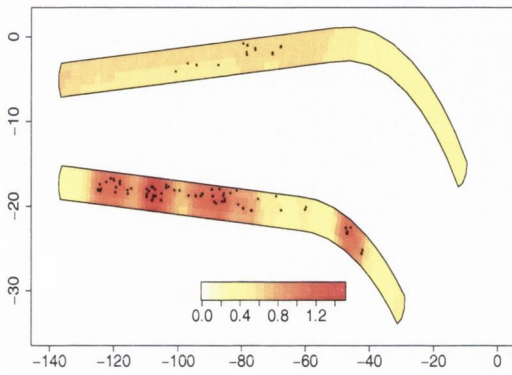
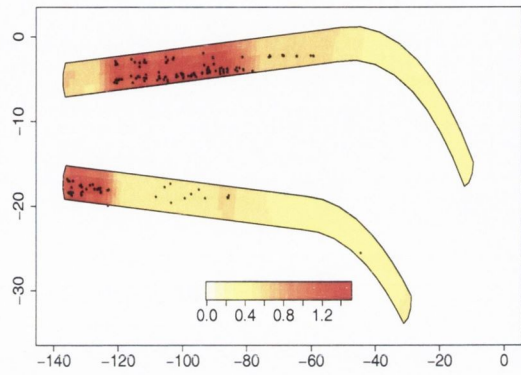


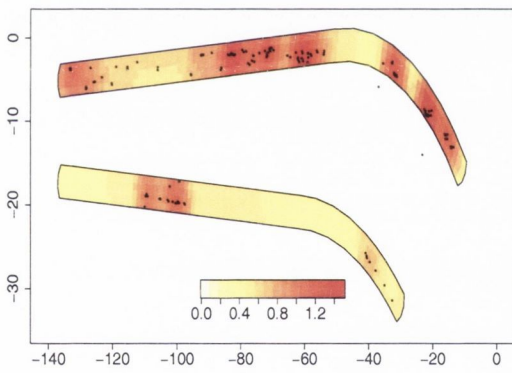
Figure 5.3: Image plot for Specimen 5 indicating the posterior mean of the Gamma random field over the two windows. The posterior mean is calculated on a 100×100 grid and the Gamma random field in each grid segment G is obtained by calculating $\int_G \Gamma(ds) \approx \sum_m \{\gamma_m : \sigma_m \in G\}$ at each iteration of the program and averaging over the iterations.



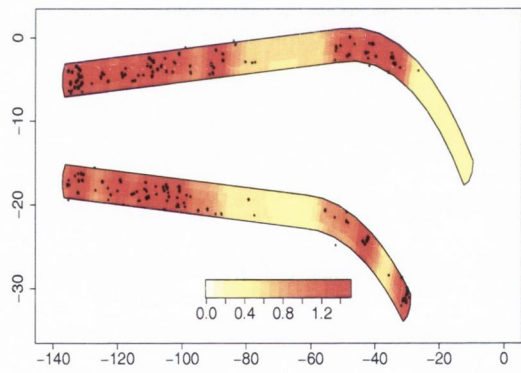
(a) Specimen 1



(b) Specimen 2

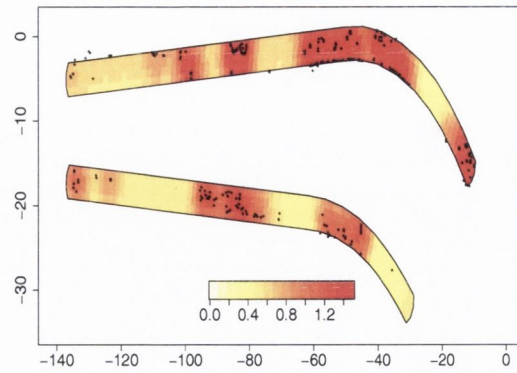


(c) Specimen 3



(d) Specimen 4

Figure 5.4: Posterior mean crack density for Specimens 1 to 4 together with actual crack locations (stars).



(a) Specimen 5

Figure 5.5: Posterior mean crack density for Specimen 5 together with actual crack locations (stars).

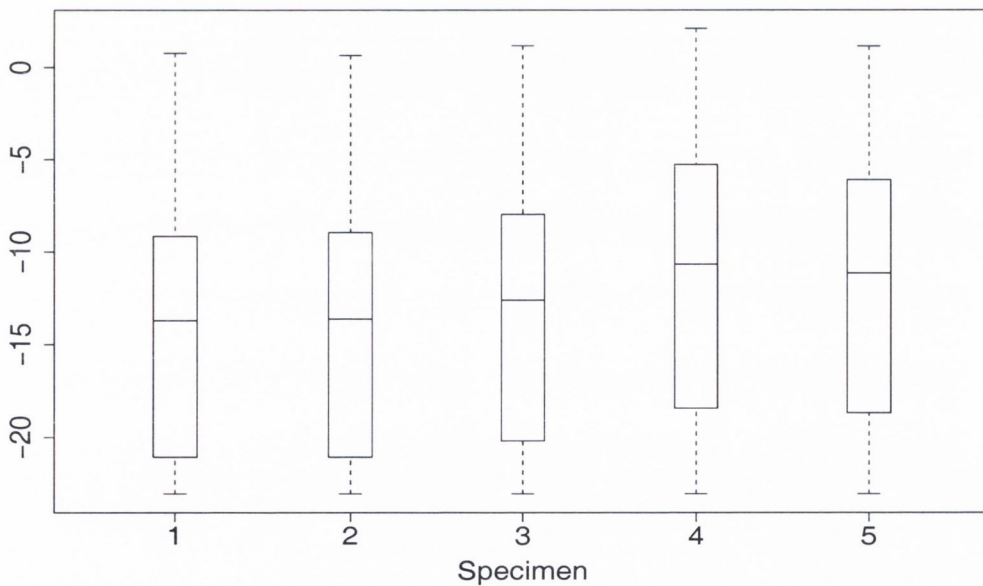
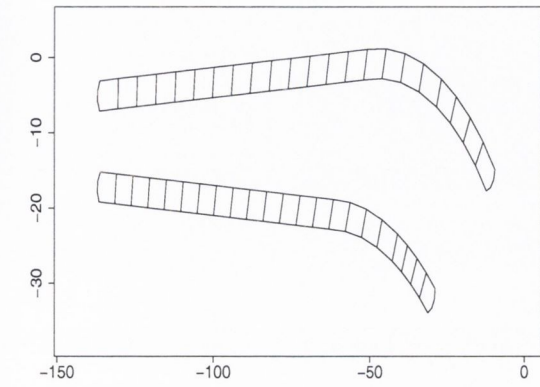
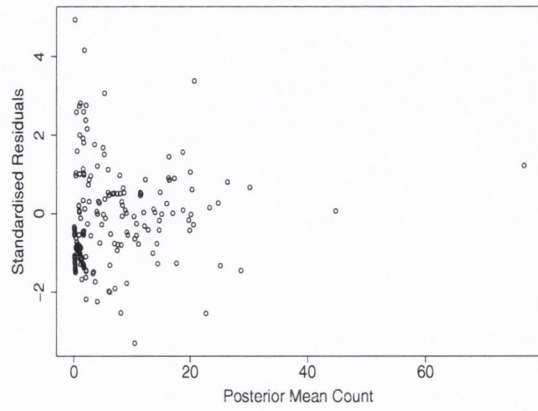


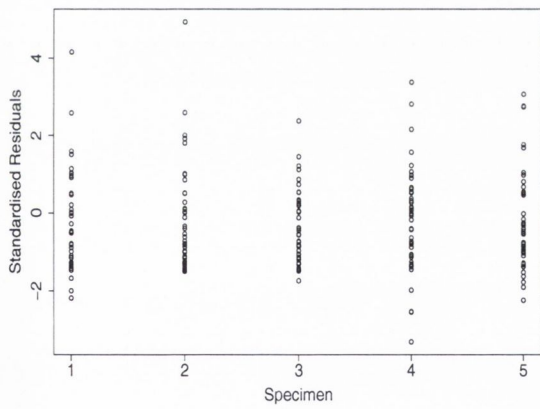
Figure 5.6: Boxplots of re-scaled $\int_G \Gamma(ds)$ where G is a square of area $(145 \cdot 40) / (100 \cdot 100) = 0.58$ on the grid used for each of the specimens in Figures 5.2 and 5.3 for each of the specimens. (The re-scaling is $\log(\int_G \Gamma(ds)e^{-9})$).



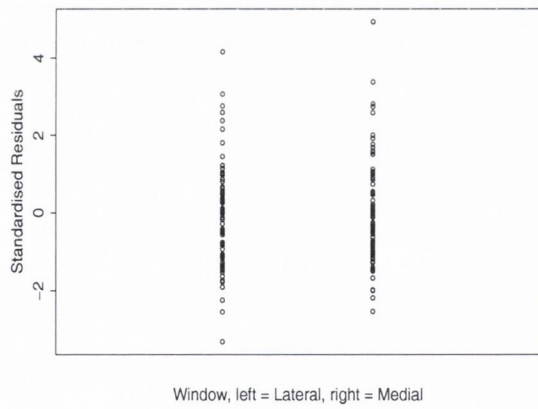
(a) Regions



(b) Residuals against Fitted Values



(c) Residuals against Specimen



(d) Residuals against Window

Figure 5.7: (a) The regions for which the residuals were calculated. The standardised residuals against the posterior mean crack count (b), against specimen (c), and against window (d).

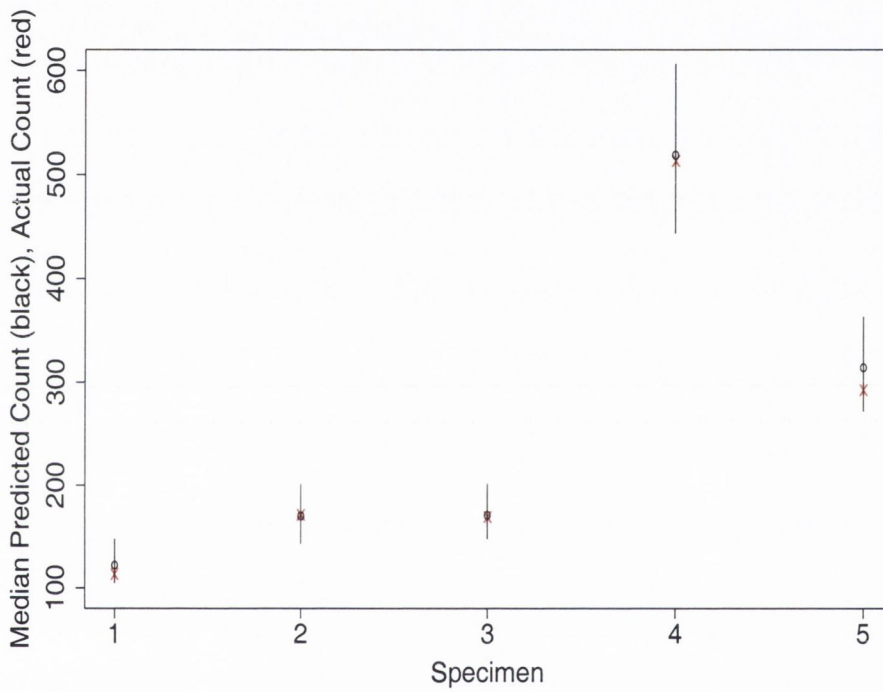


Figure 5.8: For each specimen we show the actual total crack count (red star), and the median posterior predicted count (black circle), together with 90% quantiles for the predicted counts.

Chapter 6

Growth Model

Damage accumulation consists of both crack initiation and crack growth. In order to model damage accumulation it is necessary to model the growth of the cracks in the polymer cement. A model for growth must take into account the differences between pre-cracks and load-cracks. We present a spatial model for growth that incorporates the physical properties of the cement and captures the way in which fatigue cracks, both pre-cracks and load-cracks, grow.

6.1 Preliminary Investigations

6.1.1 Crack Types

As regards examination of growth of the cracks in the bone cement, we retain the distinction between those cracks that have formed before any stress loading has been applied, i.e., the pre-cracks, and those cracks that initiate sometime during the stress loading, which are referred to as load-cracks. When the stress loading is applied the pre-cracks are still present but are now subject to the stresses that have been applied. It is necessary to take into account the extra growing time that the pre-cracks have had in a model for the growth of the cracks. Figure 6.1 shows pre-cracks and load-cracks for one particular specimen.

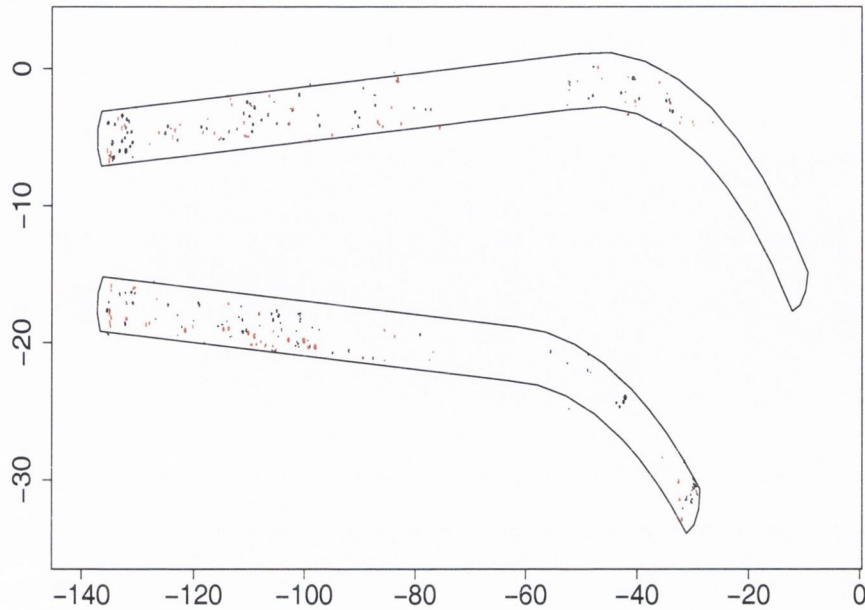


Figure 6.1: Crack lines in the two windows of one particular specimen. Red lines indicate pre-cracks and black lines indicate load-cracks.

6.1.2 Crack Lengths

As a preliminary exploration of the data we examine the growth experienced by each type of crack. In Figure 6.2 we have plotted the logarithm of the lengths of the pre-cracks (yellow) before stress loading, the logarithm of the growth of the pre-cracks (red) after the stress loading, and the logarithm of the lengths of the load-cracks (green), for all specimens. In order to make any comparisons or to draw any conclusions about the lengths of the cracks we must first examine the components that make up the lengths of each of these crack types.

The pre-cracks consist of an initiation length together with some length due to growth before stress loading. The growth in pre-cracks is due to residual stresses experienced in the cement during the curing (drying) process (Lennon and Prendergast (2002)). The lengths of the load-cracks are composed of an initiation length, similar to the pre-cracks and a growth component; the growth having occurred during the

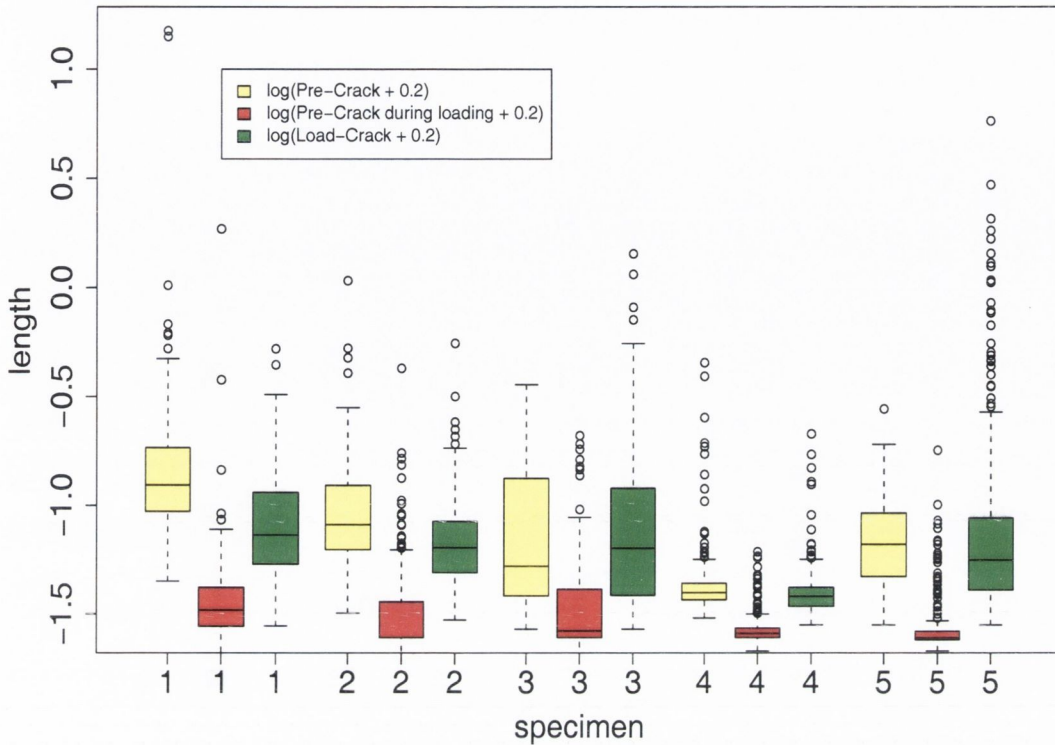


Figure 6.2: Logarithm of lengths (mm) of the various crack types.

stress loading. The amount of growth experienced by the pre-cracks during stress loading should be similar to that experienced by the load-cracks, since both types of cracks are experiencing the same stresses and they are both subject to the influence of any other factors that affect crack growth. The reason why the growth in pre-cracks during stress loading appears to be significantly smaller than the growth of the load-cracks is due to the initiation length of the load-cracks. We must also note that the pre-cracks have had the full loading time in which to grow, this is not the case for the load-cracks; they may have initiated at any time during the stress loading, with the possibility that any of these cracks could have initiated towards the end of the loading period. This would indicate that the initiation length of a crack accounts for a substantial part of the total length.

6.2 How Cracks Grow

We have two measurements of the lengths of pre-cracks. They initiate at some point before the stress loading is applied, their lengths are then measured immediately prior to stressing and again at the end of the experiment. For the load-cracks we only have one measurement of their lengths, i.e., that taken at the end of the experiment. This makes the examination of how the cracks grow, difficult, as we do not have many time points at which to examine their lengths. But it is known that fatigue cracks initiate with some length that is sufficient in order for the cracks to propagate, that they then grow intermittently with the growth consisting of both active and dormant periods (Sobczyk and Spencer 1992, Ch. 5). The active and dormant periods can be explained by the fact that the damaging stresses experienced by the cement and which cause the cracks to grow, are generated by factors such as peaks in the stress loading process.

Wilson (2005), having crack length data measured at five time points, observed that cracks initiate with some length, then some of the cracks grow slowly, while others grow very quickly. This observation can be explained by the theory of active and dormant periods in growth, in which jumps in growth (active periods) occur between periods of much slower growth (dormant periods). Wilson (2005) attributes the jumps in growth to local material properties such as dislocations in the cement, and the slower growth is attributed to global properties of the specimen such as, for example, the stress range.

6.3 Stochastic Process Model for Growth

We propose a stochastic process model for the growth of all cracks in the hip replacement specimens during stressing. Sobczyk and Spencer (1992) suggest treating the crack growth process as a discontinuous random process consisting of a random number of jumps, with each of the jumps being of random magnitude. We construct a model similar to this. In order to account for the spatial variability in stress, which

obviously would have an influence on crack growth, we propose that our crack growth model should take into account the varying stress.

6.3.1 Spatial Aspect to Growth

Consider again the division of the medial and lateral windows into 22 polygons each, as in our discrete model for crack initiation in Chapter 4. Let $l_{ijk}(t)$ be the logarithm of the length (in μm) of crack k (can be either a pre-crack or a load-crack) in region j of specimen i at time t , $0 \leq t \leq t_{\text{final}}$, where t_{final} is the time at which the final measurements were recorded.

6.3.2 Stress

As would be expected, stress has an impact on the growth of the cracks. We propose to model the influence of stress spatially and we use the same kriged values as used in the discrete crack initiation model, Chapter 4., i.e., the stress at the centroid of each of the polygons, as we believe that the growth of a crack in a given polygon is influenced by the stress in that polygon.

6.3.3 Jumps in Growth Rate

As mentioned already, it is known that the growth in cracks consists of slow periods of growth in between jumps in the growth rate, and we would like our model to incorporate these jumps in growth. Wilson (2005) allowed for just one jump in each 0.5 million cycles interval, as 0.5 million cycles was the shortest interval between the successive measurement of the cracks in the data that were analysed. Since we do not have multiple time points at which the cracks were measured we would like to allow for a random number of random sized jumps to occur, but there is a question of identifiability between the number and size of the jumps, i.e., it may not be possible to identify both the number and size of jumps since a small number of large sized jumps would have the same effect on growth as a large number of small jumps. For

this reason we allow for either a single jump of random size or no jump at all. We would hope that the jump would model pores or any other latent factors present in the cement that would have an influence on the growth of the cracks.

6.3.4 The Model

From examination of the data and following McCormack et al. (1998) and Wilson (2005) it appears that the lengths of cracks follow a Lognormal distribution and so we propose the following model for the logarithm of the length of a crack k (again either pre-crack or load-crack) in region j of specimen i at time t :

$$l_{ijk}(t) \sim \text{Normal}(\mu_{ijk}(t), \sigma^2),$$

where

$$\mu_{ijk}(t) = I_{ijk} + (\alpha C_j + \beta T_j)(t - t_{ijk}) + B_{ijk} Y_{ijk},$$

and we now explain in detail the parameters of the model. I_{ijk} is the logarithm of the initiation length of the crack. For pre-cracks this is known and it is the length of the pre-crack just prior to the start of loading. For load-cracks it is unknown and we simulate the I_{ijk} for these cracks. For a load-crack $I_{ijk} \sim \text{Normal}(M_I, \frac{1}{\tau_I})$ with some unknown mean M_I and unknown precision τ_I .

As in the discrete model for initiation, see Chapter 4, C_j and T_j are the compression and tension respectively at the centroid of polygon j . Again as in the discrete initiation model one of either C_j or T_j will be zero for a given polygon as compression and tension cannot both be present at a single location. α and β are the coefficients of compression and tension respectively, and we include them in order to model the influence that stress has in causing cracks to grow. α and β are not specimen specific, reflecting the fact that we only have one set of stress measurements for all specimens and thus do not expect the influence of stress to vary between specimens.

The initiation time of a crack is denoted by t_{ijk} . We fix t , the time at the end of the experiment to be 1, so that the duration of the experiment is from 0 to 1. For

pre-cracks $t_{ijk} = 0$ and since load-cracks initiate at some unknown time during the experiment t_{ijk^*} is unknown.

We indicate whether a crack experiences a jump in growth by B_{ijk} , where $B_{ijk} \sim \text{Bernoulli}(\lambda)$. The size of the jump is denoted by Y_{ijk} , where $Y_{ijk} \sim \text{Normal}(M_Y, 1/\tau_Y)$.

6.3.5 Prior Distributions

We would like to carry out Bayesian inference, and we use MCMC techniques in order to sample from the posterior of the unknown parameters: $\tau = 1/\sigma^2$, α , β , λ , M_I , τ_I , M_Y and τ_Y . In order to do this we must specify prior distributions for each of these parameters. For the precision parameter τ we choose a vague prior, $\text{Gamma}(1/2, 1/2)$, reflecting the lack of information available as regards the variance and also that the parameter must be non-negative. For λ the parameter of the Bernoulli distribution for the jump indicator B_{ijk} we choose a $\text{Beta}(1, 1)$ prior as we have no reason to believe a jump is more likely than not. We also choose Uniform priors for both α and β . We propose a $\text{Uniform}(0, 1)$ prior on $h_{ijk^*} = 1 - t_{ijk^*}, k^*$ indicating a load-crack.

For the means M_I and M_Y of the Normal distributions for the initiation length I_{ijk} and jump size Y_{ijk} respectively we choose Normal priors. This allows for the Gibbs sampler (see Section 3.3.5) to be used due to the conjugacy of the distributions. For the precision parameters τ_I and τ_Y of the Normal distributions for the initiation length I_{ijk} and jump size Y_{ijk} respectively we choose Gamma priors, allowing for the use of the Gibbs sampler due to the conjugacy of the distributions again. Here are the prior distributions chosen:

$$\begin{aligned}
\tau &\sim \text{Gamma}(\phi, \omega), \\
\lambda &\sim \text{Beta}(a_\lambda, b_\lambda), \\
\alpha &\sim \text{Uniform}(a_\alpha, b_\alpha), \\
\beta &\sim \text{Uniform}(a_\beta, b_\beta), \\
M_I &\sim \text{Normal}(m_I, s_I), \\
\tau_I &\sim \text{Gamma}(\phi_I, \omega_I), \\
M_Y &\sim \text{Normal}(m_Y, s_Y), \\
\tau_Y &\sim \text{Gamma}(\phi_Y, \omega_Y), \\
h_{ijk^*} &\sim \text{Uniform}(a_h, b_h).
\end{aligned}$$

6.4 Posterior Distribution

The joint posterior distribution for all the data has the following form:

$$\begin{aligned}
&\mathbb{P}(\tau, \alpha, \beta, \lambda, M_I, \tau_I, M_Y, \tau_Y, \{I_{ijk^*}\}, \{B_{ijk}\}, \{Y_{ijk}\}, \{h_{ijk^*}\} | \{l_{ijk}\}) \\
&\propto \mathbb{P}(\{l_{ijk}\} | \tau, \alpha, \beta, \{I_{ijk^*}\}, \{B_{ijk}\}, \{Y_{ijk}\}, \{h_{ijk^*}\}) \mathbb{P}(\{I_{ijk^*}\} | M_I, \tau_I) \\
&\quad \times \mathbb{P}(\{B_{ijk}\} | \lambda) \mathbb{P}(\{Y_{ijk}\} | M_Y, \tau_Y) \pi(\theta), \\
&\propto \prod_{ijk} \left\{ \sqrt{\frac{\tau}{2\pi}} \exp\left(-\frac{\tau}{2}(l_{ijk} - \mu_{ijk})^2\right) (1 - \lambda)^{1 - B_{ijk}} (\lambda)^{B_{ijk}} \right. \\
&\quad \times \left. \sqrt{\frac{\tau_Y}{2\pi}} \exp\left(-\frac{\tau_Y}{2}(Y_{ijk} - M_Y)^2\right) \right\} \\
&\quad \times \prod_{ijk^*} \left\{ \sqrt{\frac{\tau_I}{2\pi}} \exp\left(-\frac{\tau_I}{2}(I_{ijk^*} - M_I)^2\right) \right\} \\
&\quad \times \sqrt{\frac{s_I}{2\pi}} \exp\left(-\frac{s_I}{2}(M_I - m_I)^2\right) \tau_I^{\phi_I - 1} \exp(-\omega_I \tau_I) \\
&\quad \times \sqrt{\frac{s_Y}{2\pi}} \exp\left(-\frac{s_Y}{2}(M_Y - m_Y)^2\right) \tau_Y^{\phi_Y - 1} \exp(-\omega_Y \tau_Y) \\
&\quad \times \tau^{\phi - 1} \exp(-\omega \tau) \{\mathbb{I}(h_{ijk^*} \in [a_h, b_h])\} \{\mathbb{I}(\alpha \in [a_\alpha, b_\alpha])\} \\
&\quad \times \{\mathbb{I}(\beta \in [a_\beta, b_\beta])\} \lambda^{a_\lambda - 1} (1 - \lambda)^{b_\lambda - 1},
\end{aligned}$$

where $\pi(\theta)$ indicates the priors for all the unknown parameters and k^* indicates load-cracks. See Appendix A.3.1 for full details of the posterior distribution.

6.4.1 Full Conditional Distributions

We want to carry out inference for the parameters $\tau, \alpha, \beta, \lambda, M_I, \tau_I, M_Y,$ and τ_Y . In order to do this we look at the full conditional distributions for each of the parameters. Again, full details of these distributions may be found in Appendix A.3.2. The full conditionals for each of the parameters are as follows. For the precision parameter:

$$\mathbb{P}(\tau | \dots) \sim \text{Gamma} \left(\frac{K}{2} + \phi, \frac{1}{2} \sum_{ijk} (l_{ijk} - \mu_{ijk})^2 + \omega \right), \quad (6.1)$$

where K is the total number of cracks. The full conditional distributions for the coefficients for stress:

$$\mathbb{P}(\alpha | \dots) \sim \text{Normal} \left(\frac{\sum_{ijk} (L_{\alpha ij k} C_j (t - t_{ijk}))}{\sum_{ijk} (C_j^2 (t - t_{ijk})^2)}, \frac{1}{\tau \sum_{ijk} (C_j^2 (t - t_{ijk})^2)} \right), \quad (6.2)$$

where $L_{\alpha ij k} = l_{ijk} - I_{ijk} - \beta T_j (t - t_{ijk}) - B_{ijk} Y_{ijk}$ and similarly the full conditional distribution for β :

$$\mathbb{P}(\beta | \dots) \sim \text{Normal} \left(\frac{\sum_{ijk} (L_{\beta ij k} T_j (t - t_{ijk}))}{\sum_{ijk} (T_j^2 (t - t_{ijk})^2)}, \frac{1}{\tau \sum_{ijk} (T_j^2 (t - t_{ijk})^2)} \right), \quad (6.3)$$

where $L_{\beta ij k} = l_{ijk} - I_{ijk} - \alpha C_j (t - t_{ijk}) - B_{ijk} Y_{ijk}$. The full conditional distribution for the jump parameter λ , which is the probability that a crack has a jump in growth, is given by:

$$\mathbb{P}(\lambda | \dots) \sim \text{Beta} \left(\sum_{ijk} B_{ijk} + 1, K + 1 - \sum_{ijk} B_{ijk} \right). \quad (6.4)$$

The full conditional distributions for the parameters of the Normal distribution for the initiation lengths:

$$\mathbb{P}(M_I | \dots) \sim \text{Normal} \left(\frac{\tau_I \sum_{ijk^*} I_{ijk^*} + m_I s_I}{\tau_I K^* + s_I}, \frac{1}{\tau_I K^* + s_I} \right), \quad (6.5)$$

where K^* is the total number of load-cracks.

$$\mathbb{P}(\tau_I | \dots) \sim \text{Gamma} \left(\frac{K^*}{2} + \phi_I, \frac{1}{2} \sum_{ijk^*} (I_{ijk^*} - M_I)^2 + \omega_I \right), \quad (6.6)$$

and the full conditionals for M_Y and τ_Y are of similar form to those of M_I and τ_I ,

$$\mathbb{P}(M_Y | \dots) \sim \text{Normal} \left(\frac{\tau_Y \sum_{ijk} Y_{ijk} + m_Y s_Y}{\tau_Y K + s_Y}, \frac{1}{\tau_Y K + s_Y} \right), \quad (6.7)$$

and

$$\mathbb{P}(\tau_Y | \dots) \sim \text{Gamma} \left(\frac{K}{2} + \phi_Y, \frac{1}{2} \sum_{ijk} (Y_{ijk} - M_Y)^2 + \omega_Y \right). \quad (6.8)$$

Since each of the full conditional distributions is of known form we can use Gibbs sampling in order to obtain samples of each of the parameters from the posterior distribution.

6.4.2 Simulation of I_{ijk^*} , B_{ijk} , Y_{ijk} , and h_{ijk^*}

Even though we are not interested in obtaining estimates of each of the I_{ijk^*} , B_{ijk} , h_{ijk^*} , and Y_{ijk} it is still necessary that we simulate them in our MCMC algorithm and in order to do this we again look at the full conditional distributions for each of these variables. Full details of these distributions are supplied in Appendix A.3.2. For the initiation length I_{ijk^*} of a load-crack

$$\mathbb{P}(I_{ijk^*} | \dots) \sim \text{Normal} \left(\frac{\tau X_{ijk^*} + \tau_I M_I}{\tau + \tau_I}, \frac{1}{\tau + \tau_I} \right), \quad (6.9)$$

where $X_{ijk^*} = l_{ijk^*} - (\alpha C_j + \beta T_j)(t - t_{ijk^*}) + B_{ijk^*} Y_{ijk^*}$. The full conditional distribution for the jump indicator B_{ijk} is as follows:

$$\mathbb{P}(B_{ijk} = 1 | \dots) \sim \text{Bernoulli} \left(\frac{\exp \left\{ -\frac{\tau}{2} (X_{ijk} - Y_{ijk})^2 \right\} \lambda}{\exp \left\{ -\frac{\tau}{2} (X_{ijk} - Y_{ijk})^2 \right\} \lambda + \exp \left\{ -\frac{\tau}{2} (X_{ijk})^2 \right\} (1 - \lambda)} \right), \quad (6.10)$$

where $X_{ijk} = l_{ijk} - I_{ijk} - (\alpha C_j + \beta T_j)(t - t_{ijk})$. The jump sizes are simulated from the following distributions: if $B_{ijk} = 0$, then

$$\mathbb{P}(Y_{ijk} | \dots) \sim \text{Normal} (M_Y, \tau_Y), \quad (6.11)$$

and if $B_{ijk} = 1$, then

$$\mathbb{P}(Y_{ijk} | \dots) \sim \text{Normal} \left(\frac{\tau X_{ijk} + \tau_Y M_Y}{\tau + \tau_Y}, \frac{1}{\tau + \tau_Y} \right), \quad (6.12)$$

where $X_{ijk} = l_{ijk} - I_{ijk} - (\alpha C_j + \beta T_j)(t - t_{ijk})$, as before. Finally for each $h_{ijk^*} = 1 - t_{ijk^*}$, where t_{ijk^*} is the initiation time of a load-crack, the full conditional distribution is:

$$\mathbb{P}(h_{ijk^*} | \dots) \sim \text{Normal} \left(\frac{X_{ijk^*}}{(\alpha C_j + \beta T_j)}, \frac{1}{\tau(\alpha C_j + \beta T_j)^2} \right) \mathbb{I}(h_{ijk^*} \in [0, 1]), \quad (6.13)$$

where $X_{ijk^*} = l_{ijk^*} - I_{ijk^*} - B_{ijk^*} Y_{ijk^*}$.

6.5 MCMC Algorithm

We now present a brief outline of the MCMC algorithm used to obtain samples from the posterior distribution for each of the parameters of the growth model. A more detailed algorithm is contained in Appendix B.3.

Algorithm

1. Initialise $\tau, \alpha, \beta, \lambda, M_I, \tau_I, M_Y, \tau_Y$ and $\{I_{ijk^*}\}, \{B_{ijk^*}\}, \{Y_{ijk^*}\}, \{h_{ijk^*}\}$, and set the iteration counter $r = 0$.
2. Using Gibbs sampling, simulate each of the parameters $\tau^{(r)}, \alpha^{(r)}, \beta^{(r)}, \lambda^{(r)}, M_I^{(r)}, \tau_I^{(r)}, M_Y^{(r)}, \tau_Y^{(r)}$ from the appropriate distributions.
3. For each load-crack simulate its initiation length $I_{ijk^*}^{(r)}$ and its initiation time $h_{ijk^*}^{(r)}$.
4. Simulate the jump indicator $B_{ijk^*}^{(r)}$ for each crack.
5. Depending on whether there is a jump in growth or not simulate the jump length $Y_{ijk^*}^{(r)}$ appropriately.
6. $r = r + 1$. Repeat Step 2 through 6.

6.6 Results

6.6.1 Convergence Assessment

The estimates of our parameters of interest are based on sample values obtained from the posterior distribution by running the MCMC algorithm detailed above. We computed 22,000 iterations. In order to examine whether the chains showed evidence of convergence we examined trace plots for each of the parameters. Visual inspection of the traces presented no evidence for lack of convergence. We also ran multiple independent chains of the same length for each of the parameters, with each chain having a different starting point. Using R code, available on the web (Gelman and Rubin (1992)), that implements the method of convergence assessment of Gelman and Rubin (1992), see Section 3.3.6, it was not determined that the chains would benefit from further iterations. Thus we use the sample values obtained from these iterations to obtain estimates for our parameters of interest. Figure 6.3 shows the first 1500 iterations of multiple chains for two parameters, together with a magnified image of 500 of the iterations that appear to show convergence. Further trace plots may be found in Appendix B.4, Figure B.4.

6.6.2 Parameter Estimates

We present in Table 6.1 estimates of the parameters of interest. The results are based on 20,000 iterations after a burn-in of 2000 iterations. No thinning has been performed.

6.6.3 Heterogeneity of Specimens

We have also obtained estimates for the parameters based on subsets of the data, i.e., we have run the MCMC algorithm but left the data for one specimen out each time. Figures 6.4 and 6.5 show 95% credibility intervals for each of the parameter estimates. The results presented in this table would appear to suggest that heterogeneity does

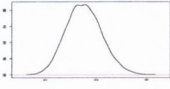
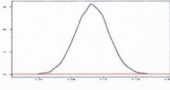
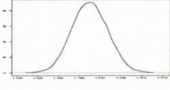
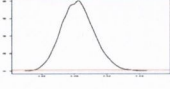
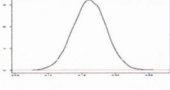

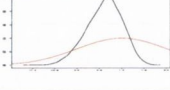
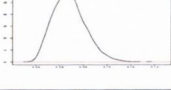
Parameter	Quantiles			KDE's and Priors
	5%	50%	95 %	
τ	21.0	23.8	26.8	
α	0.04	0.08	0.13	
β	0.05	0.06	0.06	
λ	0.02	0.03	0.04	
M_I	4.12	4.16	4.20	
τ_I	1.31	1.41	1.51	
M_Y	-0.01	0.64	1.22	
τ_Y	0.05	0.07	0.09	

Table 6.1: Quantiles and plots of kernel density estimates and priors (red) for each of the parameters of the growth model based on data from all five specimens.

exist between the specimens. Specimen 4 is seen to have a large impact on the estimates of M_Y and $\frac{1}{\sqrt{\tau_Y}}$ as is demonstrated by the sensitivity analysis in Figures 6.5 (c) and (d). The heterogeneity between specimens should be taken into account when considering the estimates of the parameters.

6.6.4 Spatial Pattern of Jump Sizes

On examination of the average jump size, conditional on there being a jump, we see that a spatial pattern does exist for the impact of jumps. See Figures 6.6 and 6.7.

This could be accommodated in the model by having a spatially varying parameter for the mean of the jumps.

6.6.5 Growth Model Validation

In order to carry out model validation for the growth model we do a prediction analysis. For a given specimen we randomly select half of the pre-crack and half of the load-crack lengths. We then carry out our analysis using this randomly selected data. Using the MCMC algorithm for the growth model, we obtain posterior estimates for μ_{ijk} for each of the cracks k in region j of the chosen specimen i . Where the index k now runs over the randomly selected half of the data. We then calculate the posterior mean of the $\{\mu_{ijk}\}$, $\bar{\mu}$, and we plot the Normal density, $\text{Normal}(\bar{\mu}, 1/\tau)$ where $1/\tau$ is the posterior estimate of the variance obtained from the randomly selected half of the data.

We then take the remaining half of the data that were not used in the analysis and we examine a histogram of the logarithm of the lengths of these cracks, comparing the histogram with the Normal density we have obtained from our analysis.

If the model fits the data reasonably well we would expect that the logarithms of the lengths of the cracks not used in the analysis to be of the same size as the posterior density estimate we have obtained.

In Figure 6.8 we show plots containing histograms of the remaining data together with the posterior density we have estimated. We have carried out this analysis for Specimen 3 and Specimen 4. For Specimen 3 the analysis was carried out using the lengths of 143 cracks (85 pre-cracks, 58 load-cracks) and the results are compared with the remaining 142 cracks in Figure 6.8(a). The majority of the logarithms of the lengths of the remaining cracks do appear to lie within two standard deviations of the posterior mean, although there are a number of small cracks that the model does not appear to capture so well.

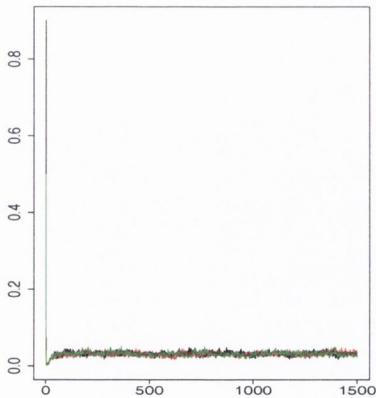
A similar analysis was carried out for Specimen 4. In this case the analysis was done on the logarithms of 418 cracks (161 pre-cracks, 257 load-cracks) and the results

are compared in Figure 6.8(b) with a histogram of the logarithms of the lengths. It would appear from this figure that they are reasonably well modelled by the Normal density whose parameters are obtained from the analysis. The model may, in the case of Specimen 4 appear to be fitting better as more data have been used in the analysis than in that carried out for Specimen 3.

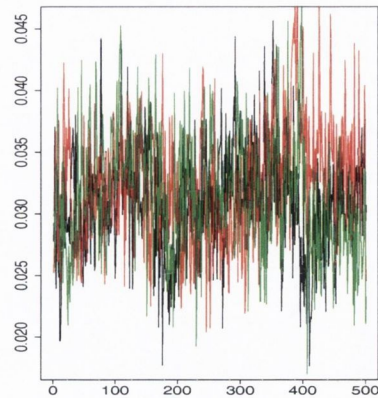
6.7 Conclusions

The model that we have presented for growth does capture some of the main features of how fatigue cracks grow. For example, the length with which cracks initiate seems to be substantial, this is also noted in the literature as cracks must initiate with a length that is sufficient in order to propagate (Sobczyk and Spencer (1992)). The model does appear to estimate reasonable initiation lengths for the load-cracks, in comparison with data analysed in Wilson (2005) the initiation lengths are of the same size.

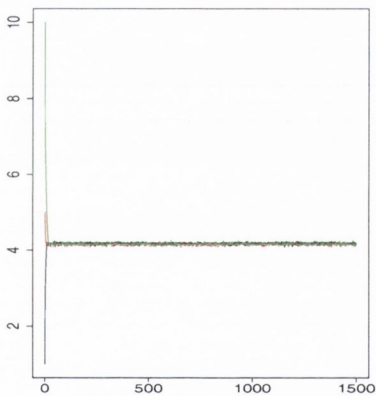
The spatial aspect to growth does appear to be important, for the jumps there seems to be spatial variability, although our model does not capture the spatial variability in jump sizes explicitly it does allow for the examination of a spatial pattern in jump size.



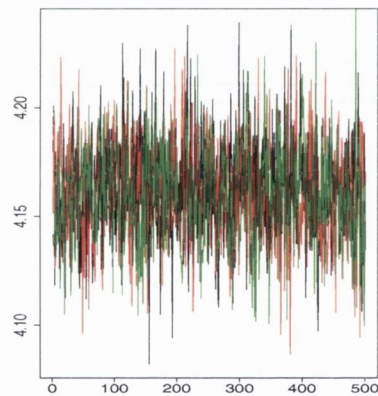
(a)



(b)

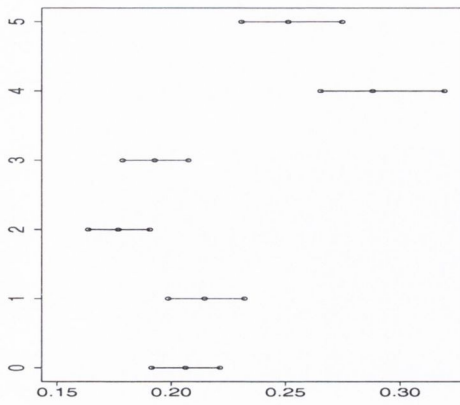


(c)

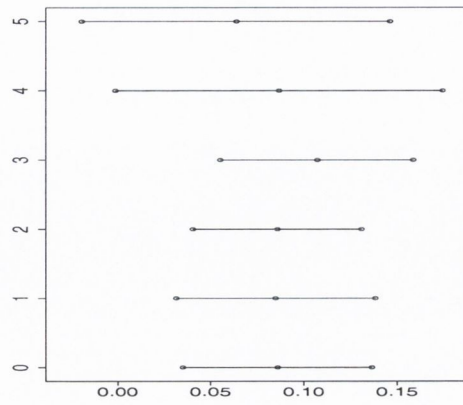


(d)

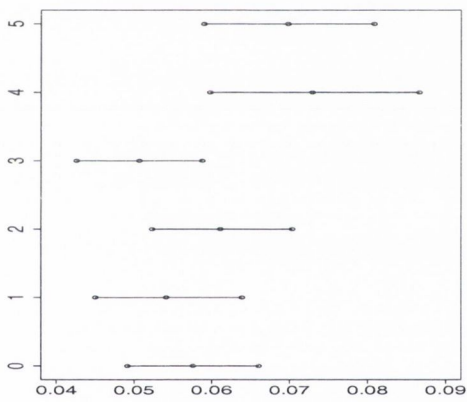
Figure 6.3: (a) shows a trace plot of sample values for λ ; the black trace having started at 0.9, the red trace at 0.1 and the green trace at 0.5. (b) shows a sample of 500 points from each of the three traces for λ when the chains appear to have converged. (c) shows a trace plot of sample values for M_I ; the black trace having started at 1, the red trace at 5 and the green trace at 10. (d) shows a sample of 500 points from each of the three traces for M_I when the chains appear to have converged.



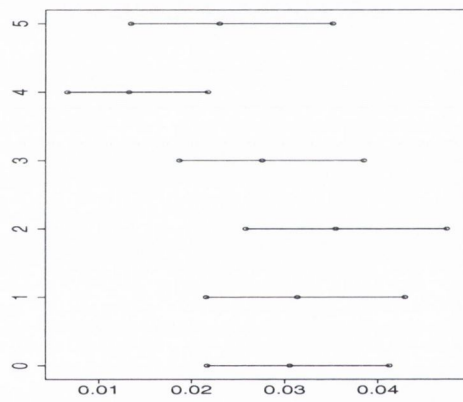
(a) $\frac{1}{\sqrt{r}}$



(b) α

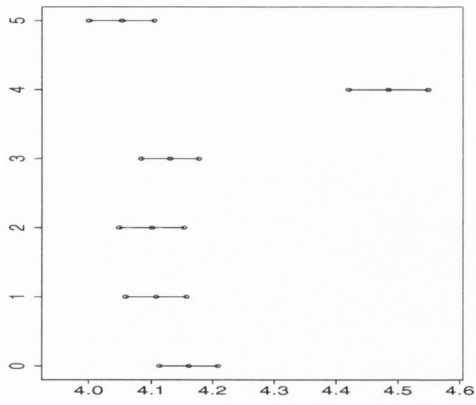


(c) β

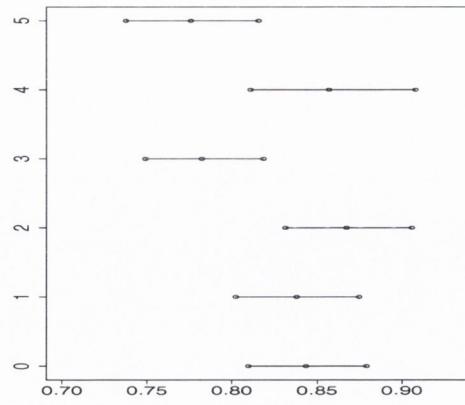


(d) λ

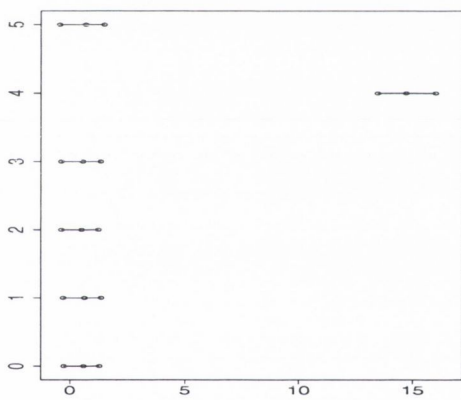
Figure 6.4: Each plot contains 95% credibility intervals for a particular parameter: $\frac{1}{\sqrt{r}}$, α , β and λ . Each plot contains five 95% credibility intervals and each interval has circles at the 0.025, 0.5 and 0.975 quantiles, left to right. An interval at $y = x$, $x = 1, \dots, 5$ represents estimates for the parameter based on data *not* containing that specimen, for example, an interval at $y = 3$ indicates that the estimates are based on data from all specimens except Specimen 3. Intervals at $y = 0$ are based on the data from all five specimens



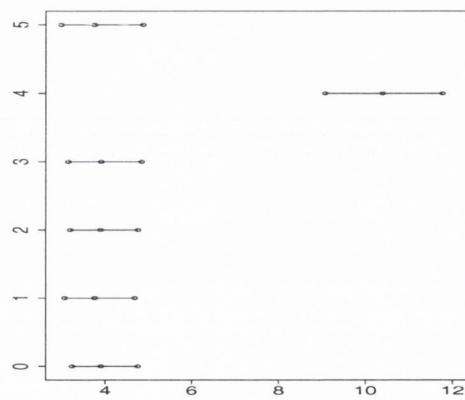
(a) M_I



(b) $\frac{1}{\sqrt{\tau_I}}$

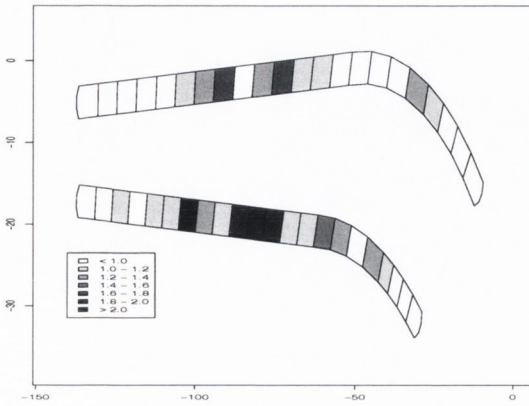


(c) M_Y

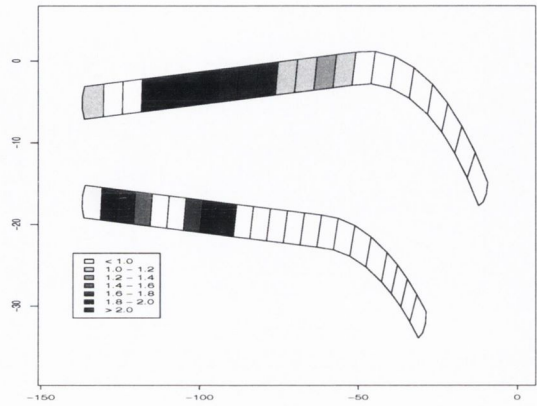


(d) $\frac{1}{\sqrt{\tau_Y}}$

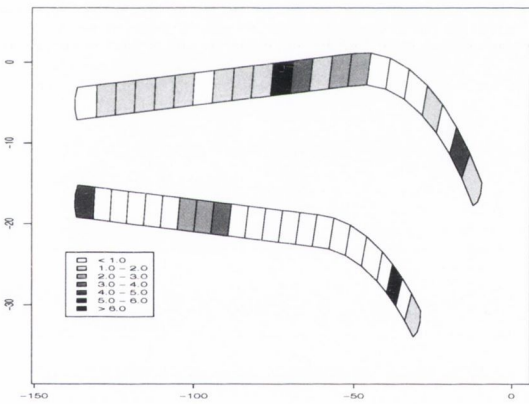
Figure 6.5: Each plot contains 95% credibility intervals for a particular parameter: M_I , $\frac{1}{\sqrt{\tau_I}}$, M_Y and $\frac{1}{\sqrt{\tau_Y}}$. Each plot contains five 95% credibility intervals and each interval has circles at the 0.025, 0.5 and 0.975 quantiles, left to right. An interval at $y = x$, $x = 1, \dots, 5$ represents estimates for the parameter based on data *not* containing that specimen, for example, an interval at $y = 3$ indicates that the estimates are based on data from all specimens except Specimen 3. Intervals at $y = 0$ are based on data from all five specimens



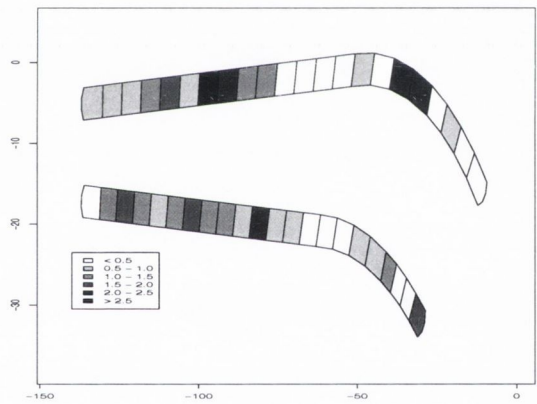
(a) Specimen 1



(b) Specimen 2



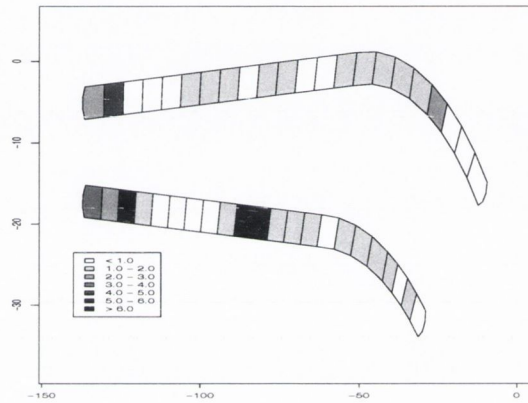
(c) Specimen 3



(d) Specimen 4

Figure 6.6: Spatial representation of the average jump size, i.e., for polygon j of specimen i the average jump size, conditional on there being a jump, is given by

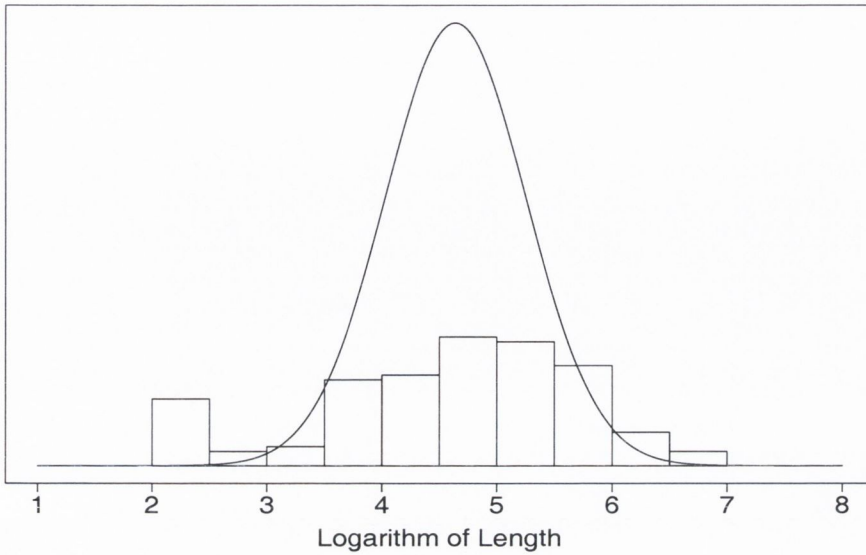
$$\sum_k \frac{B_{ijk} Y_{ijk}}{B_{ijk}}.$$



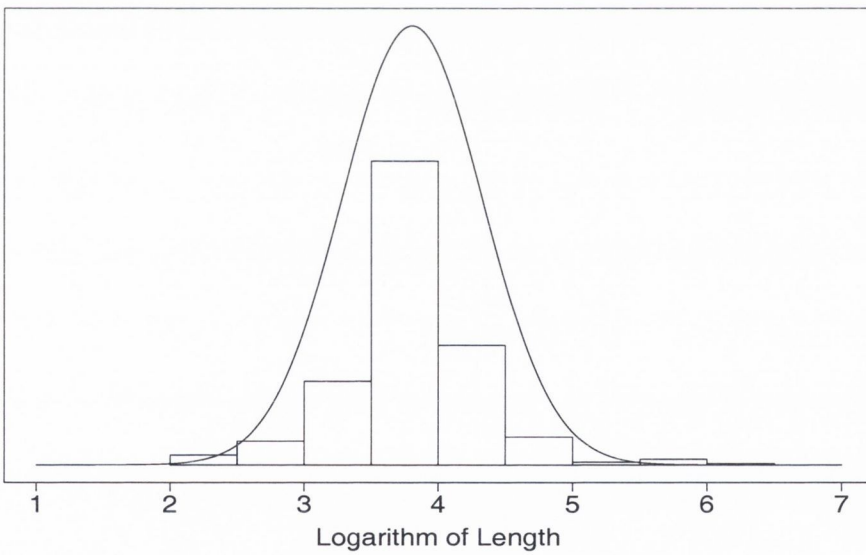
(a) Specimen 5

Figure 6.7: Spatial representation of the average jump size, i.e., for polygon j of specimen 5 the average jump size, conditional on there being a jump, is given by

$$\sum_k \frac{B_{5jk} Y_{5jk}}{B_{5jk}}.$$



(a) Specimen 3



(b) Specimen 4

Figure 6.8: The posterior density for the logarithm of the crack lengths for a random selection of half of the cracks in Specimen 3 (a) and Specimen 4 (b), together with histograms of the logarithms of the lengths of the remaining cracks not used in the analyses.

Chapter 7

Conclusions and Future Work

7.1 Conclusions

From the analysis carried out, it would appear that unmeasured, spatially varying factors have an impact on crack initiation. The influence of the unmeasured factors was modelled using latent variables (discrete model) and a Gamma random field (continuous model). In the analysis of both the discrete and continuous models, evidence was presented that spatially varying factors were present in the cement that had an influence on crack initiation in the specimens. The range over which these spatially varying factors exert an influence appears to be short ($< 4\text{mm}$).

The identification of such important factors is helpful for the understanding of why damage accumulation is so variable. Specimens that were subjected to identical stress loads under laboratory conditions did not present the same damage accumulation patterns. The knowledge that such factors exist and the identification of them as crack causing, together with the estimation of the range over which they have an influence can lead to strategies to identify the physical causes. It may then be possible to either eliminate or reduce them in order to decrease the amount of damage accumulation and ultimately prolong the lifetime of the hip replacement.

Comparing the results of the discrete and continuous models it could be argued that not much more information was gained by not aggregating the data and using

the continuous model. The continuous model would allow for more accurate estimates of the parameters but at the cost of locating each individual crack. If collecting crack counts on a discrete grid facilitates the replication of more data than would locating each individual crack, then using the discrete model with more data would be preferable. The advantage of the continuous model is that it allows for more accurate estimates of the range over which the latent parameters exert an influence.

In analysing the estimates of the parameters of the growth model evidence was also found that suggest spatial variation in the growth of cracks exists. There is also evidence of specimen variability as regards growth of the cracks.

7.2 Comparison With Other Models

Both the discrete and continuous initiation models presented are spatial models, in contrast to the initiation models presented in McCormack et al. (1998) and Wilson (2005), for example. The data analysed in this thesis readily facilitate the modelling of crack initiation spatially, as spatial information has been recorded for each crack that was observed. This is not the case in the data analysed in both McCormack et al. (1998) and Wilson (2005) (same data analysed in both), as detailed spatial information was not present in the data. Considering the spatial aspect as an important feature in modelling crack initiation, it could be argued that the data analysed in this thesis carry more information.

For the growth model, again it is possible to explore spatial aspects of crack growth in the data analysed in this thesis, as this information is contained in the data. Again such detailed information was not available in the data used in the growth models of McCormack et al. (1998) and Wilson (2005) and hence any spatial aspects to growth could not easily be examined.

The data analysed in this thesis do not have multiple time points at which cracks were observed, thus it is not possible to examine crack initiation or crack growth over time. In contrast, the data analysed in McCormack et al. (1998) and Wilson (2005)

were recorded at five time points allowing a more detailed analysis of both initiation and growth over time. From this point of view the data analysed in this thesis contain less information.

7.3 Further Work

7.3.1 Reliability Models

An obvious extension to the work carried out in this thesis would be to construct a model for the reliability of the hip replacement specimens. A model for reliability is necessarily dependent on the definition of failure. As mentioned in the introduction, the definition of failure is a subjective term. If failure is defined to be the total number of cracks exceeding some limit then it would be possible to use either of the initiation models proposed. Using one of these models it would be possible to obtain an estimate for the probability that the crack density in a region exceeds some specified limit. Beyond this limit the specimen would be deemed to have failed.

Another definition of failure could be that the total crack length (the sum of individual crack lengths) exceeds a certain threshold, again beyond which the specimen is deemed to have failed. The growth model proposed could be used to estimate the probability that the total length exceeds the threshold. Another alternative could be that a single crack length exceeds some threshold length.

7.3.2 Pre-Crack Initiation

The initiation models proposed are used to model the initiation intensity for load-cracks. Pre-cracks are also a component of damage accumulation and the initiation intensity for these cracks could also be modelled using the initiation models presented in this thesis.

Since pre-cracks by definition form before any stress loading has been applied, they are not subjected to this form of stress. However, they do experience what are

known as residual stresses when the bone cement in the specimen is curing (drying). Pre-cracks would also be subjected to unmeasured factors influencing their initiation. Given estimates of the residual stresses, it would be possible to fit one of the initiation models and thus model the initiation intensity of the pre-cracks.

7.3.3 Growth Model Extension

As briefly mentioned in Section 6.6.4, there does appear to be spatial variability in the impact of the jumps on growth. As mentioned, this feature could be modelled by incorporating a spatially varying parameter for the mean of the jumps. This could be accommodated in our model by allowing each polygon to have its own jump mean M_{Yj} , in this way accounting for the spatial variability.

7.4 Final Remarks

As mentioned in the introduction, the spatial initiation models presented in this thesis are a new application of the statistical methodology in an engineering context. Both of these models, together with the growth model, offer mathematical insight into the physical processes of damage accumulation, allowing the estimation of parameters that model the factors (both observed and unobserved) that are influential in causing damage accumulation. This collaborative work offers both the engineer and the statistician directions for further research.

Appendix A

Calculations

A.1 Discrete Model

A.1.1 Data Augmentation for Crack Count

The count of cracks in polygon P_{ij} is given by $N_{ij} \sim \text{Poisson}(\mu_{ij})$, where

$$\mu_{ij} = \lambda_{ij}A_j = \beta_1 C_j A_j + \beta_2 T_j A_j + A_j \sum_k \omega_{jk} \gamma_{ik}.$$

The likelihood function for $\beta_1, \beta_2, \{\gamma_{ik}\}$, and ρ is calculated as follows. Note the following index ranges: (specimen) $i = 1, \dots, 5$; (polygon) $j = 1, \dots, 44$; (polygon) $k = 1, \dots, 44$.

$$\mathbb{P}(N_{ij} = n_{ij} | \beta_1, \beta_2, \{\gamma_{ik}\}) = \frac{\exp(-\mu_{ij})(\mu_{ij})^{n_{ij}}}{n_{ij}!}.$$

Using the technique of data augmentation (see Example 3.1) we introduce the following random variables: $N_{ij1}, N_{ij2}, \dots, N_{ij46}$, where

$$\begin{aligned} \mathbb{P}(N_{ij1} | N_{ij}) &\sim \text{Binomial} \left(N_{ij}, \frac{\beta_1 C_j A_j}{\mu_{ij}} \right), \\ \mathbb{P}(N_{ij2} | N_{ij}) &\sim \text{Binomial} \left(N_{ij} - N_{ij1}, \frac{\beta_2 T_j A_j}{\mu_{ij} - \beta_1 C_j A_j} \right), \end{aligned}$$

$$\begin{aligned} \mathbb{P}(N_{ij3}|N_{ij}) &\sim \text{Binomial}\left(N_{ij} - N_{ij1} - N_{ij2}, \frac{\gamma_{i1}\omega_{j1}A_j}{\mu_{ij} - \beta_1 C_j A_j - \beta_2 T_j A_j}\right), \\ &\vdots \\ \mathbb{P}(N_{ij45}|N_{ij}) &\sim \text{Binomial}\left(N_{ij} - N_{ij1} - \dots - N_{ij44}, \frac{\gamma_{i43}\omega_{j43}A_j}{\gamma_{i43}\omega_{j43}A_j + \gamma_{i44}\omega_{j44}A_j}\right), \end{aligned}$$

and

$$N_{ij46} = N_{ij} - N_{ij1} - \dots - N_{ij45}.$$

It follows from Lemma 3.1 that:

$$\begin{aligned} N_{ij1} &\sim \text{Poisson}(\beta_1 C_j A_j), \\ N_{ij2} &\sim \text{Poisson}(\beta_2 T_j A_j), \\ N_{ij3} &\sim \text{Poisson}(\gamma_{i1}\omega_{j1}A_j), \\ &\vdots \\ N_{ij46} &\sim \text{Poisson}(\gamma_{i44}\omega_{j44}A_j). \end{aligned}$$

Combining this result and Lemma 3.2 we obtain the following

$$\begin{aligned} \mathbb{P}(N_{ij1}, \dots, N_{ij46} | \beta_1, \beta_2, \{\gamma_{ik}\}, \rho) &= \mathbb{P}(N_{ij1}) \cdots \mathbb{P}(N_{ij46}), \\ &= \frac{\exp(-\beta_1 C_j A_j) (\beta_1 C_j A_j)^{N_{ij1}}}{N_{ij1}!} \\ &\quad \times \frac{\exp(-\beta_2 T_j A_j) (\beta_2 T_j A_j)^{N_{ij2}}}{N_{ij2}!} \\ &\quad \times \prod_k \left\{ \frac{\exp(-\gamma_{ik}\omega_{jk}A_j) (\gamma_{ik}\omega_{jk}A_j)^{N_{ijk+2}}}{N_{ijk+2}!} \right\}. \end{aligned}$$

The joint posterior is given by

$$\begin{aligned}
\mathbb{P}(\beta_1, \beta_2, \{\gamma_{ij}\}, \rho | \{N_{ij}\}) &\propto \prod_{ij} \left\{ \frac{\exp(-\beta_1 C_j A_j) (\beta_1 C_j A_j)^{N_{ij1}}}{N_{ij1}!} \right. \\
&\quad \times \frac{\exp(-\beta_2 T_j A_j) (\beta_2 T_j A_j)^{N_{ij2}}}{N_{ij2}!} \\
&\quad \times \left. \prod_k \left(\frac{\exp(-\gamma_{ik} \omega_{jk} A_j) (\gamma_{ik} \omega_{jk} A_j)^{N_{ijk+2}}}{N_{ijk+2}!} \right) \right\} \\
&\quad \times \exp(-b_1 \beta_1) \beta_1^{\alpha_1 - 1} \\
&\quad \times \exp(-b_2 \beta_2) \beta_2^{\alpha_2 - 1} \\
&\quad \times \frac{1}{\sigma \rho} \exp \left\{ -\frac{(\log(\rho) - \mu)^2}{2\sigma^2} \right\} \\
&\quad \times \prod_{ij} \exp(-b_g \gamma_{ij}) \gamma_{ij}^{\alpha_g - 1},
\end{aligned}$$

which can also be written as:

$$\begin{aligned}
\mathbb{P}(\beta_1, \beta_2, \{\gamma_{ij}\}, \rho | \{N_{ij}\}) &\propto \exp \left\{ -\beta_1 \sum_{ij} C_j A_j \right\} (\beta_1)^{\sum_{ij} N_{ij1}} \times 5 \prod_j (C_j)^{N_{ij1}} \\
&\quad \times \exp \left\{ -\beta_2 \sum_{ij} T_j A_j \right\} (\beta_2)^{\sum_{ij} N_{ij2}} \times 5 \prod_j (T_j)^{N_{ij1}} \\
&\quad \times \prod_{ik} \left\{ \exp \left(-\gamma_{ik} \sum_j \omega_{jk} A_j \right) (\gamma_{ik})^{\sum_j N_{ijk+2}} \prod_j (\omega_{jk})^{N_{ijk+2}} \right\} \\
&\quad \times \exp(-b_1 \beta_1) \beta_1^{\alpha_1 - 1} \\
&\quad \times \exp(-b_2 \beta_2) \beta_2^{\alpha_2 - 1} \\
&\quad \times \frac{1}{\sigma \rho} \exp \left\{ -\frac{(\log(\rho) - \mu)^2}{2\sigma^2} \right\} \\
&\quad \times \prod_{ik} \exp(-b_g \gamma_{ik}) \gamma_{ik}^{\alpha_g - 1}.
\end{aligned}$$

A.1.2 Full Conditional Distributions

The full conditional distributions for β_1, β_2 , and $\{\gamma_{ij}\}$ are obtained as follows:

$$\begin{aligned}
\mathbb{P}(\beta_1 | \beta_2, \{\gamma_{ij}\}, \rho) &\propto \exp \left\{ -\beta_1 \left(5 \sum_j C_j A_j + b_1 \right) \right\} \beta_1^{\sum_{ij} N_{ij1} + \alpha_1 - 1}, \\
&\sim \text{Gamma} \left(\sum_{ij} N_{ij1} + \alpha_1, 5 \sum_j C_j A_j + b_1 \right);
\end{aligned}$$

$$\begin{aligned}\mathbb{P}(\beta_2|\beta_1, \{\gamma_{ij}\}, \rho) &\propto \exp\{-\beta_2(5 \sum_j T_j A_j + b_2)\} \beta_2^{\sum_{ij} N_{ij2} + \alpha_2 - 1}, \\ &\sim \text{Gamma}\left(\sum_{ij} N_{ij2} + \alpha_2, 5 \sum_j T_j A_j + b_2\right);\end{aligned}$$

$$\begin{aligned}\mathbb{P}(\gamma_{ik}|\beta_1, \beta_2, \rho) &\propto \exp\{-\gamma_{ik}(\sum_j \omega_{jk} A_j + b_g)\} (\gamma_{ik})^{\sum_j N_{ijk+2} + \alpha_g - 1}, \\ &\sim \text{Gamma}\left(\sum_j N_{ijk+2} + \alpha_g, \sum_j \omega_{jk} A_j + b_g\right).\end{aligned}$$

The full conditional distribution for ρ is as follows

$$\mathbb{P}(\rho|\beta_1, \beta_2, \{\gamma_{ij}\}) \propto \prod_{ij} \left\{ \exp\left(-\sum_{jk} \gamma_{ik} \omega_{jk} A_j\right) (\lambda_{ij})^{N_{ij}} \right\} \frac{1}{\sigma \rho} \exp\left\{-\frac{(\log(\rho) - \mu)^2}{2\sigma^2}\right\}.$$

Let $W(\rho) = \sum_{jk} \omega_{jk} \gamma_{ik} A_j$ and let $\lambda_{ij}(\rho) = \lambda_{ij}$, the full conditional then becomes

$$\mathbb{P}(\rho|\beta_1, \beta_2, \{\gamma_{ij}\}) \propto \prod_{ij} \left\{ \exp(-W(\rho)) (\lambda_{ij}(\rho))^{N_{ij}} \right\} \frac{1}{\sigma \rho} \exp\left\{-\frac{(\log(\rho) - \mu)^2}{2\sigma^2}\right\}.$$

This full conditional distribution is not of known form and so the use of Gibbs sampling in order to perform inference for ρ is not easily facilitated. Instead we use a random walk Metropolis step. The acceptance probability for this step is calculated as follows:

$$\text{accept}(\rho, \rho_{\text{test}}) = \min\left\{1, \frac{\mathbb{P}(\rho_{\text{test}})}{\mathbb{P}(\rho)}\right\},$$

where ρ_{test} is the new ρ proposed for the random walk. For ease of computation we consider the $\log\{\mathbb{P}(\rho_{\text{test}})/\mathbb{P}(\rho)\}$.

$$\begin{aligned}\log\left\{\frac{\mathbb{P}(\rho_{\text{test}})}{\mathbb{P}(\rho)}\right\} &= \sum_{ij} W(\rho) - \sum_{ij} W(\rho_{\text{test}}) \\ &\quad + \sum_{ij} \{N_{ij} \log(\lambda_{ij}(\rho_{\text{test}}))\} - \sum_{ij} \{N_{ij} \log(\lambda_{ij}(\rho))\} \\ &\quad + \log(\sigma \rho) - \log(\sigma \rho_{\text{test}}) \\ &\quad + \frac{(\log(\rho) - \mu)^2 - (\log(\rho_{\text{test}}) - \mu)^2}{2\sigma^2}.\end{aligned}$$

A.2 Continuous Model

For the random field model for crack initiation the count of cracks in window $j = 1, 2$ of specimen $i = 1, \dots, 5$ is given by

$$N_{ij} \sim \text{Poisson}(\Lambda_{ij}),$$

where the intensity measure is defined to be

$$\Lambda_{ij} = \beta_1 \int_{\mathcal{X}_j} X_1(x) \omega(dx) + \beta_2 \int_{\mathcal{X}_j} X_2(x) \omega(dx) + \int_{\mathcal{X}_j} \int_{\mathcal{S}_j} k(x, s) \Gamma_{ij}(ds) \omega(dx).$$

For ease of notation let $\Lambda_{ijn} = \beta_n \int_{\mathcal{X}_j} X_n(x) \omega(dx)$ for $n = 1, 2$, and let

$$\Lambda_{ij3} = \int_{\mathcal{X}_j} \int_{\mathcal{S}_j} k(x, s) \Gamma_{ij}(ds) \omega(dx). \text{ Also we let } \Gamma_{ij} = \Gamma_{ij}(ds).$$

A.2.1 Full Conditional Distributions for β_1 , β_2 and ρ

We use the technique of data augmentation (see Section 3.4) in the following way. For each crack (k) in a given specimen (i) and window (j) we augment the data with an indicator which has the effect of attributing the initiation of the crack to either compression ($n = 1$), tension ($n = 2$), or the unobserved latent spatial factor ($n = 3$). Let $I_{ijk} \in \{1, 2, 3\}$ be this indicator variable, where

$$\mathbb{P}(I_{ijk} = n) \propto X_n(x_{ijk}) \beta_n, \quad n = 1, 2, 3.$$

One method of carrying this out is for a given crack x_{ijk} let

$$P_1 = \frac{X_1(x_{ijk}) \beta_1}{\Lambda(x_{ijk})},$$

and

$$P_2 = \frac{X_2(x_{ijk}) \beta_2}{\Lambda(x_{ijk}) - X_1(x_{ijk}) \beta_1},$$

where

$$\Lambda(x_{ijk}) = \sum_{n=1}^3 X_n(x_{ijk}) \beta_n.$$

Simulate a Bernoulli random variable B_1 with probability P_1 . If $B_1 = 1$, then $I_{ijk} = 1$, and we attribute this crack to compression. If $B_1 = 0$ then simulate another Bernoulli random variable B_2 with probability P_2 . If $B_2 = 1$ then $I_{ijk} = 2$ and we attribute this crack to tension. If $B_2 = 0$ then $I_{ijk} = 3$ and we attribute this crack to the latent spatial factor.

We now introduce the random variables N_{ij1} , N_{ij2} , and N_{ij3} where

$$N_{ijn} = \#\{k : I_{ijk} = n\},$$

and it follows that

$$N_{ij} = \sum_{n=1}^3 N_{ijn}.$$

It follows from the definition of the indicator variables and from Lemma 3.1 that

$$N_{ijn} \sim \text{Poisson}(\Lambda_{ijn}).$$

Combining this result and Lemma 3.2 the joint posterior distribution for the augmented data may be written as

$$\mathbb{P}(\beta_1, \beta_2, \rho, \{\Gamma_{ij}\} | \{N_{ijn}\}) \propto \prod_{ijn} \left\{ \frac{\exp(-\Lambda_{ijn})(\Lambda_{ijn})^{N_{ijn}}}{N_{ijn}!} \pi(\Gamma_{ij}) \right\} \pi(\beta_1)\pi(\beta_2)\pi(\rho).$$

The full conditional distributions for β_1 and β_2 may be obtained as follows, the priors for β_1 and β_2 are $\pi(\beta_1) \sim \text{Gamma}(\alpha_1, b_1)$ and $\pi(\beta_2) \sim \text{Gamma}(\alpha_2, b_2)$, respectively.

$$\begin{aligned} \mathbb{P}(\beta_1 | \beta_2, \rho, \{\Gamma_{ij}\}) &\propto \prod_{ij} \left\{ \frac{\exp(-\Lambda_{ij1})(\Lambda_{ij1})^{N_{ij1}}}{N_{ij1}!} \right\} \beta_1^{\alpha_1-1} \exp(-b_1\beta_1), \\ &\propto \exp \left\{ -\beta_1 \left(\sum_{ij} \int_{\mathcal{X}_j} X_1(x)\omega(dx) + b_1 \right) \right\} (\beta_1)^{\sum_{ij} N_{ij1} + \alpha_1 - 1}, \\ &\sim \text{Gamma} \left(\sum_{ij} N_{ij1} + \alpha_1, \sum_{ij} \int_{\mathcal{X}_j} X_1(x)\omega(dx) + b_1 \right), \end{aligned}$$

and similarly for β_2 :

$$\mathbb{P}(\beta_2 | \beta_1, \rho, \{\Gamma_{ij}\}) \sim \text{Gamma} \left(\sum_{ij} N_{ij2} + \alpha_2, \sum_{ij} \int_{\mathcal{X}_j} X_2(x)\omega(dx) + b_2 \right).$$

For ρ the conditional distribution is as follows:

$$\mathbb{P}(\rho|\dots) \propto \frac{\exp -(\Lambda_{ij3})(\Lambda_{ij3})^{N_{ij3}}}{\rho} \exp\left(-\frac{(\log(\rho) - \mu)^2}{2\sigma^2}\right),$$

and we use this distribution in calculating the acceptance probability of the random-walk Metropolis step we use to generate samples of ρ .

A.2.2 Full Conditional Distribution for $\Gamma(ds)$

The following is an adaptation of a proof given in Wolpert and Ickstadt (1998a).

Lemma 5.1

$$\mathbb{P}(\Gamma(ds)|N_1, N_2, Z_2(S), \beta_1, \beta_2) \sim \text{Gamma}(\alpha(ds) + Z_2(ds), b(s) + \int_{\mathcal{X}} k(x, s)).$$

Proof:

Let $\{A_j\}$ be a finite partition of \mathcal{S} , $j = 1, \dots, J$. The realisation of a Gamma random field is almost surely discrete, consisting of countably infinitely many point masses of magnitude γ_i at locations s_i , because of this we can determine $\Gamma(A_j)$ by summing over the jumps that fall into A_j .

$$\Gamma(A_j) = \sum_i \{\gamma_i : s_i \in A_j\}.$$

We also know from the definition of a Gamma random field (Definition 5.5) that $\Gamma(A_j) \sim \text{Gamma}(\alpha(A_j), b(s_j))$, $s_j \in A_j$.

Consider the following:

$$\begin{aligned} \mathbb{P}(Z(\mathcal{X} \times A_j) = Z_2^j = Z_2(A_j)|\Gamma(ds)) &\sim \text{Poisson}\left(\int_{A_j} \int_{\mathcal{X}} k(x, s)\omega(dx)\Gamma(ds)\right), \\ &= \text{Poisson}(k(\mathcal{X}, s_j)\mu_j), \end{aligned}$$

where $k(\mathcal{X}, s_j) = \int_{\mathcal{X}} k(x, s_j)\omega(dx)$, $\int_{A_j} \Gamma(ds) = \Gamma(A_j) = \mu_j$. Hence

$$\mathbb{P}(Z(\mathcal{X} \times A_j) = Z_2^j|\Gamma(A_j) = \mu_j, \forall j) = \prod_{j=1}^J \frac{\exp(-k(\mathcal{X}, s_j)\mu_j)(k(\mathcal{X}, s_j)\mu_j)^{Z_2^j}}{Z_2^j!}.$$

We have assigned a Gamma prior, $\pi(\Gamma(ds)) \sim \text{Gamma}(\alpha(ds), b(s))$, on the Gamma random field $\Gamma(ds)$, hence $\pi(\Gamma(A_j)) \sim \text{Gamma}(\alpha(A_j), b(s_j))$, $s_j \in A_j$. Consider the following

$$\begin{aligned} & \mathbb{P}(Z_2^j, \forall j | \Gamma(A_j) = \mu_j, \forall j) \pi(\Gamma(A_j), \forall j) = \\ & \prod_{j=1}^J \left\{ \frac{\exp(-k(\mathcal{X}, s_j)\mu_j) (k(\mathcal{X}, s_j)\mu_j)^{Z_2^j} b(s_j)^{\alpha(A_j)}}{Z_2^j! \Gamma'(\alpha(A_j))} (\mu_j)^{\alpha(A_j)-1} \exp(-b(s_j)\mu_j) \right\}, \\ & \propto \prod_{j=1}^J \exp\{-\mu_j(k(\mathcal{X}, s_j) + b(s_j))\} (\mu_j)^{\alpha(A_j)+Z_2^j-1}, \end{aligned}$$

where $\Gamma'(\cdot) = \int_0^\infty e^{-x} x^{n-1} dx$, i.e., the Gamma function. Hence

$$\mathbb{P}(\Gamma(A_j) = \mu_j, \forall j | \dots) \sim \prod_{j=1}^J \text{Gamma}(\alpha(A_j) + Z_2^j, k(\mathcal{X}, s_j) + b(s_j)).$$

On refining the partition we have the following:

$$\mathbb{P}(\Gamma(ds) = \mu(ds) | \dots) \sim \text{Gamma}(\alpha(ds) + Z_2(ds), k(\mathcal{X}, s) + b(s)),$$

as required.

A.3 Growth Model

The logarithm of the length of crack k of polygon j of specimen i is given by l_{ijk} , where $l_{ijk} \sim \text{Normal}(\mu_{ijk}, \sigma^2)$, where $\mu_{ijk} = I_{ijk} + (\alpha C_j + \beta T_j)h_{ijk} + B_{ijk}Y_{ijk}$. We wish to carry out Bayesian inference for the parameters: $\tau = 1/\sigma^2$, α , β , λ , M_I , τ_I , M_Y and τ_Y . The prior distributions for each of these parameters are as in Section 6.3.5.

A.3.1 Posterior Distribution

The posterior distribution is as follows:

$$\begin{aligned}
& \mathbb{P}(\tau, \alpha, \beta, \lambda, M_I, \tau_I, M_Y, \tau_Y, \{I_{ijk^*}\}, \{B_{ijk}\}, \{Y_{ijk}\}, \{h_{ijk^*}\} | \{l_{ijk}\}) = \\
& \quad \mathbb{P}(\tau, \alpha, \beta, \{I_{ijk^*}\}, \{B_{ijk}\}, \{Y_{ijk}\}, \{h_{ijk^*}\} | \{l_{ijk}\}) \\
& \quad \times \mathbb{P}(\lambda, M_I, \tau_I, M_Y, \tau_Y | \tau, \alpha, \beta, \{I_{ijk^*}\}, \{B_{ijk}\}, \{Y_{ijk}\}, \{h_{ijk^*}\}, \{l_{ijk}\}), \\
& \propto \mathbb{P}(\tau, \alpha, \beta, \{I_{ijk^*}\}, \{B_{ijk}\}, \{Y_{ijk}\}, \{h_{ijk^*}\} | \{l_{ijk}\}) \\
& \quad \times \mathbb{P}(\lambda | \{B_{ijk}\}) \mathbb{P}(M_I, \tau_I | \{I_{ijk^*}\}) \mathbb{P}(M_Y, \tau_Y | \{Y_{ijk}\}), \\
& \propto \mathbb{P}(\{l_{ijk}\} | \tau, \alpha, \beta, \{I_{ijk^*}\}, \{B_{ijk}\}, \{Y_{ijk}\}, \{h_{ijk^*}\}) \\
& \quad \times \mathbb{P}(\{B_{ijk}\} | \lambda) \mathbb{P}(\{I_{ijk^*}\} | M_I, \tau_I) \mathbb{P}(\{Y_{ijk}\} | M_Y, \tau_Y) \\
& \quad \times \pi(\tau) \pi(\alpha) \pi(\beta) \pi(\lambda) \pi(M_I) \pi(\tau_I) \pi(M_Y) \pi(\tau_Y) \prod_{ijk^*} \pi(h_{ijk^*}), \\
& \propto \prod_{ijk} \left\{ \sqrt{\frac{\tau}{2\pi}} \exp\left(-\frac{\tau}{2}(l_{ijk} - \mu_{ijk})^2\right) (1 - \lambda)^{1-B_{ijk}} (\lambda)^{B_{ijk}} \right. \\
& \quad \times \left. \sqrt{\frac{\tau_Y}{2\pi}} \exp\left(-\frac{\tau_Y}{2}(Y_{ijk} - M_Y)^2\right) \right\} \\
& \quad \times \prod_{ijk^*} \left\{ \sqrt{\frac{\tau_I}{2\pi}} \exp\left(-\frac{\tau_I}{2}(I_{ijk^*} - M_I)^2\right) \right\} \\
& \quad \times \sqrt{\frac{s_I}{2\pi}} \exp\left(-\frac{s_I}{2}(M_I - m_I)^2\right) \tau_I^{\phi_I - 1} \exp(-\omega_I \tau_I) \\
& \quad \times \sqrt{\frac{s_Y}{2\pi}} \exp\left(-\frac{s_Y}{2}(M_Y - m_Y)^2\right) \tau_Y^{\phi_Y - 1} \exp(-\omega_Y \tau_Y) \\
& \quad \times \tau^{\phi - 1} \exp(-\omega \tau) \{\mathbb{I}(h_{ijk^*} \in [0, 1])\} \{\mathbb{I}(\alpha \in [a_\alpha, b_\alpha])\} \\
& \quad \times \{\mathbb{I}(\beta \in [a_\beta, b_\beta])\} \lambda^{a_\lambda - 1} (1 - \lambda)^{b_\lambda - 1},
\end{aligned}$$

where $h_{ijk^*} = t - t_{ijk^*}$.

A.3.2 Full Conditional Distributions

The full conditional distributions for each of the parameters of interest are as follows:

$$\begin{aligned} \mathbb{P}(\tau | \dots) &\propto \prod_{ijk} \left\{ \sqrt{\frac{\tau}{2\pi}} \exp\left(-\frac{\tau}{2}(l_{ijk} - \mu_{ijk})^2\right) \right\} \tau^{\phi-1} \exp(-\omega\tau), \\ &\propto \tau^{\frac{K}{2} + \phi - 1} \exp\left\{-\frac{\tau}{2} \left(\sum_{ijk} (l_{ijk} - \mu_{ijk})^2\right)\right\} \exp(-\omega\tau), \\ &\sim \text{Gamma}\left(\frac{K}{2} + \phi, \frac{1}{2} \sum_{ijk} (l_{ijk} - \mu_{ijk})^2 + \omega\right), \end{aligned}$$

where K is the total number of cracks over all specimens and polygons. For the full conditional distribution for α we use the method of ‘‘completing the square’’:

$$\begin{aligned} \mathbb{P}(\alpha | \dots) &\propto \prod_{ijk} \exp\left\{-\frac{\tau}{2}(l_{ijk} - \mu_{ijk})^2\right\}, \\ &= \prod_{ijk} \exp\left\{-\frac{\tau}{2}(L_{\alpha ij k} - \alpha C_j h_{ijk})^2\right\}, \\ &= \exp\left\{-\frac{\tau}{2} \left(\sum_{ijk} L_{\alpha ij k}^2 + \alpha^2 \sum_{ijk} (C_j^2 h_{ijk}^2) \right. \right. \\ &\quad \left. \left. - 2\alpha \sum_{ijk} (L_{\alpha ij k} C_j h_{ijk})\right)\right\}, \\ &= \exp\left\{-\frac{\tau \sum_{ijk} (C_j^2 h_{ijk}^2)}{2} \left(\frac{\sum_{ijk} L_{\alpha ij k}^2}{\sum_{ijk} (C_j^2 h_{ijk}^2)} + \alpha^2 \right. \right. \\ &\quad \left. \left. - 2\alpha \frac{\sum_{ijk} (L_{\alpha ij k} C_j h_{ijk})}{\sum_{ijk} (C_j^2 h_{ijk}^2)}\right)\right\}, \\ &\propto \exp\left\{-\frac{\tau \sum_{ijk} (C_j^2 h_{ijk}^2)}{2} \left(\alpha - \frac{\sum_{ijk} (L_{\alpha ij k} C_j h_{ijk})}{\sum_{ijk} (C_j^2 h_{ijk}^2)}\right)^2\right\} \\ &\sim \text{Normal}\left(\frac{\sum_{ijk} (L_{\alpha ij k} C_j h_{ijk})}{\sum_{ijk} (C_j^2 h_{ijk}^2)}, \frac{1}{\tau \sum_{ijk} (C_j^2 h_{ijk}^2)}\right), \end{aligned} \tag{A.1}$$

where $L_{\alpha ijk} = l_{ijk} - I_{ijk} - \beta T_j h_{ijk} - B_{ijk} Y_{ijk}$. Similarly for the parameter β :

$$\mathbb{P}(\beta | \dots) \sim \text{Normal} \left(\frac{\sum_{ijk} (L_{\beta ijk} T_j h_{ijk})}{\sum_{ijk} (T_j^2 h_{ijk}^2)}, \frac{1}{\tau \sum_{ijk} (T_j^2 h_{ijk}^2)} \right),$$

where $L_{\beta ijk} = l_{ijk} - I_{ijk} - \alpha C_j h_{ijk} - B_{ijk} Y_{ijk}$. For λ the full conditional distribution is as follows:

$$\begin{aligned} \mathbb{P}(\lambda | \dots) &\propto \prod_{ijk} \{ (1 - \lambda)^{1 - B_{ijk}} (\lambda)^{B_{ijk}} \} \\ &\propto (1 - \lambda)^{K - \sum_{ijk} B_{ijk}} (\lambda)^{\sum_{ijk} B_{ijk}} \\ &\sim \text{Beta} \left(\sum_{ijk} B_{ijk} + 1, K + 1 - \sum_{ijk} B_{ijk} \right). \end{aligned}$$

For the mean of the initiation lengths of the load-cracks M_I :

$$\begin{aligned} \mathbb{P}(M_I | \dots) &\propto \prod_{ijk^*} \left\{ \exp \left(-\frac{\tau_I}{2} (I_{ijk^*} - M_I)^2 \right) \right\} \exp \left(-\frac{s_I}{2} (M_I - m_I)^2 \right) \\ &= \exp \left\{ -\frac{\tau_I}{2} \sum_{ijk^*} (I_{ijk^*} - M_I)^2 - \frac{s_I}{2} (M_I - m_I)^2 \right\} \\ &= \exp \left\{ -\frac{1}{2} \left((\tau_I K^* + s_I) M_I^2 - (\tau_I \sum_{ijk^*} I_{ijk^*} + m_I s_I) 2M_I \right. \right. \\ &\quad \left. \left. + (\tau_I \sum_{ijk^*} I_{ijk^*}^2 + m_I^2 s_I) \right) \right\} \\ &= \exp \left\{ -\frac{1}{2} (A M_I^2 - 2B M_I + C) \right\} \\ &= \exp \left\{ -\frac{A}{2} \left(M_I - \frac{2B}{A} M_I + \frac{C}{A} \right) \right\} \\ &\propto \exp \left\{ -\frac{A}{2} \left(M_I - \frac{B}{A} \right)^2 \right\} \\ &\sim \text{Normal} \left(\frac{B}{A}, \frac{1}{A} \right), \end{aligned}$$

where k^* refers to a load-crack, K^* is the total number of load-cracks, $A = \tau_I K^* + s_I$, $B = \tau_I \sum_{ijk^*} I_{ijk^*} + m_I s_I$, and $C = \tau_I \sum_{ijk^*} I_{ijk^*}^2 + m_I^2 s_I$. The mean of the Normal

distribution for the jump size M_Y is also of the same form:

$$\begin{aligned}\mathbb{P}(M_Y|\dots) &\propto \prod_{ijk} \left\{ \exp\left(-\frac{\tau_Y}{2}(Y_{ijk} - M_Y)^2\right) \right\} \exp\left(-\frac{s_Y}{2}(M_Y - m_Y)^2\right), \\ &\sim \text{Normal}\left(\frac{B}{A}, \frac{1}{A}\right),\end{aligned}$$

where $A = \tau_Y K + s_Y$ and $B = \tau_Y \sum_{ijk} Y_{ijk} + m_Y s_Y$.

The full conditional distribution for the precision parameter of the Normal distribution for the initiation lengths is as follows:

$$\begin{aligned}\mathbb{P}(\tau_I|\dots) &\propto \prod_{ijk^*} \left\{ \sqrt{\frac{\tau_I}{2\pi}} \exp\left(-\frac{\tau_I}{2}(I_{ijk^*} - M_I)^2\right) \right\} \tau_I^{\phi_I - 1} \exp(-\omega_I \tau_I) \\ &\sim \text{Gamma}\left(\frac{K^*}{2} + \phi_I, \frac{1}{2} \sum_{ijk^*} (I_{ijk^*} - M_I)^2 + \omega_I\right).\end{aligned}$$

The precision parameter of the Normal distribution for the jump size is also of the same form:

$$\begin{aligned}\mathbb{P}(\tau_Y|\dots) &\propto \prod_{ijk} \left\{ \sqrt{\frac{\tau_Y}{2\pi}} \exp\left(-\frac{\tau_Y}{2}(Y_{ijk} - M_Y)^2\right) \right\} \tau_Y^{\phi_Y - 1} \exp(-\omega_Y \tau_Y) \\ &\sim \text{Gamma}\left(\frac{K}{2} + \phi_Y, \frac{1}{2} \sum_{ijk} (Y_{ijk} - M_Y)^2 + \omega_Y\right).\end{aligned}$$

Finally the full conditional distributions for the parameters I_{ijk} , B_{ijk} and Y_{ijk} are as follows:

$$\mathbb{P}(I_{ijk^*}|\dots) \propto \exp\left(-\frac{\tau}{2}(X_{ijk^*} - I_{ijk^*})^2\right) \exp\left(-\frac{\tau_I}{2}(I_{ijk^*} - M_I)^2\right)$$

in a similar way to Equation A.1 we use the method of ‘‘completing the square’’, giving

$$\mathbb{P}(I_{ijk^*}|\dots) \sim \text{Normal}\left(\frac{\tau X_{ijk^*} + \tau_I M_I}{\tau + \tau_I}, \frac{1}{\tau + \tau_I}\right)$$

where $X_{ijk} = l_{ijk} - (\alpha C_j + \beta T_j)h_{ijk} + B_{ijk}Y_{ijk}$. The full conditional distribution for the jump indicator is:

$$\begin{aligned}\mathbb{P}(B_{ijk}|\dots) &\propto \exp\left\{-\frac{\tau}{2}(l_{ijk} - \mu_{ijk})^2\right\} (1 - \lambda)^{1 - B_{ijk}} (\lambda)^{B_{ijk}} \\ &= \exp\left\{-\frac{\tau}{2}(X_{ijk} - B_{ijk}Y_{ijk})^2\right\} (1 - \lambda)^{1 - B_{ijk}} (\lambda)^{B_{ijk}},\end{aligned}$$

where $X_{ijk} = l_{ijk} - I_{ijk} - (\alpha C_j + \beta T_j)h_{ijk}$. Let

$$\begin{aligned} A_0 &= \mathbb{P}(B_{ijk} = 0) \propto \exp\left(-\frac{\tau}{2}X_{ijk}^2\right)(1 - \lambda), \\ A_1 &= \mathbb{P}(B_{ijk} = 1) \propto \exp\left(-\frac{\tau}{2}(X_{ijk} - Y_{ijk})^2\right)\lambda, \end{aligned}$$

thus we have

$$\mathbb{P}(B_{ijk} = 1 | \dots) \sim \text{Bernoulli}\left(\frac{A_1}{A_0 + A_1}\right).$$

The full conditional distribution for the size of an individual jump is:

$$\mathbb{P}(Y_{ijk} | \dots) \propto \exp\left(-\frac{\tau}{2}(l_{ijk} - \mu_{ijk})^2\right) \exp\left(-\frac{\tau_Y}{2}(Y_{ijk} - M_Y)^2\right),$$

if $B_{ijk} = 0$

$$\mathbb{P}(Y_{ijk} | \dots) \sim \text{Normal}(M_Y, \tau_Y),$$

and if $B_{ijk} = 1$, then

$$\mathbb{P}(Y_{ijk} | \dots) \sim \text{Normal}\left(\frac{\tau X_{ijk} + \tau_Y M_Y}{\tau + \tau_Y}, \frac{1}{\tau + \tau_Y}\right),$$

where $X_{ijk} = l_{ijk} - I_{ijk} - (\alpha C_j + \beta T_j)h_{ijk}$. The full conditional distribution for $h_{ijk^*} = 1 - t_{ijk^*}$, where t_{ijk^*} is the initiation time of a load-crack is:

$$\begin{aligned} \mathbb{P}(h_{ijk^*} | \dots) &\propto \exp\left\{-\frac{\tau}{2}(X_{ijk^*} - (\alpha C_j + \beta T_j)h_{ijk^*})^2\right\} \mathbb{I}(h_{ijk^*} \in [0, 1]), \\ &\propto \exp\left\{-\frac{\tau(\alpha C_j + \beta T_j)^2}{2}\left(h_{ijk^*} - \frac{X_{ijk^*}}{(\alpha C_j + \beta T_j)}\right)^2\right\} \mathbb{I}(h_{ijk^*} \in [0, 1]) \\ &\sim \text{Normal}\left(\frac{X_{ijk^*}}{(\alpha C_j + \beta T_j)}, \frac{1}{\tau(\alpha C_j + \beta T_j)^2}\right) \mathbb{I}(h_{ijk^*} \in [0, 1]), \end{aligned}$$

where $X_{ijk^*} = l_{ijk^*} - I_{ijk^*} - B_{ijk^*}Y_{ijk^*}$.

Appendix B

Algorithms and Trace Plots

B.1 MCMC Algorithm for Discrete Initiation Model

We now present the MCMC algorithm used to obtain samples from the posterior distribution for each of the parameters: $\beta_1, \beta_2, \{\gamma_{ij}\}$, and ρ of the discrete initiation model.

1. For $i = 1, \dots, 5; j = 1, \dots, 44$, input the data: N_{ij}, C_j, T_j , and the coordinates of the centroids of the polygons.
2. Initialise $\beta_1, \beta_2, \{\gamma_{ij}\}$, and ρ .
3. Set parameter values for the priors: $\alpha_1, b_1, \alpha_2, b_2, \alpha_g, b_g, \mu$, and σ .
4. Initialise the iteration counter $r = 0$.
5. **For $r \leq \text{total number of iterations}$:**
 - (a) For $j = 1, \dots, 22, k = 1, \dots, 22$ calculate

$$\omega_{jk}^{(r)} = \frac{1}{2\pi\rho^{(r-1)2}} \exp\left(\frac{-|d_{jk}|^2}{2\rho^{(r-1)2}}\right),$$

where $|d_{jk}|$ is the Euclidean distance between the centroid of polygon P_{ij} and the centroid of polygon P_{ik} for a particular i (as the weights are the same for each specimen).

(b) For $j = 1, \dots, 22, k = 23, \dots, 44$

$$\omega_{jk}^{(r)} = 0,$$

i.e., initiation of cracks in a given polygon is only affected by latent variables in the window that contains the polygon.

(c) For $j = 23, \dots, 44, k = 23, \dots, 44$ repeat Step (a).

(d) For $j = 23, \dots, 44, k = 1, \dots, 22$ repeat Step (b).

(e) For $i = 1, \dots, 5, j = 1, \dots, 44$ define

$$\text{top}_{1ij}^{(r)} = \beta_1^{(r-1)} C_j A_j;$$

$$\text{top}_{2ij}^{(r)} = \beta_2^{(r-1)} T_j A_j;$$

$$\text{top}_{3ij}^{(r)} = \gamma_{i1}^{(r-1)} \omega_{j1}^{(r)} A_j;$$

⋮

$$\text{top}_{45ij}^{(r)} = \gamma_{i43}^{(r-1)} \omega_{j43}^{(r)} A_j,$$

and

$$\text{bottom}_{1ij}^{(r)} = \sum_{k=1}^{46} \text{top}_{kij}^{(r)};$$

$$\text{bottom}_{2ij}^{(r)} = \text{bottom}_{1ij}^{(r)} - \text{top}_{1ij}^{(r)};$$

$$\text{bottom}_{3ij}^{(r)} = \text{bottom}_{2ij}^{(r)} - \text{top}_{2ij}^{(r)};$$

⋮

$$\text{bottom}_{45ij}^{(r)} = \text{bottom}_{44ij}^{(r)} - \text{top}_{44ij}^{(r)};$$

(f) **Data Augmentation**

For each $i = 1, \dots, 5, j = 1, \dots, 44$ simulate

$$N_{ij1}^{(r)} \text{ from Binomial} \left(N_{ij}, \frac{\text{top}_{1ik}^{(r)}}{\text{bottom}_{1ij}^{(r)}} \right);$$

$$N_{ij2}^{(r)} \text{ from Binomial} \left(N_{ij} - N_{ij1}^{(r)}, \frac{\text{top}_{2ik}^{(r)}}{\text{bottom}_{2ij}^{(r)}} \right);$$

⋮

$$N_{ij45}^{(r)} \text{ from Binomial} \left(N_{ij} - N_{ij1}^{(r)} - \dots - N_{ij44}^{(r)}, \frac{\text{top}_{45ik}^{(r)}}{\text{bottom}_{45ij}^{(r)}} \right).$$

(g) Set $N_{ij46}^{(r)} = N_{ij} - \sum_{k=1}^{45} N_{ijk}^{(r)}$.

(h) **Gibbs Sampling**

Simulate $\beta_1^{(r)}$ from $\text{Gamma}\left(\sum_{ij} N_{ij1}^{(r)} + \alpha_1, 5 \sum_j C_j A_j + b_1\right)$.

Simulate $\beta_2^{(r)}$ from $\text{Gamma}\left(\sum_{ij} N_{ij2}^{(r)} + \alpha_2, 5 \sum_j T_j A_j + b_2\right)$.

For each $i = 1, \dots, 5$, $k = 1, \dots, 44$,

simulate $\gamma_{ik}^{(r)}$ from $\text{Gamma}\left(\sum_j N_{ijk+2}^{(r)} + \alpha_g, \sum_j \omega_{jk}^{(r)} A_j + b_g\right)$.

(i) **Random Walk Metropolis Step to Update ρ**

i. Simulate $\rho_{\text{test}} = \rho^{(r-1)} + \text{Normal}(\text{mean}, \text{var})$ such that $\rho_{\text{test}} \geq 0$.

ii. For $j = 1, \dots, 22$, $k = 1, \dots, 22$ calculate

$$\omega_{jk}^{(r)}(\text{test}) = \frac{1}{2\pi\rho_{\text{test}}^2} \exp\left(\frac{-|d_{jk}|^2}{2\rho_{\text{test}}^2}\right),$$

iii. For $j = 1, \dots, 22$, $k = 23, \dots, 44$

$$\omega_{jk}^{(r)} = 0,$$

iv. For $j = 23, \dots, 44$, $k = 23, \dots, 44$ repeat Step (i)ii.

v. For $j = 23, \dots, 44$, $k = 1, \dots, 22$ repeat Step (i)iii.

vi. Accept ρ_{test} with probability

$$\min\left\{1, \frac{\mathbb{P}(\rho_{\text{test}})}{\mathbb{P}(\rho^{(r-1)})}\right\},$$

see Appendix A.1.2 for full details of the acceptance probability.

vii. If ρ_{test} is accepted set $\rho^{(r)} = \rho_{\text{test}}$, otherwise $\rho^{(r)} = \rho^{(r-1)}$.

(j) $r = r + 1$.

B.2 MCMC Algorithm for Continuous Initiation Model

The following is the MCMC algorithm used to obtain samples from the posterior distribution for each of the parameters: β_1, β_2, ρ and $\Gamma_{ij}(ds)$ of the continuous spatial initiation model.

1. Input of Data and Initialisation of Parameters

- (a) For $i = 1, \dots, 5$ (specimen); $j = 1, 2$ (window); $k = 1, \dots, K_{ij}$, (K_{ij} is the total number of cracks in window j of specimen i) input the data: for each crack we have its spatial location l_{ijk} and its attribute vector $a_{ijk} = (C_{ijk}, T_{ijk})$.
- (b) In order to calculate $\sum_j \int_{\mathcal{X}_j} X_1(x)\omega(dx)$ and $\sum_j \int_{\mathcal{X}_j} X_2(x)\omega(dx)$ (see Equations 5.4 and 5.5) we use an approximation. We divide each window into a fine grid and calculate the stress value, through kriging, at the centroid of each segment of the grid. Thus each segment on the grid has a vector (C_{jg}, T_{jg}) and one of C_{jg} and T_{jg} will be zero as there cannot be both a compression and a tension value at a single point. For $g = 1, \dots, G$ and $j = 1, 2$ input the vector (C_{jg}, T_{jg}) . Also input the area of each segment of the grid, A_{jg} and the coordinates of the centroid of each segment c_{jg} . The approximations are as follows: $\int_{\mathcal{X}_j} X_1(x)\omega(dx) \approx \sum_g C_{jg}A_{jg}$ and $\int_{\mathcal{X}_j} X_2(x)\omega(dx) \approx \sum_g T_{jg}A_{jg}$.
- (c) Set the parameter values for each of the priors, $\alpha_1, b_1, \alpha_2, b_2, \alpha_g, b_g, \mu$, and σ .
- (d) Initialise the parameters, β_1, β_2, ρ , and $\Gamma_{int}(ijk)$ for all i, j , and k , where $\Gamma_{int}(ijk) \approx \int_{S_j} k(l_{ijk}, s)\Gamma_{ij}(ds)$.
- (e) Initialise the Gamma random field.

2. For $r \leq$ total number of iterations:

(a) **First Data Augmentation Step**

- i. For each crack calculate

$$\Lambda_{ijk}^{(r)} = C_{ijk}\beta_1^{(r-1)} + T_{ijk}\beta_2^{(r-1)} + \Gamma_{int}(ijk)^{(r-1)}.$$

- ii. Set $P_1 = C_{ijk}\beta_1^{(r-1)} / \Lambda_{ijk}^{(r)}$.

- iii. Simulate $B_1 \sim \text{Bernoulli}(P_1)$. If $B_1 = 1$ increase N_{ij1} by 1.

- iv. If $B_1 = 0$ set $P_2 = T_{ijk}\beta_2^{(r-1)} / (\Lambda_{ijk}^{(r)} - C_{ijk}\beta_1^{(r-1)})$.

- v. Simulate $B_2 \sim \text{Bernoulli}(P_2)$. If $B_2 = 1$ increase N_{ij2} by 1.

- vi. If $B_2 = 0$ increase N_{ij3} by 1, and keep a record of this crack location that has been attributed to the latent factor by setting $H_{N_{ij3}} = l_{ijk}$.

(b) **Second Data Augmentation Step**

- i. For each $i, j, k = 1, \dots, N_{ij3}$, and for each $m = 1, \dots, M$ calculate the following:

$$P_{ijm} = \frac{\gamma_{ijm} \mathbf{k}(H_k, \sigma_{ijm})}{\sum_{m=1}^M \gamma_{ijm} \mathbf{k}(H_k, \sigma_{ijm})}.$$

For each latent crack choose a corresponding point σ_{ij*} in S_j based on the probabilities P_{ijm} . Let $s_{ijk} = \sigma_{ij*}$.

- ii. **Random Walk Metropolis Step** see Note 1.

Let $s_{ijk} = \sigma_{ij*} + r$, where $r \sim \text{Gaussian}$. Accept s_{ijk} with probability $\min\{1, a\}$ where

$$a = \frac{\frac{\mathbf{k}(H_{ijk}, s_{ijk})}{\sum_{m \neq *} \gamma_{ijm} \mathbf{k}(H_{ijk}, \sigma_{ijm}) + \gamma_{ij*} \mathbf{k}(H_{ijk}, s_{ijk})}}{\frac{\mathbf{k}(H_{ijk}, \sigma_{ij*})}{\sum_m \gamma_{ijm} \mathbf{k}(H_{ijk}, \sigma_{ijm})}}.$$

If $s_{ijk} = \sigma_{ij*} + r$ is not accepted then $s_{ijk} = \sigma_{ij*}$.

(c) **Simulation of the Gamma Random Field**

- i. Set $\sigma_{ijm} = s_{ijm}$, $1 \leq m \leq N_{ij3}$.

- ii. Generate independent locations $\sigma_{ijm} \sim \Pi(ds)$ for $N_{ij3} \leq m \leq M$.

- iii. Set $bGRF_m = b_g + \sum_g k(c_{jg}, \sigma_{ijm})A_{jg}$, where we use the approximation $\sum_g k(c_{jg}, \sigma_{ijm})A_{jg} \approx \int_{\mathcal{X}_j} k(x, \sigma_{ijm})\omega(dx)$.
- iv. Generate successive jump times of a standard Poisson process by generating M exponentially distributed random variables, $\{e_t\}$, then setting $t_m = \sum_{t=1}^m e_t$, for each m .
- v. If $N_{ij3} > 0$,
 - let $\gamma_{ij1} = e_1.bGRF_1$;
 - for $m = 2, \dots, N_{ij3}$ let $\gamma_{ijm} = (e_m - e_{m-1})bGRF_m$;
 - for $m > N_{ij3}$ let $\gamma_{ijm} = E_1^{-1}((e_m - e_{N_{ij3}})/\alpha_g)bGRF_m$.
- vi. If $N_{ij3} = 0$, then for $m = 1, \dots, M$ let $\gamma_{ijm} = E_1^{-1}(e_m/\alpha_g)bGRF_m$.

(d) **Simulation of the β 's**

Simulate

$$\beta_1^{(r)} \sim \text{Gamma}(\sum_{ij} N_{ij1} + \alpha_1, 5 \sum_g C_{jg}A_g + b_1) \text{ and}$$

$$\beta_2^{(r)} \sim \text{Gamma}(\sum_{ij} N_{ij2} + \alpha_2, 5 \sum_g T_{jg}A_g + b_2).$$

(e) **Random Walk Metropolis Step for ρ 's**

Let $\rho_{\text{test}} = \rho + r$, where $r \sim \text{Gaussian}$. Accept ρ_{test} with probability $\min\{1, a\}$, where

$$a = \prod_{ij} \left\{ \exp(-\Lambda_{ij3}(\rho_{\text{test}}) + \Lambda_{ij3}(\rho^{(r-1)})) \times \left(\frac{\Lambda_{ij3}(\rho_{\text{test}})}{\Lambda_{ij3}(\rho^{(r-1)})} \right)^{N_{ij3}} \times \left(\frac{\rho^{(r)}}{\rho_{\text{test}}} \right) \times \exp\left(\frac{-(\log(\rho_{\text{test}}) - \mu)^2 + (\log(\rho^{(r-1)}) - \mu)^2}{2\sigma^2} \right) \right\},$$

where the approximation

$$\begin{aligned} \Lambda_{ij3}(\rho) &= \int_{\mathcal{X}_j} \int_{\mathcal{S}_j} k(x, s)\Gamma_{ij}(ds)\omega(dx), \\ &\approx \sum_m \gamma_{ijm} \left\{ \sum_g k(c_{jg}, \sigma_{ijm})A_{jg} \right\} \end{aligned}$$

is used.

- (f) Set $\Gamma_{int}^{(r)}(ijk) = \sum_m k(l_{ijk}, \sigma_{ijm})\gamma_{ijm}$.

(g) $r = r + 1$.

Note 1: Step 2(b)(ii) is optional. Without this extra random walk Metropolis step it is highly likely that the same augmentation points (σ_{ij*}) will be continuously chosen and this can slow the convergence of the algorithm, this was also noted by Wolpert and Ickstadt (1998a).

B.3 MCMC Algorithm for Growth Model

We present the MCMC algorithm used to obtain samples from the posterior distribution for each of the parameters: τ , α , β , λ , M_I , τ_I , M_Y and τ_Y for the growth model. When simulating from a distribution, a reference is given to the equation number that provides full details of the parameters of the distribution.

1. Input of Data and Initialisation of Parameters

- (a) For $i = 1, \dots, 5$ (specimen); $j = 1, \dots, 44$ (polygon); $k = 1, \dots, K_{ij}$, (K_{ij} is the total number of cracks in polygon j of specimen i) input the data: l_{ijk} , C_j and T_j . For each pre-crack input I_{ijk} , the logarithm of the length of the pre-crack at the start of stressing.
- (b) For each pre-crack set $t_{ijk} = 0$.
- (c) Initialise τ , α , β , λ , M_I , τ_I , M_Y , τ_Y , $\{I_{ijk*}\}$, $\{B_{ijk}\}$, $\{Y_{ijk}\}$, and $\{h_{ijk*}\}$.
- (d) Set the parameter values for each of the prior distributions for each of the parameters, see Section 6.3.5.

2. For $r \leq$ total number of iterations:

(a) Gibbs Sampling

Simulate the following parameters:

$$\tau^{(r)} \sim \text{Gamma}(,) \text{ 6.1;}$$

$$\alpha^{(r)} \sim \text{Normal}(,) \text{ 6.2;}$$

$$\beta^{(r)} \sim \text{Normal}(,) \text{ 6.3;}$$

$$\lambda^{(r)} \sim \text{Beta}(,) \text{ 6.4;}$$

$$M_I^{(r)} \sim \text{Normal}(,) \text{ 6.5;}$$

$$\tau_I^{(r)} \sim \text{Gamma}(,) \text{ 6.6;}$$

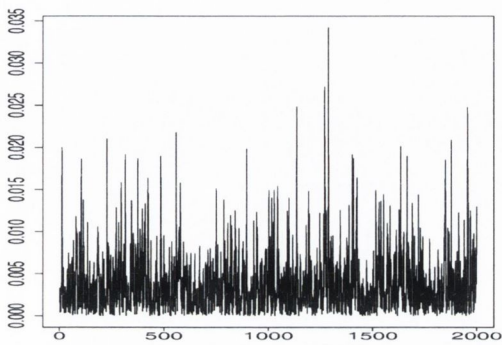
$$M_Y^{(r)} \sim \text{Normal}(,) \text{ 6.7;}$$

$$\tau_Y^{(r)} \sim \text{Gamma}(,) \text{ 6.8.}$$

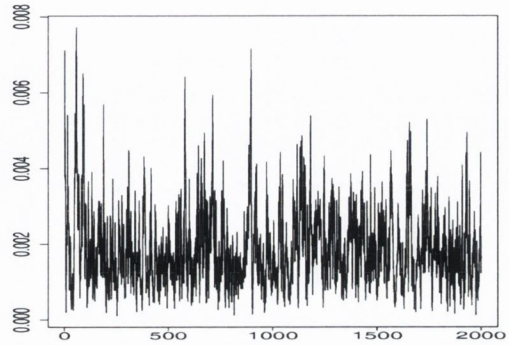
- (b) For each load-crack simulate its initiation length: $I_{ijk^*}^{(r)} \sim \text{Normal}(,)$ (6.9) and simulate its initiation time $h_{ijk^*}^{(r)} \sim \text{Normal}(,)$ (6.13).
- (c) For each crack simulate whether or not there is a jump in its length: $B_{ijk}^{(r)} \sim \text{Bernoulli}(.)$ (6.10).
- (d) Depending on whether or not $B_{ijk}^{(r)}$ is 1 simulate a jump size accordingly: for each crack k : $Y_{ijk}^{(r)} \sim \text{Normal}(.)$ (6.11) if $B_{ijk}^{(r)} = 0$ and $Y_{ijk}^{(r)} \sim \text{Normal}(.)$ (6.12) if $B_{ijk}^{(r)} = 1$.
- (e) $r = r + 1$.

B.4 Trace Plots

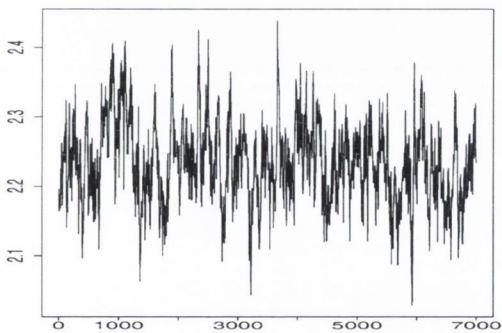
We present in the following figures trace plots for the various parameters of the three models discussed in this thesis. As detailed in Section 3.3.6, after a number of iterations (burn-in) the Markov chain resulting from the MCMC algorithm, is said to have converged. When examining trace plots an indication that convergence has been reached is if the chain exhibits the same qualitative behaviour. It appears that the trace plots presented in the following figures exhibit the same qualitative behaviour and so we conclude that there exists no evidence for lack of convergence and we believe that the chains presented are samples from the corresponding posterior distributions.



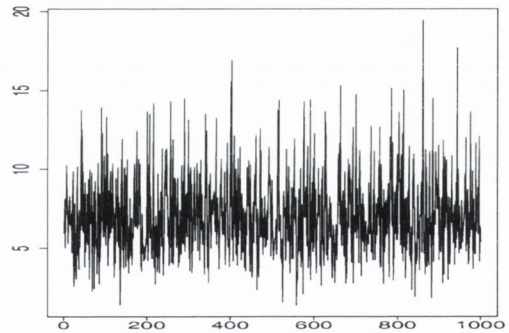
(a)



(b)

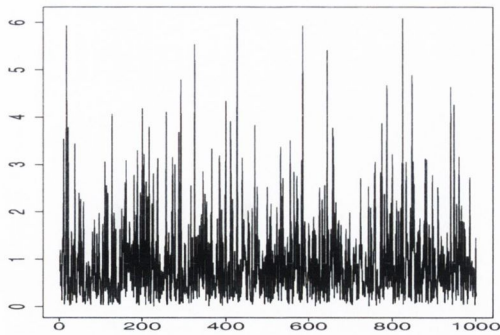


(c)

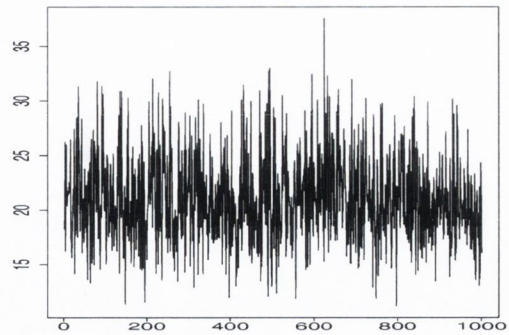


(d)

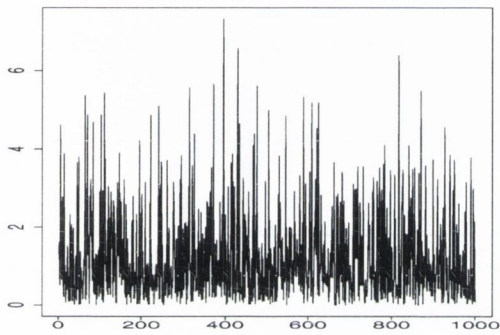
Figure B.1: Trace plots of samples obtained after convergence for parameters of the discrete initiation model. (a) shows a trace plot of sample values for β_1 (2000 samples); (b) shows a trace plot of sample values for β_2 (2000 samples); (c) shows a trace plot of sample values for ρ (7000 samples); (d) shows a trace plot of sample values for $A_{10} \sum_k \omega_{10,k} \gamma_{1,k}$ (1000 samples).



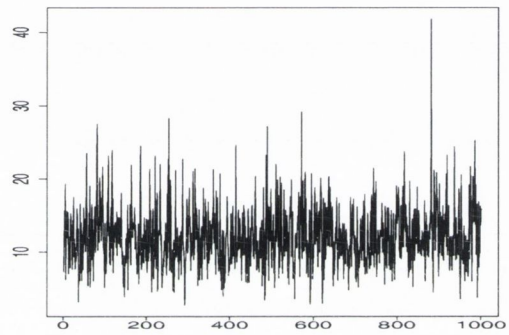
(a)



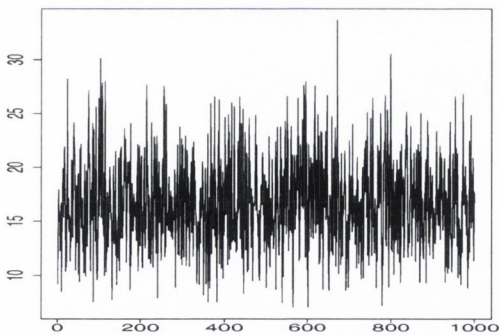
(b)



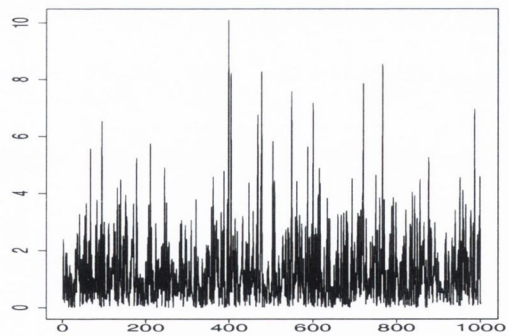
(c)



(d)

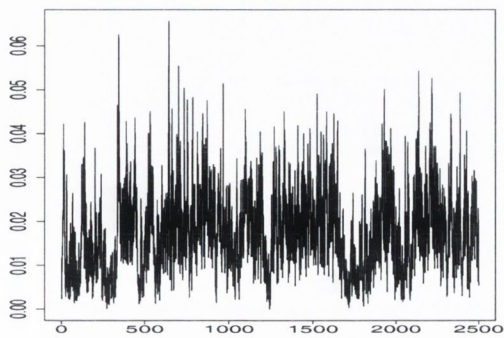


(e)

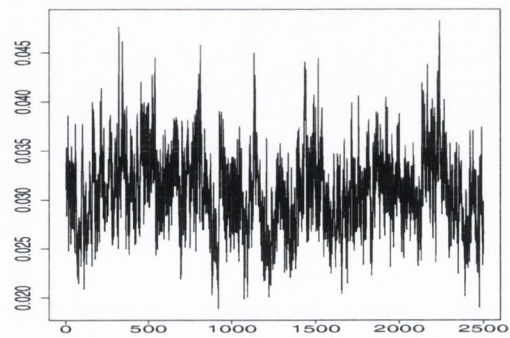


(f)

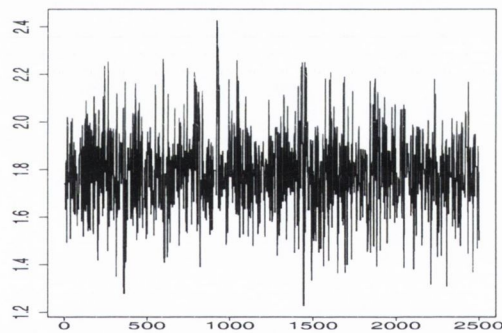
Figure B.2: Trace plots of samples, for various parameters of the discrete initiation model, obtained after convergence. (a) $A_{15} \sum_k \omega_{15,k} \gamma_{2,k}$ (1000 samples); (b) $A_{40} \sum_k \omega_{40,k} \gamma_{4,k}$ (1000 samples); (c) $\gamma_{1,22}$ (1000 samples); (d) $\gamma_{3,29}$ (1000 samples); (e) $\gamma_{4,6}$ (1000 samples); (f) $\gamma_{5,21}$ (1000 samples).



(a)

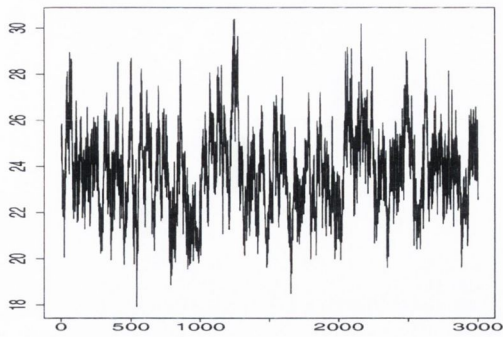


(b)

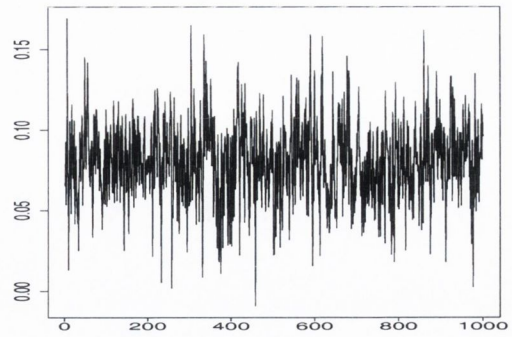


(c)

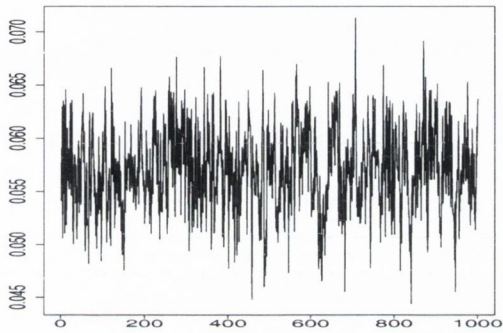
Figure B.3: Trace plots of samples obtained after convergence for the parameters of the continuous initiation model. (a) shows a trace plot of sample values for β_1 (2500 samples); (b) shows a trace plot of sample values for β_2 (2500 samples); (c) shows a trace plot of sample values for ρ (2500 samples).



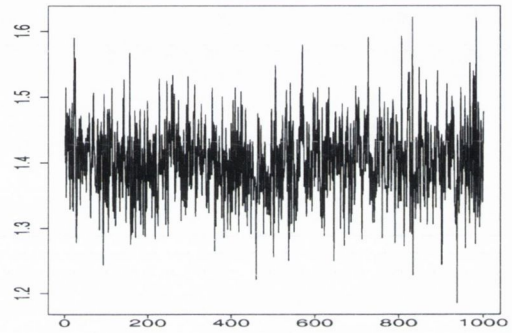
(a)



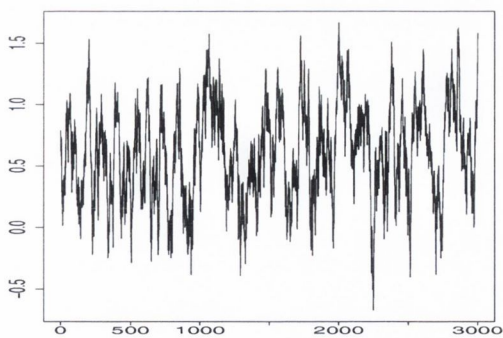
(b)



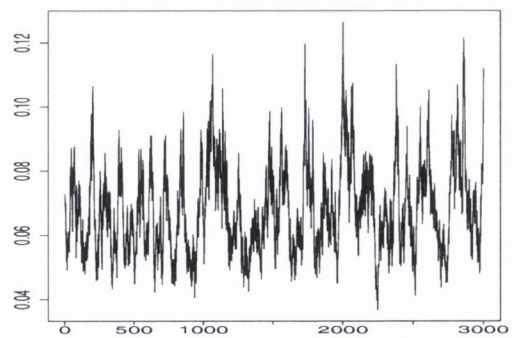
(c)



(d)



(e)



(f)

Figure B.4: Trace plots of samples, for various parameters of the growth model, obtained after convergence. (a) τ (3000 samples); (b) α (1000 samples); (c) β (1000 samples); (d) τ_I (1000 samples); (e) M_Y (3000 samples); (f) τ_Y (3000 samples).

Bibliography

- Abramowitz, M. and Stegun, IE.** *Handbook of Mathematical Functions with Formulas, Graphs and Mathematical Tables*. Applied Mathematics Series, 55. Washington, DC: National Bureau of Standards, 1964.
- Bergmann, G., Graichen, F., and Rohlmann, A.** Hip joint loading during walking and running, measured in two patients. *Journal of Biomechanics*, 26(8): 969–990, 1993.
- Best, N., Ickstadt, K., and Wolpert, R.** Spatial Poisson Regression for Health and Exposure Data Measured at Disparate Resolutions. *Journal of the American Statistical Association*, 95(452):1076–1088, 2000a.
- Best, N., Ickstadt, K., Wolpert, R., and Briggs, D.** *Spatial Epidemiology: Methods and Applications*, chapter : Combining Models of Health and Exposure Data: The SAVIAH Study, Eds. P. Elliott, J.C. Wakefield, N.G. Best, and D.J. Briggs, pages 393–414. Oxford University Press, 2000b.
- Brooks, S. and Roberts, G.** Convergence assessment techniques for Markov chain Monte Carlo. *Statistics and Computing*, 8(4):319–335, 1998.
- Casella, G. and Robert, C.** Rao-Blackwellisation of sampling schemes. *Biometrika*, 83(1):81–94, 1996.
- Chatfield, C.** *Statistics for Technology*. Chapman and Hall, 3rd edition, 1983.

- Chib, S. and Greenberg, E.** Understanding the Metropolis Hastings Algorithm. *The American Statistician*, 49(4):327–335, 1995.
- Cowles, M. and Carlin, B.** Markov Chain Monte Carlo Convergence Diagnostics: A Comparative Study. *Journal of the American Statistical Association*, 91(434): 883–904, 1996.
- Cox, D. and Isham, V.** *Point Processes*. Chapman and Hall, 1st edition, 1980.
- Cressie, N.** *Statistics for Spatial Data*. John Wiley and Sons, Inc., revised edition, 1993.
- Culleton, T., Prendergast, P., and Taylor, D.** Fatigue failure in the cement mantle of an artificial hip joint. *Clinical Materials*, 12:95–102, 1993.
- Dempster, A., Laird, N., and Rubin, D.** Maximum Likelihood from Incomplete Data via the EM Algorithm (with discussion). *Journal of the Royal Statistical Society, Series B (Methodological)*, 39(1):1–38, 1977.
- Diggle, P.** *Statistical Analysis of Spatial Point Patterns*. Arnold, 2nd edition, 2003.
- Diggle, P. and Ribeiro Jr., P.** Model-based geostatistics. *Caxambu: Associação Brasileira de Estatística (XIV SINAPE - Simpósio Nacional de Probabilidade e Estatística)*, 2000.
- Dobson, A.** *An Introduction To Generalized Linear Models*. Chapman and Hall/CRC, 2nd edition, 2002.
- Elliott, P., Wakefield, J., Best, N., and Briggs, D.** *Spatial Epidemiology: Methods and Applications*. Oxford University Press, 2000.
- Gamerman, D.** *Markov Chain Monte Carlo: Stochastic Simulation for Bayesian Inference*. Chapman and Hall, 1st edition, 1997.
- Garthwaite, P., Kadane, J., and O'Hagan, A.** Elicitation. *Journal of the American Statistical Association (to appear)*.

- Gelfand, A., Hills, S., Racine-Poon, A., and Smith, A.** Illustration of Bayesian Inference in Normal Data Models Using Gibbs Sampling. *Journal of the American Statistical Association*, 85(412):972–985, 1990.
- Gelfand, A. and Smith, A.** Sampling-Based Approaches to Calculating Marginal Densities. *Journal of the American Statistical Association*, 85(410):398–409, 1990.
- Gelman, A. and Rubin, DB.** Inference from Iterative Simulation Using Multiple Sequences (<http://www.stat.columbia.edu/~gelman>). *Statistical Science*, 7(4):457–511, 1992.
- Geman, S. and Geman, D.** Stochastic Relaxation, Gibbs Distributions and the Bayesian Restoration of Images. *IEEE Transactions on Pattern Analysis and Machine Intelligence*, 6:721–741, 1984.
- Gilks, W., Richardson, S., and Spiegelhalter, D.** *Markov Chain Monte Carlo in Practice*. Chapman and Hall, 1st edition, 1996.
- Grasa, J., Pérez, M., Ferrer, R., Bea, J., García, J., and Doblaré, M.** A probabilistic damage model for acrylic cements. Application to the life prediction of cemented hip implants. *International Journal of Fatigue (submitted)*, 2003.
- Grimmett, G. and Stirzaker, D.** *Probability and Random Processes*. Oxford Science Publications, 3rd edition, 2001.
- Hastings, W.** Monte Carlo sampling methods using Markov chains and their applications. *Biometrika*, 57(1):97–109, 1970.
- Huiskes, R.** Failed innovation in total hip replacement. Diagnosis and proposals for a cure. *Acta Orthopaedica Scandinavica*, 64(6):699–716, 1993.
- Huiskes, R. and Verdonshot, N.** *Basic Orthopaedic Biomechanics*, Eds. Mow, V.C. and Hayes, W.C., chapter : Biomechanics of artificial joints: The hip., pages 395–460. Lipincott-Raven, Philadelphia, 2nd edition, 1997.

- Ickstadt, K. and Wolpert, R.** *Multiresolution Assessment of Forest Inhomogeneity in Case Studies in Bayesian Statistics, Lecture Notes in Statistics, No. 121, Eds. Gatsonis, C., Hodges, J.S., Kass, R.E., McCulloch, R., Rossi, P., and Singpurwalla, N.D.*, volume 3, pages 371–386. Springer-Verlag: New York, 1997.
- Ickstadt, K. and Wolpert, R.** Spatial Regression for Marked Point Processes (with discussion). In Bernardo, J., Berger, J., Dawid, A., and Smith, A., editors, *Bayesian Statistics 6*, pages 323–341. Oxford University Press, 1999.
- Jasty, M., Maloney, W., Bragdon, C., O'Connor, D., Haire, T., and Harris, W.** The Initiation of Failure in Cemented Femoral Components of Hip Arthroplasties. *Journal of Bone and Joint Surgery*, 73-B:551–558, 1991.
- Kingman, J.** *Poisson Processes*. Clarendon Press, Oxford, 1st edition, 1993.
- Lee, P.** *Bayesian Statistics: An Introduction*. Arnold, 2nd edition, 1997.
- Lennon, A.** *A stochastic model of damage accumulation in acrylic bone cement. Application to failure modelling of cemented hip replacement*. PhD thesis, 2002. University of Dublin, Trinity College.
- Lennon, A. and Prendergast, P.** Evaluation of cement stresses in finite element analyses of cemented orthopaedic implants. *Journal of Biomechanical Engineering, Transactions of the ASME*, 123:623–628, 2001.
- Lennon, A. and Prendergast, P.** Residual stress due to curing can initiate damage in porous bone cement: experimental and theoretical evidence. *Journal of Biomechanics*, 35:311–321, 2002.
- Lévy, P.** *Théorie de L'Addition des Variables Aléatoires*. Paris: Gauthier-Villars, 1937.
- Malchau, H. and Herberts, P.** Prognosis of Total Hip Replacement, Revision and Re-revision rate in THR: a revision-risk study of 148,359 primary operations.

- In Proceedings of the 65th Annual Meeting of American Academy of Orthopaedic Surgeons, New Orleans, USA, 1998.*
- Malchau, H., Herberts, P., Söderman, P., and Odén, A.** Prognosis of total hip replacement: Update and validation from the Swedish National Hip Arthroplasty Registry 1979-1998. *Scientific Exhibition presented at the 67th Annual Meeting of the American Academy of Orthopaedic Surgeons, Orlando, USA*, pages 1-16, 2000.
- McCormack, B. and Prendergast, P.** Microdamage accumulation in the cement layer of hip replacements under flexural loading. *Journal of Biomechanics*, 32: 467-475, 1999.
- McCormack, B., Walsh, C., Wilson, S., and Prendergast, P.** A statistical analysis of microcrack accumulation in PMMA under fatigue loading: applications to orthopaedic implant fixation. *International Journal of Fatigue*, 20(3):581-593, 1998.
- Metropolis, N., Rosenbluth, A., Rosenbluth, M., Teller, A., and Teller, E.** Equations of State Calculations by Fast Computing Machines. *Journal of Chemical Physics*, 21(6):1087-1092, 1953.
- Murphy, B. and Prendergast, P.** Measurement of non-linear microcrack accumulation rates in polymethylmethacrylate bone cement under cyclic loading. *Journal of Materials Science: Materials in Medicine*, 10:779-781, 1999.
- O'Hagan, A.** Eliciting expert beliefs in substantial practical applications. *The Statistician*, 47(1):21-35, 1998.
- O'Hagan, A. and Forster, J.** *Kendall's Advanced Theory of Statistics: Volume 2B Bayesian Inference*. Arnold, 2nd edition, 2004.
- Press, W., Flannery, B., Teukolsky, S., and Vetterling, W.** *Numerical Recipes in C: The Art of Scientific Computing*. Cambridge University Press, 2nd edition, 1992.

- Ridout, M., Demétrio, C., and Hinde, J.** Models for count data with many zeros. In *Proceedings of the XIXth International Biometric Conference, Cape Town, South Africa*, pages 179–192, 1998.
- Ross, S.** *Introduction to Probability Models*. Academic Press, 8th edition, 2003.
- Smith, P.** *Analysis of Failure and Survival Data*. Chapman and Hall/CRC, 2002.
- Sobczyk, K. and Spencer, B.** *Random Fatigue: From Data to Theory*. San Diego: Academic Press, 1st edition, 1992.
- Swendsen, RH. and Wang, JS.** Non-universal Critical Dynamics in Monte Carlo Simulation. *Physical Review Letters*, 58(2):86–88, 1987.
- Tanner, MA. and Wong, WH.** The Calculation of Posterior Distributions by Data Augmentation. *Journal of the American Statistical Association*, 82(398):528–540, 1987.
- Tsukrov, I. and Kachanov, M.** Stress Concentrations and Microfracturing Patterns in a Brittle-Elastic Solid with Interacting Pores of Diverse Shapes. *International Journal of Solids and Structures*, 34(22):2887–2904, 1997.
- van Dyk, D. and Meng, X.** The Art of Data Augmentation (with discussion). *Journal of Computational and Graphical Statistics*, 10(1):1–50, 2001.
- Wang, J., Toksvig-Larsen, S., Müller-Willie, P., and Franzeén, H.** Is there any difference between vacuum mixing systems in reducing bone cement porosity? *Journal of Biomedical Materials Research*, 33:115–119, 1996.
- Wilson, S.** Hierarchical Modelling of Orthopaedic Hip Replacement Damage Accumulation and Reliability. *Journal of the Royal Statistical Society. Series C (Applied)*, 54(2):425–441, 2005.
- WinBUGS.** Lecture Notes from Workshop: Bayesian Models in Environmental Applications using WinBUGS, Imperial College, London, UK. June 2003.

- Wolpert, R. and Ickstadt, K.** Poisson/gamma random field models for spatial statistics. *Biometrika*, 85(2):251–267, 1998a.
- Wolpert, R. and Ickstadt, K.** *Practical Nonparametric and Semiparametric Bayesian Statistics*, Eds. Müller, P., Dey, D. and Sinha, D., chapter Simulation of Lévy Random Fields, pages 227–242. Springer-Verlag, 1998b.